

**STUDY THE RHEOLOGICAL
PROPERTIES OF NON-NEWTONIAN
POLYMER SOLUTIONS AND SOLID
SUSPENSIONS**

A Thesis
Submitted to the College of Engineering
of Nahrain University in Partial Fulfillment
of the Requirements for the Degree of
Master of Science
in
Chemical Engineering

by

Manar Taher Nasser
(B.Sc. in Chemical Engineering 2006)

Jumada AL-Aker

1430

May

2009

Certification

I certify that the thesis entitled “**Study the Rheological Properties of Non-Newtonian Polymer Solutions and Solid Suspensions**” was prepared by “**Manar Taher Nasser**” under my supervision at Nahrain University / College of Engineering in partial fulfillment of the requirements for the degree of Master of Science in Chemical Engineering.

Signature: *K.S. Abdulmasih*

Name: **Dr. Kamal Shakir Abdul Masih.**

(Supervisor)

Date: *7/6/2009*

Signature: *Q. J. Slaiman*

Name: **Prof. Dr. Qasim J. Slaiman**
(Head of Department)

Date: *7/6/2009*

Certificate

We certify, as an expermining committee, that we have read this thesis entitled "Study the Rherological Properties of Non-Newtonian Polymer Solutions and Solid Suspensions", examined the student "Manar Taher Nasser" in its content and found it meets the standard of thesis for the degree of Master of Science in Chemical Engineering.

Signature: *K.S. Abdulmasih*

Name: Dr. Kamal S. Abdul Masih.

(Supervisor)

Date: 7/6/2009

Signature: *Wadood*

Name: Ass. Prof. Dr. Wadood T. Mohammed

(Member)

Date: 7/6/2009

Signature: *Malek*

Name: Ass. Prof. Dr. Malek M. Mohammed

(Member)

Date: 7/6/2009

Signature: *Nada*

Name: Prof. Dr. Nada B. Nakkash

(Chairman)

Date: 7/6/2009

Approval of the College of Engineering.

Signature: *M. J. Jweeg*

Name: Prof. Dr. Muhsin J. Jweeg.

(Dean)

Date: 10/6/2009

Abstract

This research deals with experimental study of the rheological behavior of polymer solutions, solid suspension and the effect of adding polymers to solid suspensions. All polymers studied in this work are water soluble and used in industries as a rheology control additive (rheology modifiers), these are: CMC-Carboxymethyl cellulose, XC-Xanthan Gum, HEC-Hydroxyethyl cellulose and PVA-polyvinyl alcohol. Solid suspensions used are: Bentonite, Graphite and Corn starch.

The rheological properties of these materials were investigated using a Couette coaxial cylinder rotational viscometer Fann model 35A with range between 3-600 rpm; by measuring shear stresses versus shear rates (i.e. Flow curve).

Seventy Six runs were performed with the range concentration for all polymer solutions used: CMC, HEC, XC (4-40) g/L, PVA (2-10) g/L and the range concentration of solid suspensions: Bentonite 50-120 g/L, Graphite 30-90 g/L and Corn Starch 300-800 g/L. The range temperature for runs: 0-55 °C

It was found that as polymer concentration was increased, the flow behavior index (n) decreased, and the range of n was between 0.7-0.4 at 20°C. Increase the concentration of solid suspension the flow behavior index (n), the range of n was between 1-1.3 at 35°C. Correlations were developed that describe the effect of polymer solutions and solid suspensions concentration on flow behavior index for each material used in this study and presented in a linear form.

The viscosities of three polymers CMC, XC and HEC were decreased with increasing temperature and shear rate. It was found that XC polymer was more affected by concentration than other polymer used in this study and it has higher viscosity than other polymer used.

It was found that the viscosities of solid suspensions were increased with increasing shear rate. The flow curve of experimental polymer solution and solid suspension was studied using the power law model.

The variations in temperature influence the value of n and k . The increases in temperature cause are increase in flow behavior index (n) and decrease in consistency index (k).

By using the Solver Add-in in Microsoft Excel, the Bingham plastic model was found to be the best fits the experimental results of adding polymer to solid suspensions (PVA to Bentonite suspensions).

The effect of PVA polymer on the rheological properties of the Bentonite slurry was modifier the data for apparent viscosity. This experimental evidence shows that the apparent viscosity of Bentonite/PVA decreases with increasing shear rate, while the experimental data for Bentonite/water (with out polymer) show that increase of apparent viscosity with increase in shear rate

The Bingham yield stress decreases when adding PVA polymer, when the concentration reaches 14-15g/l the yield stress start to increase.

List of Contents

	<u>Contents</u>	<u>Page</u>
	Abstract	I
	List of contents.	III
	Nomenclature	VII
	List of table.	IX
	List of figures.	XI
	Chapter One: Introduction.	1
1.1	Introduction.	1
1.2	Aim of this work.	4
	Chapter Two: Literature Survey.	5
2.1	Introduction.	5
2.2	Understanding rheology: viscous and elastic response.	6
2.3	Fundamentals of rheological terms.	7
2.3.1	Deformation.	7
2.3.1.1	Elastic deformation.	7
2.3.1.2	Shear deformation.	8
2.3.2	Viscoelastic.	10
2.3.3	Shear rate.	10
2.4	Shear viscosity.	13
2.5	The general form of the viscosity curve for suspensions.	14
2.6	The general form of the viscosity curve for polymer solution.	16
2.7	Newtonian fluids.	17
2.8	Non-newtonian fluid.	18

2.8.1	Non-newtonian fluids-time independent.	19
2.8.1.1	Pseudo plastic (shear-thinning) behavior.	19
2.8.1.2	Dilatants (shear-thickening) behavior	20
2.8.1.3	Bingham behavior	22
2.8.2	Non-newtonian fluids-time dependent.	23
2.8.2.1	Thixotropic fluids.	23
2.8.2.2	Rheopectic fluids.	24
2.9	Water soluble polymers.	26
2.10	Cellulose and cellulose derivatives	27
2.11	Polymer solutions.	29
2.11.1	Solubility of polymer.	30
2.11.2	Dilute and concentrated polymer solutions.	31
2.12	Previous works	32
Chapter Three: Experimental Work.		41
3.1	Solid suspension used.	41
3.2	Polymers used.	41
3.3	Sets of experiments	42
3.4	Equipments used.	44
3.5	Instruments to measure rheological properties.	46
3.6	Viscometer (the model 35 viscometer).	47
3.7	Calibration of viscometer.	48
3.8	Solid suspension.	50
3.8.1	Bentonite suspension.	50
3.8.2	Corn starch suspension.	50
3.8.3	Graphite suspension.	51
3.9	Polymer definition.	51

3.9.1.1	Sodium carboxymethyl cellulose (CMC).	51
3.9.1.2	Hydroxyethyl cellulose (HEC).	52
3.9.2	XC polymer (xanthan gum)	52
3.9.3	Polyvinyl alcohol (PVA).	53
3.10	Preparation of CMC, HEC and XC polymer solutions.	53
3.11	Preparation of PVA solution.	54
3.12	Rheological measurements	55
3.13	Preparation and measuring of rheological properties of solid suspension (bentonite, graphite and corn starch).	55
3.14	Preparation of add PVA to bentonite suspensions.	56
Chapter Four: Results and Discussion.		56
4.1	Introduction.	56
4.2	Results of polymer solution.	58
4.2.1	Study shears flow behavior.	58
4.2.2	Effect of polymer concentration on flow behavior index	62
4.2.3	Effect polymer concentration on flow curves.	64
4.2.4	Apparent viscosity of polymer solution.	68
4.2.5	Effect of temperature on polymer solution viscosity.	71
4.2.6	Effect of polymer type on viscosity.	74
4.3	Results of solid suspension	76
4.3.1	Shear flow behavior.	75
4.3.2	Effect o f solid suspension concentration on flow curves.	77
4.3.3	Effect of solid suspension on flow behavior index (n).	79
4.3.4	Viscosity of solid suspension.	82

4.4	Steady the effect of adding PVA to bentonite for different concentration.	84
4.4.1	General of rheological properties.	84
4.4.2	Flow model selection.	87
4.4.3	Bingham plastic model.	92
4.4.4	Effect concentration PVA polymer on bingham yield stress.	95
4.4.5	Apparent viscosity of bentonite/PVA.	96
Chapter Five: Conclusions and Recommendations for Future Work.		99
5.1	Conclusions.	99
5.2	Recommendations for future work.	100
References.		101
Appendices.		
Appendix A: The flow curves of the experiments (shear stress versus shear rate).		A-1
Appendix B: Experimental data shear stress versus shear rate.		B-1

Nomenclature

<u>Symbol</u>	<u>Meaning</u>	<u>Unit</u>
A	Area	m ²
b	Outer radius coaxial rheometer	cm
E	Young's modulus	N/m ²
F	Force	N
h	Length of inner cylinder	m
K	Consistency index	Pa. s ⁿ
k ₁ k ₂	Conversion factors in Equations (4.1) and (4.2)	-
L	Length	m
l ₀	Initial length	m
n	Flow behavior index	-
N	Rotational speed	rpm
P	Pressure	Pa
R	Radius	m
r ^o	Inner radius of cylinder.	cm
R _c	Radius of the cone	m
R _i	Radius of inner cylinder	m
R _o	Radius of the outer cylinder	m
t	Time	s
V	Velocity	m/s

	Greek Letters	<u>Unit</u>
$\dot{\gamma}$	Shear rate	s^{-1}
α	Constant	-
ε	Strain or deformation	-
θ	Dial reading	deg
σ	Normal stress	Pa
τ	Shear stress	Pa
τ_c	Shear stress critical	Pa
Δp	Pressure difference	N/m^2
τ_{PI}	Plastic viscosity	Pa
G''	Storage modules	Pa
G'	Elastic modules	Pa
η	Viscosity	Pa. s

Abbreviations

CMC	Carboxymethyl Cellulose.
HEC	Hydroxyethyl Cellulose.
PVA	Polyvinyl Alcohol.
XC	Xanthomonas Campestris.

List of Tables

<u>Table</u>	<u>Title</u>	<u>Page</u>
2-1	Characteristic shear-rate ranges (in s^{-1}) occurring in some industrial processes.	11
3-1	List of all experiments.	42
4-1	Flow behavior index (n) and consistency index (k).	62
4-2	The influence of the temperature on the values of n and k for polymer solutions at 10 g/l.	73
4-3	Flow behavior index (n) and consistency index (k)	82
4-4	Model selection for (Bentonite/PVA) using add-in solver microsoft excel.	89
4-5	Flow equations for flow models.	90
B-1	Shear stress versus shear rate for CMC polymer at concentration 4, 10, 20, 30 and 40 g/L.	B-1
B-2	Shear stress versus shear rate for CMC polymer at concentration 7, 15, 25 and 35 g/L.	B-1
B-3	Shear stress versus shear rate for HEC polymer.	B-1
B-4	Shear stress versus shear rate for XC polymer.	B-2
B-5	Shear stress versus shear rate for PVA polymer.	B-2
B-6	Apparent viscosity versus shear rate for CMC polymer.	B-2
B-7	Apparent viscosity versus shear rate for CMC Polymer.	B-3
B-8	Apparent viscosity versus shear rate for HEC polymer.	B-3
B-9	Apparent viscosity versus shear rate for XC polymer.	B-3
B-10	Effect of temperature in apparent viscosity for CMC at 10 g/L.	B-4
B-11	Effect of temperature in apparent viscosity for CMC at 15 g/L.	B-4
B-12	Effect of temperature in apparent viscosity for CMC at 25 g/L.	B-4
B-13	Effect of temperature in apparent viscosity for CMC at 40 g/L.	B-4

B-14	Effect of temperature in apparent viscosity for HEC at 10 g/L.	B-5
B-15	Effect of temperature in apparent viscosity for HEC at 20 g/L.	B-5
B-16	Effect of temperature in apparent viscosity for HEC at 30 g/L.	B-5
B-17	Effect of temperature in apparent viscosity for HEC at 40 g/L.	B-5
B-18	Effect of temperature in apparent viscosity for XC at 4 g/L.	B-6
B-19	Effect of temperature in apparent viscosity for XC at 10 g/L.	B-6
B-20	Effect of temperature in apparent viscosity for XC at 20 g/L.	B-6
B-21	Effect of temperature in apparent viscosity for XC at 40 g/L.	B-6
B-22	Shear rate versus shear stress for bentonite suspension.	B-7
B-23	Shear rate versus shear stress for graphite suspension.	B-7
B-24	Shear rate versus shear stress for corn starch suspension.	B-7
B-25	Apparent viscosity versus shear rate for bentonite suspension.	B-8
B-26	Apparent viscosity versus shear rate for graphite suspension.	B-8
B-27	Apparent viscosity versus shear rate for corn starch suspension.	B-8
B-28	Shear stress versus shear rate for (bentonite/PVA).	B-9
B-29	Shear stress versus shear rate for (bentonite/PVA).	B-9
B-30	Bingham yield point and plastic viscosity versus shear rate for (bentonite/PVA).	B-9
B-31	Model selection for bentonite/PVA at concentration (80+4) g/L using add-in in microsoft excel.	B-10
B-32	Model selection for bentonite/PVA at concentration (80+10) g/L using add-in in microsoft excel	B-10
B-33	Model selection for bentonite/PVA at concentration (80+14) g/L using add-in in microsoft excel	B-10
B-34	Model selection for bentonite/PVA at concentration (80+20) g/L using add-in in microsoft excel.	B-11

List of Figures

<u>Figure</u>	<u>Title</u>	<u>Page</u>
2-1	Laminar flow of a Newtonian liquid in simple shear.	6
2-2	Elastic deformation.	7
2-3	Shear deformation in space.	8
2-4	Shear deformation of a fluid placed in between two parallel planes.	9
2-5	Schematic representation of the flow curve of a concentrated suspension (A) and (B).	13
2-6	Schematic representation of the flow curve of polymer solutions.	14
2-7	A characteristic of Newtonian liquids (A) shear stress is directly proportional to rate of shear. (B) Viscosity is independent of rate of shear.	15
2-8	Alignment of particles.	17
2-9	Breaking down of particles.	17
2-10	The structure of shear thinning behavior.	18
2-11	τ versus $\dot{\gamma}$, η versus $\dot{\gamma}$ in shear thinning behavior.	18
2-12	Packing of particles.	19
2-13	The structure of shear thickening behavior.	19
2-14	τ versus $\dot{\gamma}$ and η versus $\dot{\gamma}$ in shear thickening behavior.	20
2-15	τ versus $\dot{\gamma}$ and η versus $\dot{\gamma}$ in Bingham plastic model.	21
2-16	Viscosity dependence on time for Thixotropic fluids.	22
2-17	Viscosity and shear rate dependence on time for rheopectic fluids.	22
2-18	The setup of the particle tracking velocimetry.	33

2-19	Schematic representation of adsorption of PVA polymer on bentonite particles as a function of concentration of polymer.	34
2-20	Coaxial rotating cylinder, couette flow device the outer cylinder (red) rotates while the inner cylinder remains fixed.	39
3-1	Fann VG-viscometer, model 35A	44
3-2	Hamilton beach mixer and cup	45
3-3	Classification of rheological instruments	46
3-4	The essential elements of rotational viscometer	47
3-5	Shear stresses versus shear rate for water at 20 °C	49
3-6	Molecular structure of Bentonite slurry.	50
3-7	Molecular structure of graphite.	51
3-8	Molecular structure of CMC	52
3-9	Molecular structure of HEC	52
3-10	Molecular structure of XC polymer	53
3-11	Molecular structure of PVA	53
4-1	Flow curve for CMC polymer solution at concentration 20g/l at 20°C.	59
4-2	Flow curve for HEC polymer solution at concentration 20g/l at 20°C.	59
4-3	Flow curve for XC polymer solution at concentration 20 g/l at 20°C.	60
4-4	Flow curve for CMC polymer pollution at concentration 20g/l at 20°C.	60
4-5	Flow curve for HEC polymer solution at concentration 20 g/l at 20°C.	61
4-6	Flow curve for XC polymer solution at concentration 20 g/l at 20°C.	61

4-7	Effect of XC polymer concentration on flow behavior index at 20°C.	64
4-8	Effect of HEC polymer concentration on flow behavior index at 20°C.	64
4-9	Effect of CMC polymer concentration on flow behavior index at 20°C.	65
4-10	Effect of HEC polymer concentration on flow curves at 20°C.	66
4-11	Effect of XC polymer concentration on flow curves at 20°C.	66
4-12	Effect of CMC polymer concentration on flow curves at 20°C.	67
4-13	Effect of HEC polymer concentration on flow curves at 20°C.	68
4-14	Effect of XC polymer concentration on flow curves at 20°C.	68
4-15	Effect of CMC polymer concentration on flow curves at 20°C.	69
4-16	Apparent viscosity of CMC polymer solutions at different concentration at 20°C.	70
4-17	Apparent viscosity of XC polymer solutions at different concentration at 20°C.	70
4-18	Apparent viscosity of HEC polymer solutions at different concentration at 20°C.	71
4-19	Effect of temperature in CMC polymer viscosity at concentration 10g/l at 20°C.	72
4-20	Effect of temperature in XC polymer viscosity at concentration 10g/l at 20°C.	72
4-21	Effect of temperature in HEC polymer viscosity at concentration 10g/l at 20°C.	73

4-22	Effect of polymer type on viscosity at polymer concentration of 10g/l at 20°C.	74
4-23	Effect of polymer type on viscosity at polymer concentration of 20g/l at 20°C.	75
4-24	Flow curve for bentonite suspension at concentration 50g/L at 35°C.	76
4-25	Flow curve for graphite at concentration 70 g/L at 35°C.	76
4-26	Flow curve for corn starch at concentration 700 g/L at 35°C.	77
4-27	Effect of bentonite in different concentration on flow curves at 35°C.	78
4-28	Effect of graphite in different concentration on flow curves at 35°C.	79
4-29	Effect of corn starch in different concentration on flow curve at 35°C.	79
4-30	Effect the bentonite suspension on flow behavior index at 35°C.	81
4-31	Effect the corn starch on flow behavior index at 35°C.	81
4-32	Effect the graphite on flow behavior index at 35°C.	82
4-33	Apparent viscosity of bentonite suspension at concentration 120 g/l at 35°C.	83
4-34	Apparent viscosity of corn starch at concentration 700g/l at 35°C.	84
4-35	Apparent viscosity of graphite at concentration 30 g/l at 35°C.	84
4-36	Changing result from the shape in flow curve caused by adding 2g/0.5L PVA polymer to bentonite slurry at 35°C.	86
4-37	Changing result from the shape in flow curve caused by adding 5 g/0.5L PVA polymer to bentonite slurry at 35°C.	86

4-38	Changing result from the shape in flow curve caused by adding 7 g/0.5L PVA polymer to bentonite slurry at 35°C.	87
4-39	Changing result from the shape in flow curve caused by adding 10g/0.5L PVA polymer to bentonite slurry at 35°C.	87
4-40	Experimental results and flow models representation for PVA/ Bentonite suspension at concentration (2+40) g/l at 35°C.	90
4-41	Experimental results and flow models representation for PVA/ Bentonite suspension at concentration (5+40) g/l at 35°C.	91
4-42	Experimental results and flow models representation for PVA/ Bentonite suspension at concentration (7+40) g/l at 35°C.	91
4-43	Experimental results and flow models representation for PVA/ Bentonite Suspension at Concentration (10+40) g/l at 35°C.	92
4-44	Rheogram for PVA/Bentonite suspension at concentration (2 in 40) g/L at 35°C.	93
4-45	Rheogram for PVA/Bentonite suspension at concentration (5 in 40) g/L at 35°C.	93
4-46	Rheogram for PVA/Bentonite suspension at concentration (7 in 40)g/L at 20°C.	94
4-47	Rheogram for PVA/Bentonite suspension at concentration (10 in 40)g/L at 20°C.	94
4-48	The influence of PVA on the bingham yield value of 8% (w/w) bentonite water system at 20°C.	96

4-49	Viscosity as a function of shear rate for Bentonite/ PVA polymer at concentration (2 in 40) g/L at 35°C.	97
4-50	Viscosity as a function of shear rate for Bentonite/ PVA polymer at concentration (5 in 40) g/L at 35°C.	97
4-51	Viscosity as a function of shear rate for Bentonite/ PVA polymer at concentration (7 in 40) g/L at 35°C.	98
4-52	Viscosity as a function of shear rate for Bentonite/ PVA polymer at concentration (10 in 40) g/L at 35°C.	98
A-1	Shear stress versus shear rate for CMC polymer at 4, 7, 10 and 15 g/l.	A-1
A-2	Shear stress versus shear rate for CMC polymer at 20, 25, 30, 35, 40 g/l	A-1
A-3	Shear stress versus shear rate for CMC polymer in 10 g/l at 20, 35 45 and 55°C	A-2
A-4	Shear stress versus shear rate for CMC polymer in 15 g/l at 20, 35 45 and 55°C.	A-2
A-5	Shear stress versus shear rate for CMC polymer in 25 g/l at 20, 35 45 and 55°C	A-3
A-6	Shear stress versus shear rate for CMC polymer in 40 g/l at 20, 35 45 and 55°C.	A-3
A-7	Shear stress versus shear rate for XC polymer at 4, 10, 20, 30, 40 g/l	A-4
A-8	Shear stress versus shear rate for HEC polymer at 4, 10, 20, 30 and 40 g/l.	A-4
A-9	Shear stress versus shear rate for XC polymer in 4 g/l at 20, 35 45 and 55°C.	A-5

- A-10 Shear stress versus shear rate for XC polymer in 10 g/l at 20, 35 45 and 55°C. A-5
- A-11 Shear stress versus shear rate for XC polymer in 30 g/l at 20, 35 45 and 55°C. A-6
- A-12 Shear stress versus shear rate for XC polymer in 40 g/l at 20, 35 45 and 55°C. A-6
- A-13 Shear stress versus shear rate for HEC polymer in 10 g/l at 20, 35 45 and 55°C. A-7
- A-14 Shear stress versus shear rate for HEC polymer in 20 g/l at 20, 35 45 and 55°C. A-7
- A-15 Shear stress versus shear rate for HEC polymer in 30 g/l at 20, 35 45 and 55°C. A-8
- A-16 Shear stress versus shear rate for HEC polymer in 40 g/l at 20, 35 45 and 55°C. A-8
- A-17 Shear stress versus shear rate for PVA polymer at 2, 5, 7 and 10 g/0.5L. A-9
- A-18 Shear stress versus shear rate for Bentonite suspension at 50, 80 and 120 g/l. A-9
- A-19 Shear stress versus shear rate for Graphite suspension at 30, 40, 70 and 90 g/l. A-10
- A-20 Shear stress versus shear rate for Corn Starch suspension at 300, 400, 500, 600, 700 and 800 g/l. A-10
- A-21 Shear stress versus shear rate for PVA to Bentonite suspension at concentration 2, 5, 7 and 10 g/0.5L to 40 g/0.5L. A-11

Chapter One

1.1 Introduction.

Rheology is the branch of science that deals with the flow and deformation of materials. Rheological instrumentation and rheological measurements have become essential tools in the analytical laboratory for characterizing component materials and final products, monitoring process conditions, and predicting product performance and consumer acceptance [1].

Deformation is the relative displacement of points of a body. It can be divided into two types: flow and elasticity. Flow is irreversible deformation; when the stress is removed the material does not revert to its original form. This means that the work is converted to heat. Elasticity is reversible deformation; the deformed body recovers its original shape, and the applied work is largely recoverable. Viscoelastic materials show both flow and elasticity, which bounces like a rubber ball when dropped, but slowly flows when allowed to stand [2].

Flow curves are basic rheology characteristics showing static properties of flowing materials. They express a relation (function) between shear rate and shear stress applied to a material, which flow [3].

There are two main types of fluids: Newtonian and non-Newtonian fluids. Newtonian fluids possess a constant viscosity at a constant temperature, while for non-Newtonian fluids the apparent viscosity depends on shear rate [4].

In polymer solutions, polymer molecules are long chain molecules composed of many repeating units. The bonds along the polymer backbone are continually rotating, and as a result, the molecule itself is continually changing orientation and configuration on a length scale much smaller than the equilibrium size [5].

In dilute polymer solutions, the rheology of solution is dependant solely on the dynamics of an individual chain and the number of chains (i.e. concentration) in the system. At high concentrations, interactions between polymer molecules impact the rheology in a significant way. As concentration further increases, polymer solutions exhibit a change from fluid-like to more elastic-like behavior [5].

The rheology of suspensions, colloidal dispersions and emulsions provide critical information for product and process performance in many industrial applications, and in order for them to give proper product performance, or to process efficiently, they must be stable. But these are often complex formulations of solvents (or fluids), suspended particles of varying size and shape, and various additives used to affect stability [6].

Dispersion of a solid or liquid in a liquid affects the viscosity. In many cases Newtonian flow behavior is transformed into non-Newtonian flow behavior, shear thickening results from the ability of the solid particles or liquid droplets to come together to form network structures when at rest or under low shear. With increasing shear the interlinked structure gradually breaks down, and the resistance to flow decreases. The viscosity of adispersed system depends on hydrodynamic interactions between particles or droplets and liquid [2].

The determination of rheological properties of Bentonite-water systems is very important for its characterization. Bentonite dispersions have colloid structure. The control of the rheological properties of these systems is not only important from a technological but also from a scientific point of view [5].

The rheological behavior of the system is determined by a mutual effect of attractive and repulsive forces between clay particles, which interact with each other through Coulombic and Van der Waals forces. These interactions can be

changed to gain the desired properties with the addition of various electrolytes, polymers, surfactants, and organic matters [5].

Addition of polymer greatly changed the rheological properties of bentonite dispersion. The degree of interaction between polymer molecules and clay particles depended on the polymer concentration in the dispersion. The experiments carried out by [7] showed that the rheological properties of the sample can be brought to desired values by use of polymer concentrations. The polymers added to the bentonite dispersions interact with the clay particles, according to their ionic or non-ionic character. The ionic polymers induce electrostatic interactions, but the non-ionic polymers are adsorbed on the surface by steric interactions (PVA molecules attached on the net negatively charged clay particles) [7].

Viscosity is the measure of the internal friction of a fluid. This friction becomes apparent when a layer of fluid is made to move in relation to another layer. The greater the friction the greater the amount of force required to causing this movement which is called shear [8]. Viscosity is a property of a fluid which is a measure of it's resistance to flow. Viscosities can be measured using a viscometer, which has the ability to determine changes in viscosity with time or with shear rate or shear stress. Viscometers can also detect if a solution undergoes shear thinning or thickening with time. Shear thinning is when a solution's viscosity decreases with increasing shear. The property called the apparent viscosity is defined as a ratio between shear stress and resulting shear rate of flowing material [8].

Many flow models have been proposed, which are useful for the treatment of experimental data or for describing flow behavior [2]. Such mathematical models range from the very simple to the very complex. Some of them merely involve the plotting of data on graph paper. Others require calculating the ratio of two numbers. Some are quite sophisticated and require use of computers.

This kind of analysis is the best way for getting the most from our data and often results in one of two constants which summarize the data and can be related to product or process performance. Once a correlation has been developed between rheological data and product behavior, the procedure can then be reversed and rheological data may be used to predict performance and behavior [9].

1.2 Aim of This Work.

- 1- Study experimentally the rheological behavior of solid suspensions in water.
- 2- Study experimentally the rheological behavior of polymer solutions.
- 3- Study the effect of adding polymers to solid suspensions on the rheological properties.
- 4- To obtain the best model to calculate the rheological properties of solid suspensions and polymer solution.
- 5- Study the effect of temperature on the rheological properties of polymer solutions.

Chapter Two

Literature Survey

2.1 Introduction.

The word “rheology” normally refers to the flow and deformation of “non-classical” materials such as rubber, molten plastic, polymer solutions, slurries and pastes, electrorheological fluids, blood, muscle composites, soils, and paints. These materials can exhibit varied and striking rheological properties that classical fluid mechanics and elasticity cannot describe. Though the word “rheology” was coined in 1929, the rapid development of the subject began 20 years later [10].

Rheology is used to predict a material's response to differing modes of flow and deformation at any point from the processing step through its final end use.

Matter can be rheologically classified into two extreme types: elastic solid, which obeys Hooke's law, and a viscous fluid, which obeys Newton's law. The application of a constant shear stress to an elastic solid will result in a constant shear strain. This leads to Hooke's law,

$$\sigma = G.\gamma \quad \dots (2.1)$$

Where σ is the shear stress, γ is the shear strain and G is the shear modulus. The application of a constant shear stress to a viscous fluid will result in a continuous deformation at a constant shear rate. This leads to Newton's Law,

$$\sigma = \eta. \dot{\gamma} \quad \dots (2.2)$$

Where η is viscosity and $\dot{\gamma}$ is the shear rate. However, most materials cannot be solely described by either of these classical extreme laws, because the shear stress is dependant on both the shear strain and the shear rate. This leads to

the concept of viscoelasticity, where a material possesses both solid-like and fluid-like behavior under different experimental conditions [11].

2.2 Understanding Rheology: Viscous and Elastic Response.

Fluid-like behavior is associated with flow: matter being deformed continually with time. Fundamental rheological variables can be defined by reference to an imaginary purely fluid sample confined between two parallel plates, figure 2-1. The plates are separated by a distance x that is small compared to the linear dimensions of the plates. The bottom plate is held stationary, while parallel to the top plate a certain force per unit area (or shear stress, F/A) is applied so that it moves. The fluid in contact with the upper plate moves equally fast, with velocity.

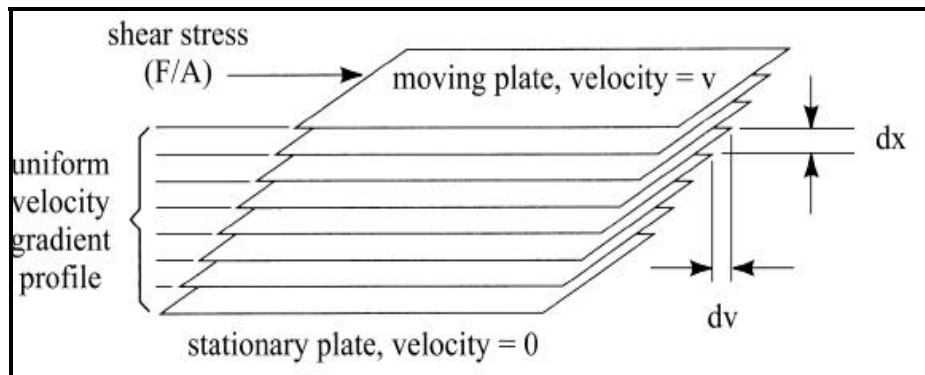


Figure 2-1 Laminar Flow of a Newtonian Liquid in Simple Shear [12].

The fluid in contact with the bottom plate is stationary. Hence, there is a difference in the fluid's velocity throughout the bulk: the sample experiences a velocity gradient dv/dx , which is the shear rate. If the force ceases to be applied, the upper plate comes to a rest. Isaac Newton discovered that the resistance that arises from the lack of slipperiness originating in a fluid - other things being equal - is proportional to the velocity by which the parts of the fluid

are being separated from each other. The proportionality constant is the shear viscosity of the liquid η [12]:

$$\sigma = \eta \dot{\gamma} \quad \dots(2.3)$$

Where:

$$\sigma = F/A, \dot{\gamma} = dv/dx, \quad (= v/x)$$

2.3 Fundamentals of Rheological Terms.

2.3.1 Deformation.

Deformation is the movement of parts or particles of a material body relative to one another such that the continuity of the body is not destroyed, resulting in a change of shape or volume or both. Deformation is a change in shape due to an applied force. This can be a result of tensile (pulling forces) or of compressive (pushing forces) loads being applied [8].

2.3.1.1 Elastic Deformation.

Elastic: A conservative property in which part of the mechanical energy used to produce deformation is stored in the material and recovered on release of stress. Elastic deformation as shown in figure 2-2 applies only to elastic solids.

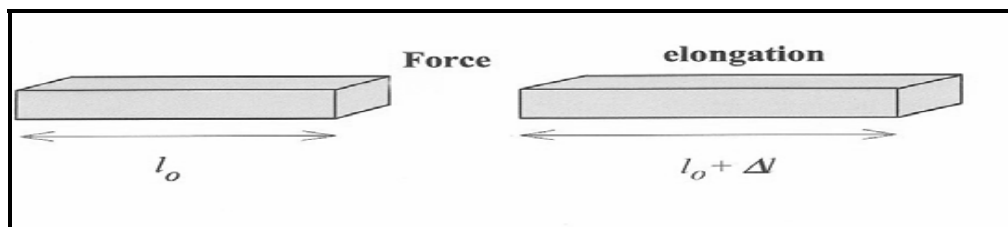


Figure 2-2 Elastic deformation [8].

Strain or deformation is defined as:

$$\varepsilon = dL/L \quad \dots(2.4)$$

Stress is the internal distribution of forces within a body that balance and react the loads applied to it. In other words: stress = Force / unit area. In between stress and strain exists a linear relation given by Hooke's law that is valid only in perfectly elastic bodies [7]:

$$\sigma = E \varepsilon \quad \dots$$

(2.5)

Where E is Young's modulus [N/m²].

2.3.1.2 Shear Deformation.

Shear stress is a stress state where the shape of a material tends to change (usually by sliding forces) without particular volume change [8]. When a shear deformation with a constant speed applied on a liquid, the flow phenomenon takes place [5].

Figure 2-3 illustrates the concept. Two large parallel plates bound a fluid. The area A, separated by a small distance H, the bottom plate is held fixed. Application of a force F to the upper plate causes it to move at a velocity V. The fluid continuous to deform as long as the force is applied, unlike a solid, which would undergo only a finite deformation [13].

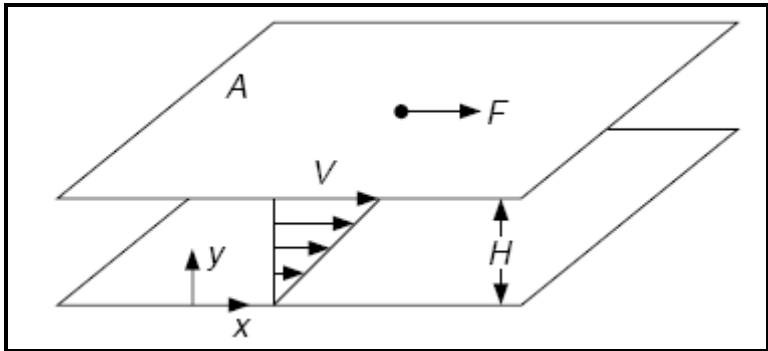


Figure 2-3 Shear Deformation in Space [13].

The force is directly proportional to the area of the plate. Within the fluid a linear velocity profile is established, due to non-slip condition, the fluid bounding the lower plate has zero velocity and the fluid bounding the upper plate move at plate velocity V . The flow in figure 2-4 is a simple shear flow.

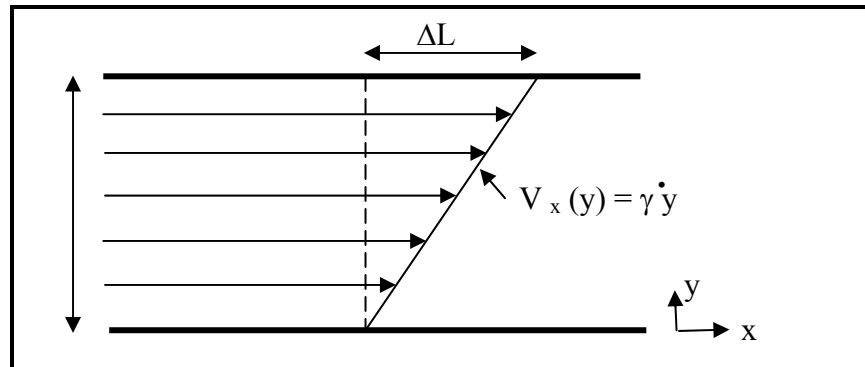


Figure 2-4 Shear Deformation of a Fluid Placed in Between Two Parallel Planes [8].

The next formulae are derived in accordance with figure 2-4.

$$\tau = F/A = - \eta(dv/dy) \quad \dots(2.6)$$

2.3.2 Viscoelastic.

The word “viscoelastic” means the simultaneous existence of viscous and elastic properties in a material. It is not unreasonable to assume that all real materials are viscoelastic (in all materials, both viscous and elastic properties coexist). The particular response of a sample in a given experiment depends on the time-scale of the experiment in relation to a natural time of the material. Thus, if the experiment is relatively slow, the sample will appear to be viscous rather than elastic, whereas, if the experiment is relatively fast, it will appear to be elastic rather than viscous. At intermediate time-scales mixed is appeared viscoelastic behavior [14].

2.3.3 Shear Rate.

The shear rate $\dot{\gamma}$ is the time dependent response of a fluid to any force acting on it. It is the time derivative of the strain $\gamma = \Delta L / \Delta y$, where ΔL is the deformation of the body as a result of the applied stress [7]. Shear rates of typical familiar material and processes are presented in table 2-1. Sedimentation of particle may involve very low shear rates, spray drying will involve high shear rates, and pipe flow of fluid will usually occur over a moderate shear rate range [15].

Table 2-1 Characteristic Shear-Rate Ranges (in s^{-1}) Occurring in Some Industrial Processes [15].

Situation	Shear rate (1/s)	Application
Sedimentation of particles in a suspending liquid	$10^{-6} - 10^{-3}$	Medicines, paints, spice in salad dressing
Leveling due to surface tension	$10^{-2} - 10^{-1}$	Frosting, paints, printing inks
Draining under gravity	$10^{-1} - 10^1$	Vats, small food containers, painting and coating
Extrusion	$10^0 - 10^3$	Snack and pet foods, tooth-paste, cereals, polymers
Pouring from a bottle	$10^1 - 10^2$	Food, cosmetics, toiletries
Chewing and swallowing	$10^1 - 10^2$	Foods
Dip coating	$10^1 - 10^2$	Paints, Confectionary
Mixing and stirring	$10^1 - 10^2$	Food processing
Pipe flow	$10^0 - 10^3$	Food processing, blood flow

Situation	Shear rate (1/s)	Application
Rubbing	$10^2 - 10^4$	Topical application of creams and lotions
Brushing	$10^3 - 10^4$	Brushing, painting, lipstick, nail polish
Spraying	$10^3 - 10^5$	Spray drying, spray painting, fuel atomization
High speed coating	$10^4 - 10^6$	Paper
Lubrication	$10^3 - 10^7$	Bearings, gasoline engines

2.4 Shear Viscosity.

Viscosity is defined as the internal friction of a fluid. The microscopic nature of internal friction in a fluid is analogous to the macroscopic concept of mechanical friction in the system of an object moving on a stationary planar surface. In a fluid, energy must be supplied: To create viscous flow units by breaking bonds between atoms and molecules and cause the flow units to move relative to one another.

The shear viscosity of most liquids decreases with temperature and increases with pressure. An increase in temperature usually causes expansion and a corresponding reduction in liquid bond strength, which in turn reduces the internal friction. Pressure causes a decrease in volume and a corresponding increase in bond strength, which in turn enhances the internal friction. For most situations, including engineering applications, temperature effects dominate the antagonistic effects of pressure.

If the viscosity throughout the fluid is independent of strain rate, then the fluid is said to be a Newtonian fluid. The constant of proportionality is called the coefficient of viscosity, and a plot of stress vs. strain rate for Newtonian fluids yields a straight line with a slope of η .

$$\tau = \eta \cdot \dot{\gamma} \quad \dots (2.7)$$

The term viscosity has no meaning for a non-Newtonian fluid unless it is related to a particular shear rate $\dot{\gamma}$. An apparent viscosity can be defined as:

$$\eta_{\text{app.}} = \tau / \dot{\gamma} \quad \dots (2.8)$$

The fundamental unit of viscosity is the poise. A material requiring a shear stress of one dyne per square centimeter to produce a shear rate of s^{-1} has a viscosity of one poise. One (Pa.s) equal 10 poise [16, 17, and 18].

2.5 The General Form of the Viscosity Curve for Suspensions.

The general viscosity/shear rate curve for all suspensions is shown schematically in figure 2-5. The first Newtonian plateau at low shear rate is followed by the power-law shear-thinning region and then by a flattening-out to the upper (second) Newtonian plateau. At some point, usually in this upper Newtonian region, there can be an increase in viscosity for suspensions of solid particles, given the appropriate conditions. In certain situations, the first Newtonian plateau is sometimes so high as to be inaccessible to measurement.

In such cases, the low-shear rate behavior is often described by an apparent yield stress. The factors controlling the details of the general flow curve in particular cases will now be considered. One point worth stressing here is that the relevant measure of the amount of material suspended in the liquid is that

fraction of space of the total suspension that is occupied by the suspended material.

This is the volume-per-volume fraction, and not the weight-per-weight fraction that is often used in defining concentration. The reason why phase volume is so important is that the rheology depends largely on the hydrodynamic forces, which act on the surface of particles or aggregates of particles, generally irrespective of the particle density [14].

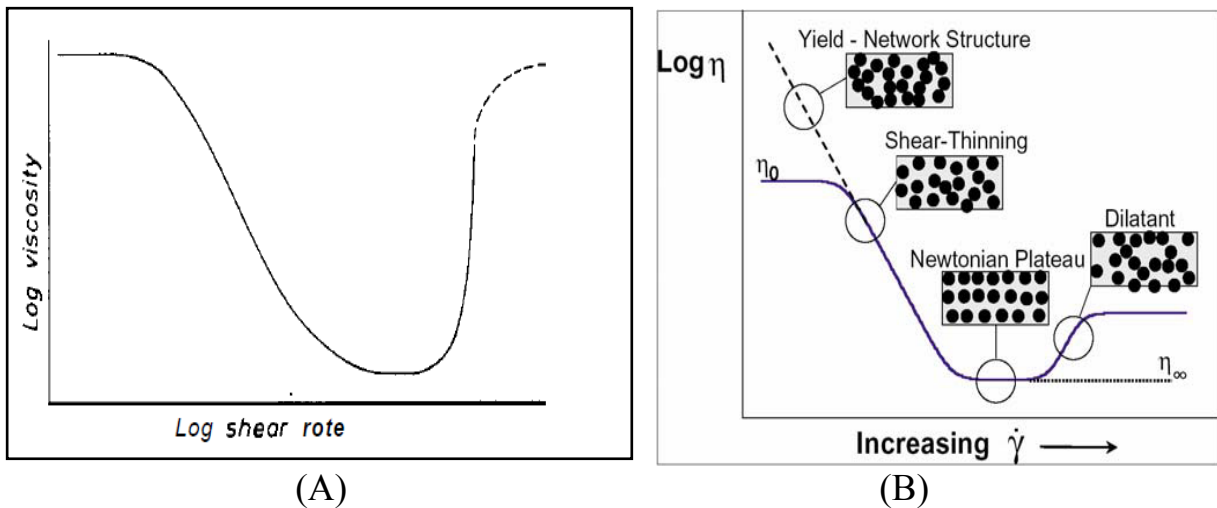


Figure 2-5 Schematic Representation of the Flow Curve of a Concentrated Suspension (A) [14] and (B) [19].

2.6 The General Form of the Viscosity Curve for Polymer Solution.

The viscosity curve for polymer solution will exhibit Newtonian behavior at extreme shear rates, both low and high. For such fluids, when the apparent viscosity is plotted against log shear rate, we see a curve like figure 2-6 [20].

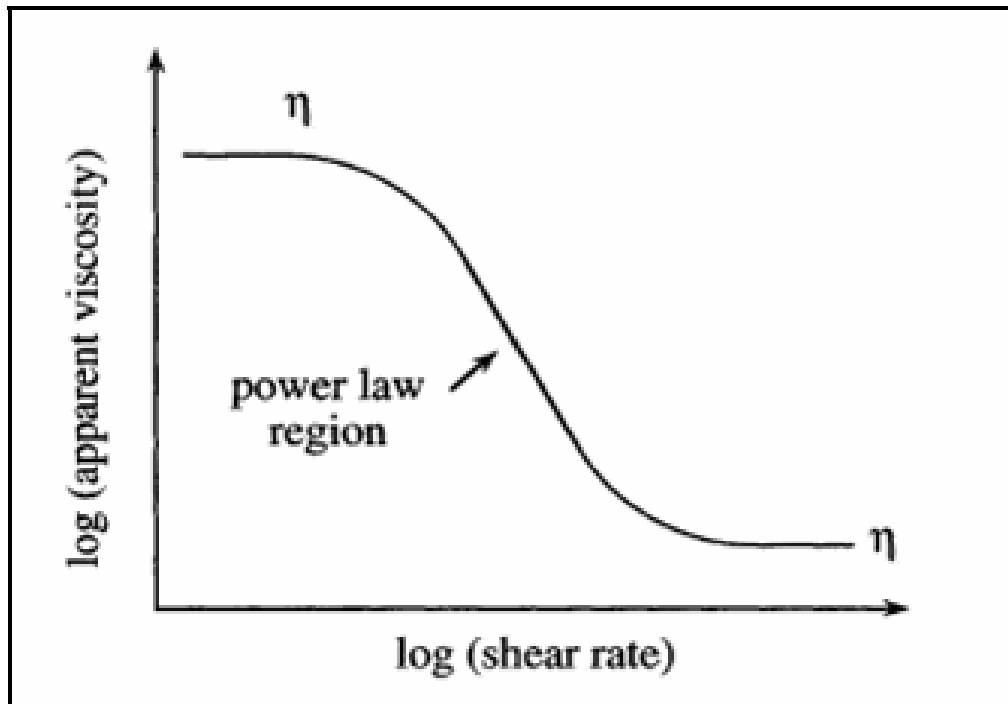


Figure 2-6 Schematic Representation of The Flow Curve of Polymer Solutions [21].

Three regions may be distinguished [21]:

1. Constant-viscosity region in which the behavior of the solution is Newtonian. This region is associated with low shear rates and/or low concentrations.
2. Transition region, which corresponds to the polymer molecules undergoing deformation due to the effect of the increasing shear rate.
3. Region in which the viscosity decreases as the shear rate increases. The greater the shear, the more the molecular chains orient in the flow direction. The behavior of the solution is pseudo plastic.

2.7 Newtonian Fluids.

Newton deduced that the viscosity of a given liquid should be constant at any particular temperature and pressure and independent of the rate of shear, as illustrated in figure 2-7 below. In such “Newtonian fluids”, shear stress is directly proportional to rate of shear.

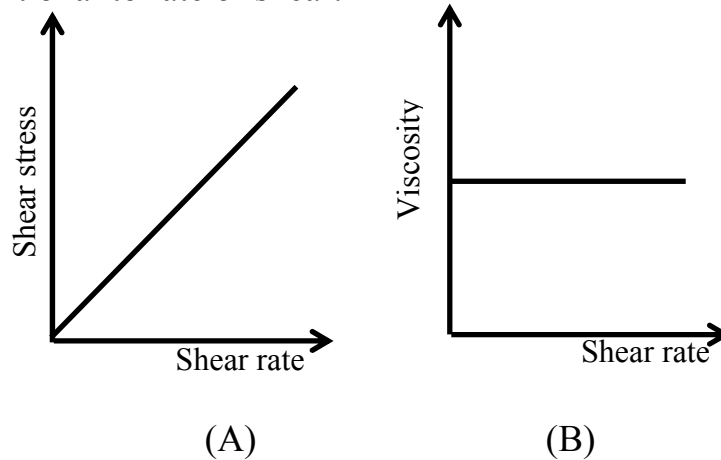


Figure 2-7 Characteristics of Newtonian Liquids (A) Shear Stress is Directly Proportional to Rate of Shear. (B) Viscosity is Independent of Rate of Shear [8].

Newtonian fluids have direct proportionality between shear stress and shear rate in laminar flow.

$$\tau = \eta \cdot (dv/dy) = \eta \cdot \gamma^\circ \quad \dots (2.9)$$

The proportionality constant is thus equal to the viscosity of the material. The flow curve, which is a plot of shear stress versus shear rate, will therefore be a straight line with slope η for a Newtonian fluid. The viscosity curve, which is a plot of viscosity versus shear rate, will show a straight line at a constant value equal to η .

A Newtonian fluid can therefore be defined by a single viscosity value at a specified temperature. Water, mineral, vegetable oils and pure sucrose solutions are examples of Newtonian fluids [22].

2.8 Non-Newtonian Fluid.

A non-Newtonian fluid is characterized by not having a unique value for viscosity. The viscosity of these fluids will depend on the shear rate applied. Any fluid that does not obey the Newtonian relationship between the shear stress and shear rate is called non-Newtonian. The subject of “Rheology” is devoted to the study of the behavior of such fluids. High molecular weight liquids which include polymer melts and solutions of polymers, as well as liquids in which fine particles are suspended (slurries and pastes), are usually non-Newtonian.

In this case, the slope of the shear stress versus shear rate curve will not be constant as we change the shear rate. When the viscosity decreases with increasing shear rate, we call the fluid shear thinning. In the opposite case where the viscosity increases as the fluid is subjected to a higher shear rate, the fluid is called shear thickening. Shear-thinning behavior is more common than shear-thickening [23].

The measured viscosity is the apparent viscosity. In the category of non-Newtonian fluids, one can include most dispersions, blood etc. The viscosity is function of the shear rate. The complexity of the microstructure of the system is influencing the viscosity measurements. If shear forces are applied, the structure of the material may change, therefore the viscosity is changing. Rheology can be used to learn about the dispersions’ microstructure [5, 10]. In equation (2.5), time reflects the structural changes.

$$\eta = \eta(\dot{\gamma}, \text{Time}) \quad \dots (2.10)$$

There are several types of non-Newtonian flow behavior and they are characterized by the way a fluid's viscosity changes in response to variations in shear rate. The most common types of non-Newtonian fluids you may encounter include:

2. 8 .1 Non-Newtonian Fluids-Time Independent.

2. 8 .1 .1 Pseudo Plastic (Shear-Thinning) Behavior.

One of the reasons for shear thinning behavior lies in the alignment of particles with the flow of the slurry, as stated before. Figure 2-8 illustrates these phenomena. Breaking down of structures is another important reason for shear thinning, figure 2-9. Because of electrical charges, polymer particles tend to form structures. Resistance to flow of particles is lower than that of structures. Also water phase can be partly locked inside the structures. When freed, this water lubricates the flow, decreasing viscosity [16].

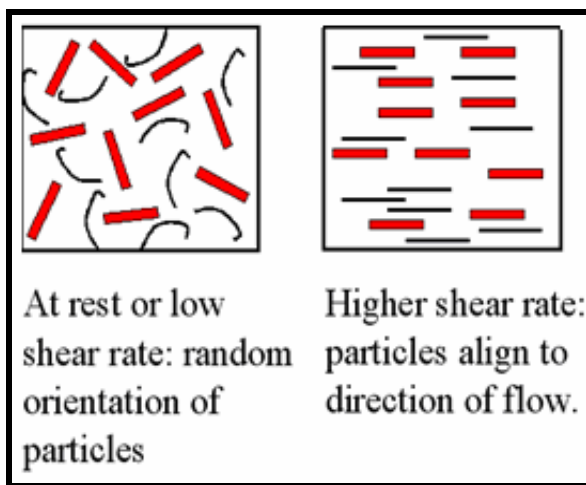


Figure 2-8 Alignment of particles [19].

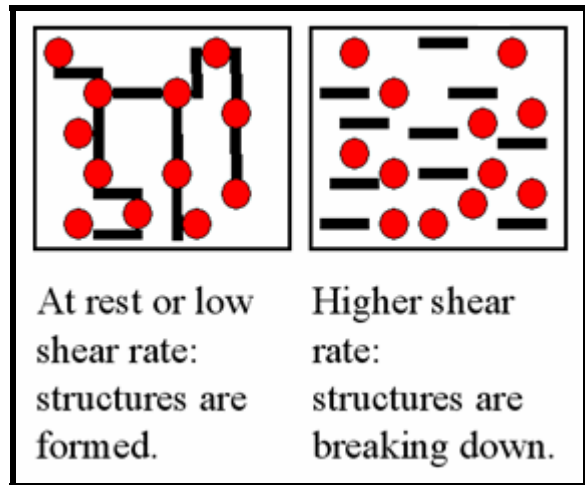


Figure 2-9 Breaking Down of Particles [19].

If the critical shear rate $\dot{\gamma}_c$ is greater than shear rate, the repulsive interactions is greater than hydrodynamic forces. The structure of shear-thinning behavior at rest while flowing is shown in figure 2-10.

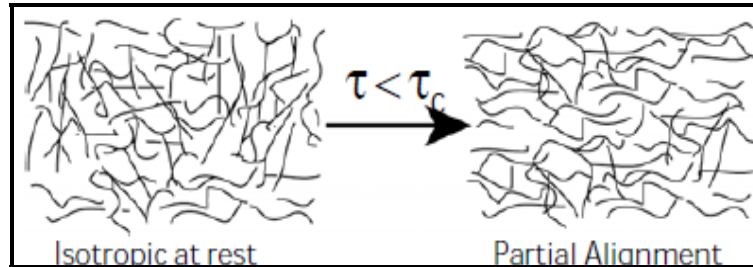


Figure 2-10 The Structure of Shear Thinning Behavior [24].

In this case, fluid displays a decreasing viscosity with an increasing shear rate as shown in figure 2-11.

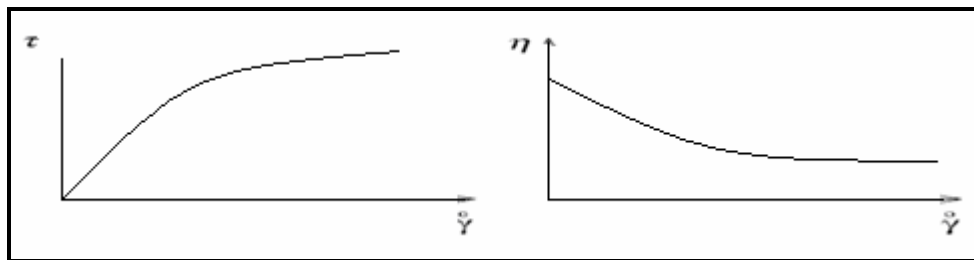


Figure 2-11 τ versus $\dot{\gamma}$, η versus $\dot{\gamma}$ in Shear Thinning Behavior [25].

Power law model describing flow behavior of shear thinning is given below [7]:

$$\tau = k (\dot{\gamma}^o)^n \quad n < 1 \quad \dots (2.11)$$

2.8.1.2 Dilatants (Shear – Thickening) Behavior.

In solid suspensions, shear thickening occurs due to rearrangements in the microstructure evoked by shear. When shear rate is increased further, the flow is disturbed and particles cause more friction between one another. In figure 2-12a (at rest) the particles are closely packed and the figure 2-12b at (flowing material), layers have different velocity [19].

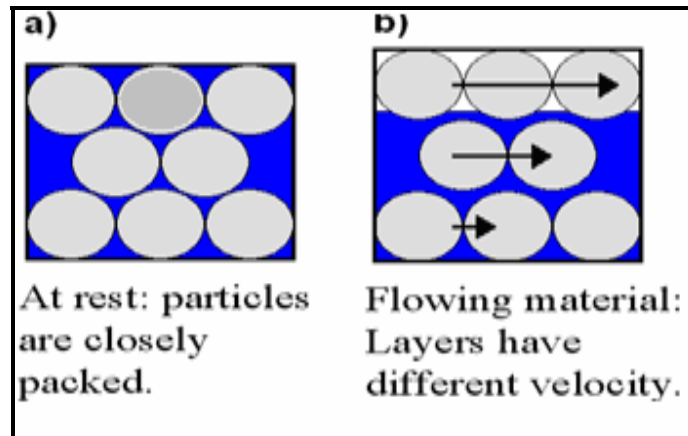


Figure 2-12 Packing of Particles [19].

If the critical shear rate $\dot{\gamma}_c$ is less than shear rate, the repulsive interactions and hydrodynamic forces is balance. The structure of shear-thickening behavior is shown in figure 2-13.

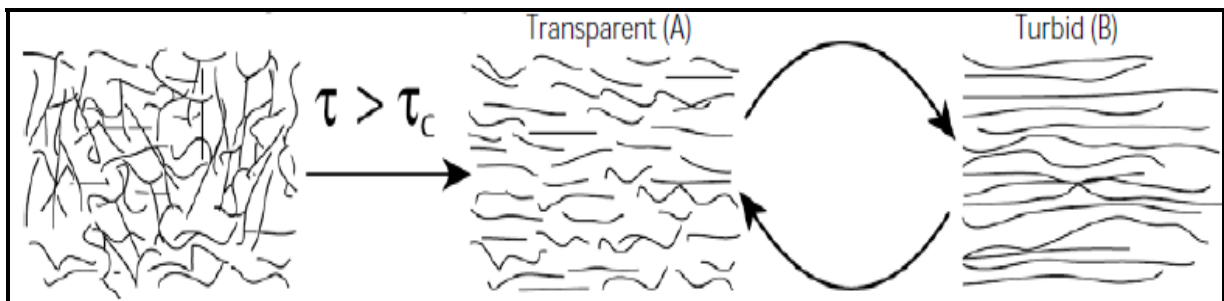


Figure 2-13 The Structure of Shear Thickening Behavior [24].

An increasing viscosity characterizes dilatants fluids with an increase in shear rate. Examples are some particulate solutions such as clay slurries and cornstarch in water etc. The figure 2-14 illustrates the shear stress versus shear rate and apparent viscosity versus shear rate in the shear thickening behavior.

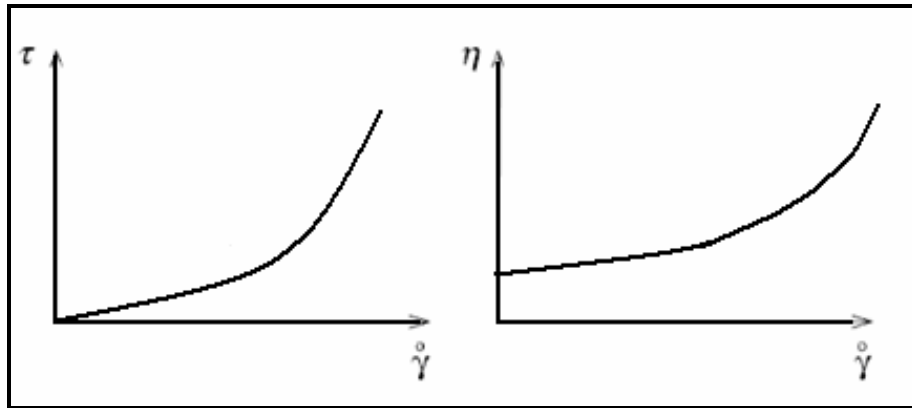


Figure 2-14 τ versus $\dot{\gamma}$ and η versus $\dot{\gamma}$ in Shear Thickening Behavior [25].

Power law model describing flow behavior of shear thickening is given below [8]:

$$\tau = k (\dot{\gamma})^n \quad n > 1 \quad \dots (2.12)$$

2.8.1.3 Bingham Behavior.

The yield stress in fluids can be defined as the stress (the shear force per unit area) going to a finite nonzero value, the yield stress, while the shear rate (velocity gradient) goes to zero. In practice, the yield stress is due to the microstructure of the fluid that resists large rearrangements. Because of the effect of the flow on the system's microstructure, it is in fact impossible to unambiguously define a yield stress [4].

In this case, the liquid behaves like a solid under static conditions. A certain amount of force must be applied to the fluid before any flow is induced. This threshold is called the yield stress value. Tomato ketchup is an example of such fluid. Once the yield value is exceeded, flow begins. This fluid flow can display Newtonian, pseudo plastic or dilatants flow characteristics [5]

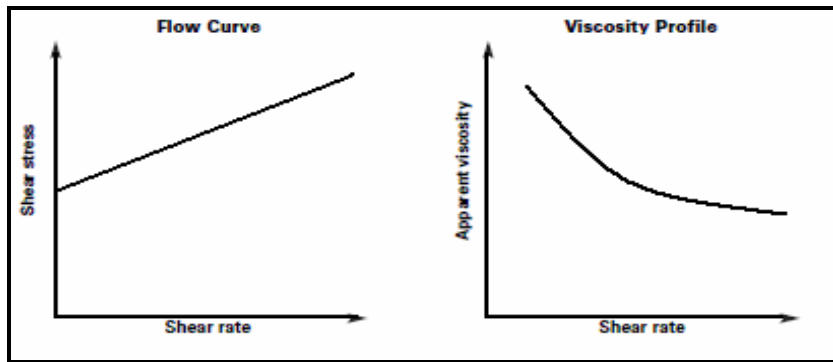


Figure 2-15 τ versus $\dot{\gamma}$ and η versus $\dot{\gamma}$ in Bingham Plastic Model [25].

2.8.2 Non – Newtonian Fluids – Time Dependent.

Some fluids display a change in viscosity with time, under conditions of constant shear rate. Time-dependent fluid behavior may be further subdivided into two categories: thixotropy and rheopectic or negative thixotropy [10].

2.8.2.1 Thixotropic fluids.

In this case, the fluid undergoes a decrease in viscosity with time, while it is subject to constant shearing as shown in figure 2-16. An example is greases. It is known from practice that non-dripping paint can flow with decreasing viscosity upon stirring in the paint-pot. Such behavior, where systems that look rather solid like but upon stirring become liquid like, with decreasing viscosity, is called thixotropy.

At rest, the viscosity increases again, so the paint does not form drips at the wall. Quicksand is also a well-known example of thixotropy: the movements of victim simply decrease the viscosity of the trap and worsen his troubles. The behavior of non-Newtonian fluids is often the result of special structures (networks, colloidal crystals) that are disturbed upon loading. At rest the structures are building up again and consequently the viscosity increases again.

If the structure disturbance and build up need some time, then the viscosity is decreasing or increasing with time upon loading or release, respectively [5, 10].

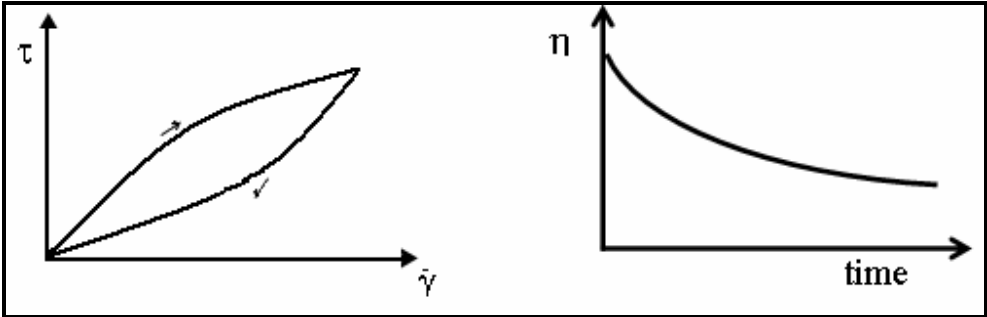


Figure 2-16 Viscosity Dependence on Time for Thixotropic Fluids [5].

2.8.2.2 Rheopectic fluids.

In this case the fluid’s viscosity increases with time as it sheared at a constant rate as shown in figure 2-17. A rheopectic liquid exhibit a behavior opposite to that of a thixotropic liquid, i.e. the apparent viscosity of the liquid will increase over time at a constant shear rate. Once the shear stress is removed, the apparent viscosity gradually decreases and returns to its original value. Rheopectic fluids are rare. Examples include specific printer’s inks [26].

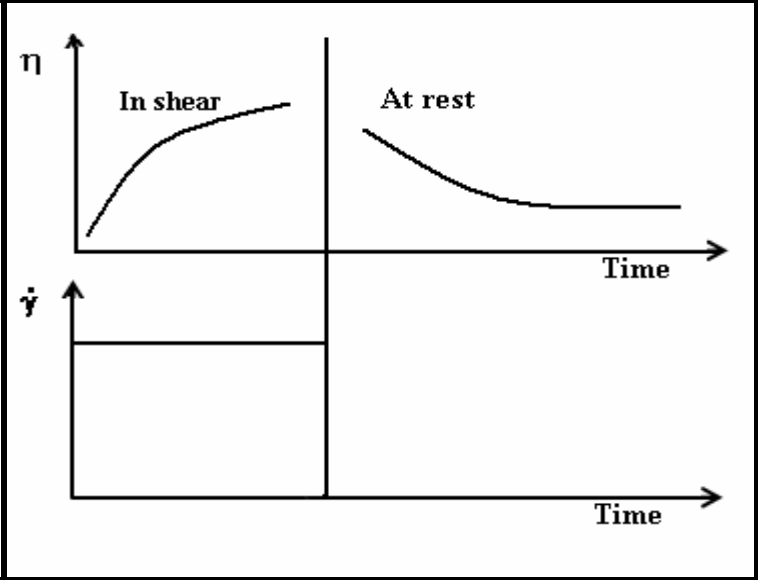


Figure 2-17 Viscosity and Shear Rate Dependence on Time for Rheopectic Fluids [8].

2.9 Water Soluble Polymers.

Polymers are large organic molecules composed of seed extracts (guar, starch), modified cellulose (CMC, HEC), biosynthetic gums (Xanthan), and synthetic polymers (PVA) [27].

The simple molecules, from which polymers are formed, are called monomer that is containing primarily of compounds of carbon. To function as monomer, a compound must have at least two reactive sites at which other monomer units can be joined.

Polymers are either linear or branch. In linear polymers, the macromolecule is a long single chain of monomer units. The linear polymers are either "homopolymers" which are containing repeat units of only one chemical composition, or "copolymers" which are containing two or more repeating units, where they have a different chemical composition. For branch polymers, their chains branch off from each other [28].

The selection of best polymer for a certain application depends on the cost of the polymer and on the performance of the polymer

2.10 Cellulose and Cellulose Derivatives

Cellulose is a widely used organic polymer. It is extracted from wood and other vegetable products. Wood contains 40 to 50% cellulose [29]. Cellulose is insoluble in water due to strong hydrogen bonding. Thus, water particles do not penetrate the solid particles of cellulose. An accorded, chemical modification is required to these polymers to become soluble in water. The most important kinds of chemically modified cellulose are: CMC and HEC polymers.

2.11 Polymer Solutions.

Polymer molecules are long chain molecules composed of many repeating units. The bonds along the polymer backbone are continually rotating, and as a result, the molecule itself is continually changing orientation and configuration on a length scale much smaller than the equilibrium size. Polymer solutions can be considered as liquid mixtures made of long macromolecular chains, and small, light molecules of solvent [27].

Polymer solutions, in general exhibit non-Newtonian pseudo plastic behavior i.e., its viscosity decreases with increasing shear rate. At rest, the chains of polymers are randomly entangled, but they do not set up a structure because the electrostatic forces and predominately repulsive when the fluid is in motion, the chains tend to align themselves parallel to the direction of flow, this tendency increases with increase in shear rate, so that the effective viscosity decreases [30].

The solution viscosity of the polymers being compared must be obtained under the same conditions of shear rate, shear stress, temperatures and polymer concentration. The choice of the best polymer for a given application depends on the both economic and performance considerations. Polymer solution properties that effect performance include solution viscosity in the solvent to be used (formation fluids can be very important).

2.11.1 Solubility of Polymer.

It should be pointed out that not all polymers can be dissolved, and even though when they can, the dissolution process may take up to several days or weeks.

The dissolution of polymers depends not only on their physical properties, but also on their chemical structure, such as polarity, molecular weight, branching, cross-linking degree, and crystallinity. Polar macromolecules like poly (acrylic acid), poly (acryl amide) and polyvinyl alcohol, among others, are soluble in water. Conversely, non-polar polymers or polymer showing a low polarity such as polystyrene, poly (methyl methacrylate), poly (vinyl chloride), and poly (isobutylene), are soluble in non-polar solvents. Chains containing long branches, cause dense entanglements making the penetration of solvent molecule difficult. Therefore, the rate of dissolution in these cases becomes slower than if it was short branching, where the interaction between chains is practically non-existent [31].

There are two stages involved in the dissolution process: the first is the polymer swelling and the second is the dissolution step itself. When a polymer is added to a given solvent, attraction as well as dispersion forces begin acting between its segments, according to their polarity, chemical characteristics, and solubility parameter. If the polymer solvent interactions are higher than the polymer-polymer attraction forces, the chain segment start to absorb solvent molecules, increasing the volume of the polymer matrix, and loosening out from their coiled shape. The segments are now "solvated" instead of "aggregated", as they were in the solid state [27].

The completely “solvation-unfolding-swelling” process takes a long time, and is influenced only by the polymer-solvent interactions; stirring plays no role in this case. However, it is desirable to start with fine powdered material, in order to expose more of their area for polymer-solvent interactions. The "solvation-unfolding-swelling" process will continue until all segments are solvated. Thus, the whole loosened coil will diffuse out of the swollen polymer, dispersing into a solution. At this stage, the disintegration of the swollen mass can be favored by stirring, which increases the rate of dissolution. The polymer coil, along with solvent molecules held within, adopts a spheric or ellipsoid form, occupying a volume known as hydrodynamic volume of the polymer coil [27].

2.11.2 Dilute and Concentrated Polymer Solutions.

Dilute solutions are those in which each polymer chain is believed (or assumed) to be completely isolated from the other polymer chains, and forms a coil at equilibrium. When the concentration is increased polymer molecules begin to interact by becoming entangled. The concentration (known as the critical concentration) required for a solution to become entangled will decrease as the molecule becomes longer and occupies a larger equilibrium volume.

In response to a deformation, the polymer molecule itself can change both its shape and orientation. In dilute solutions, the rheology of the solution is dependent solely on the dynamics of an individual chain and the number of chains (i.e. the concentration) in the system. At higher concentrations in the entangled region, interactions between polymer molecules due to entanglements impact the rheology in a significant way [27].

There is no interaction at all between the dissolved coils in dilute solutions. Even when the solution is highly viscous, such coils remain as unique entities moving freely among the solvent molecules, without exerting forces of any kind on each other. Consequently, no links can be established between them.

The situation is different in concentrated solutions. As the number of molecules is increased, they are forced to come closer and interaction between them turns noticeable. The summation of intermolecular forces becomes a key factor.

Therefore, the viscosity increases drastically, and the solution begins to exhibit a transition from a concentrated solution to a gel, because such coils will establish linkages at some points, constituting gradually an only giant cross linked coil, called a macroscopic gel. Such macroscopic gel showing the cross-links as solid circles [27]

2.12 Previous Works

In this section, we will focus on the recent works that studied the rheology of polymer solutions, solid suspension and mixed of these materials.

Alloncle, et al. (1989) [32], studied a rheological characterization of Cereal Starch-Galactomannan Mixtures. The aim of the investigation is to describe the rheology of cereal starch/galactomannan mixtures on a similar basis, assuming the hydrocolloid located mainly inside the continuous phase. Viscosity measurements (on starch pastes, gum solutions, and blends) were performed using a coaxial-cylinders viscometer (Rheomat 30, Contraves, Zurich) with the following specifications for the cylinders: internal radius, 22.9 mm; external radius, 24.2 mm; height, 56.5 mm.

Flow curves of these starch-galactomannans mixtures were compared with the curves obtained from starch or galactomannans alone. A strong synergistic effect was observed, resulting in a dramatic increase in the viscosity of the mixtures compared with starch or galactomannan alone. A simple model was proposed to interpret such effects. Because starch pastes are described as suspensions of swollen particles dispersed in a macromolecular medium, it was suggested that galactomannans are located within the continuous phase. Thus, the volume of this phase, accessible to the galactomannan, was therefore reduced. This yielded an increase of the galactomannan concentration within the continuous phase and a dramatic increase in the viscosity of the continuous medium owing to the thickening properties of this polysaccharide. Because the overall viscosity of a suspension depends upon the viscosity of the continuous phase as well as on the volume fraction of the dispersed phase, the respective contribution of each phase could be estimated. Validity of this model was supported by experiments where the galactomannan concentration in the continuous medium was kept constant (1%) while the volume fraction of the dispersed phase was varied between (0.1 and 0.9).

Hassan (1992) [33], studied viscometric behavior of single strength and concentrated Date-Water Extracts.

Viscometric behavior of single strength and concentrated date-water extracts of the cultivar anbari was experimentally investigated using a concentric cylinders rotational viscometer (A Haake viscometer, model viscotester VT.181). The date-water extracts in the concentration range 22.5% - 78.5%, temperature range 24.0 – 95.0 °C, and shear rate range 2.5 – 979.0 s⁻¹, exhibited shear

thinning behavior (pseudoplastic), evident from the consistent decrease of viscosity with increasing shear rate.

Viscosity of all concentrations within the temperature and shear rate ranges investigated was in the range 1.08 – 5622.61 (mPa.s). The power law model described adequately the flow behavior of the data-water extracts at various concentration and temperature. The flow index (n) and the consistency index (k) were within the ranges 0.57 – 0.98, and 6.49 – 5720 mPa. s ^{n} , respectively.

Petroyl and Denkoyski (1995) [34], studied the power law for some polyacrylonitrile solutions. In this study, concentrated solutions of a ternary copolymer of acrylonitrile methyl acrylate and itaconic acid, in aqueous NaSCN (51%) solution were used. The data from the measuring performed with rotational viscometer "HAAKE" RV-3, MK 500. The flow index (n) decreases and the coefficient of consistency (k) increases when $\dot{\gamma}$ increased but due to the complexity of the dependence, this results in the decrease of η_a as $\dot{\gamma}$ increases.

The increase of the temperature of the solution was always accompanied by a decrease of its viscosity. This could be connected to decrease of the anomaly of the viscosity as temperature increases and may be explained with the disintegration of the elements of the structure and the macromolecular nets in the solution under the action of the heat fluctuations that result in viscosity decrease.

Rossi, et al. (1997) [35], studied the influence of low molecular weight polymers on the rheology of bentonite suspension. The objective of this work was to determine the effect of relatively low molecular weight non-ionic polymers on the rheological behaviour of bentonite suspensions. Finally, some

preliminary measurements have made at high temperature and high pressure for bentonite alone and a bentonite/polyethylene oxide system.

The rheological properties were measured at room 25, $\pm 0.1^\circ\text{C}$ for both steady state and oscillatory measurements. The rheological properties were measured in two rheometer, A Bohlin VOR rheometer and Haake Searle type HTHP. It was possible to measure pressures up to 1000 bar and temperatures up to 150°C . The shear range was between $(0.1-1160) \text{ s}^{-1}$ and $(0-1130) \text{ s}^{-1}$. The flow curves were analyzed and fitted to the bingham model and the Herschel-Bulkley model ($\tau = \tau_B + \eta_{pl} \dot{\gamma}$), ($\tau = \tau_y + k \dot{\gamma}^n$) respectively.

The Bingham yield stress values for the high polymer contents were found to be higher than the suspension without polymer and the plastic viscosity increased with increase in polymer content. The values of the elastic G' and storage G'' modules as a function of polymer concentration G' was significantly higher than G'' indicating that the suspension was highly elastic.

It was found that, the rheological properties were increased (η and n) with increased pressure in the system while decreasing (τ and k) and the temperature affected the system. the shear stress increase with increasing temperature.

Hadar and Keren (2002) [36], studied anionic polyacrylamide polymers (PAM) effect on rheological behavior of sodium-montmorillonite suspensions.

The aim of the study was to determine the effects of molecular weight (MW) and degrees of hydrolysis (DH) of anionic PAM on the rheological properties of Na-montmorillonite suspensions at various electrolyte concentrations.

The rheological measurements for the Na-montmorillonite suspensions were performed with a commercial couette-type viscometer with an outer rotating cylinder and a stationary inner cylinder (Haake Model RV2, Sensor system CV20). The gap between the outer cylinder housing was temperature controlled at $25.0 \pm 0.2^\circ\text{C}$. The measurements were carried out at shear rates of (0 to 1000) s^{-1} during 2 min. The flow curves were analyzed and fitted to the Bingham model and the power law model.

Rheological measurements were found to be a useful tool in determining the effectiveness of anionic PAM in modifying the interactions between clay particles in suspensions. The effectiveness of the polymers was depended upon their MW and DH. These results suggest that high MW and high DH of negative PAM together with low electrolyte concentration in soil solution could be more effective in soil aggregate stabilization than those with lower MW and DH.

David and Blakey (2004) [37], compared the rheologies of laterite and goethite suspensions.

The comparisons in this study show distinct differences in the rheology of laterite and goethite suspensions. At the same solid volume concentration, the goethite suspensions were much more viscous and have much higher yield stresses. The rheometer was a Haake RV30 viscometer with a couette fixture. The rheometer worked with range (100 - 1000) s^{-1} . The instrument was capable of generating step changes and ramp sequences in shear rate, in addition to normal steady shear rate. This rheometer cannot measure G' and G'' , the usual properties to characterize the dynamic response of a fluid.

The viscosity of a goethite suspension was found to be about ten times than that of a laterite suspension at the same concentration. This finding may be unexpected in view of the higher aspect ratio for laterite particles.

Alemdar, et al. (2005) [38], studied the effect of polyethylene (PEI) adsorption on of bentonite suspension.

The addition of PEI at concentration ranges of 10^{-5} – 4.5 g/l to the slurry of stability of bentonite suspensions (2%, w/w). The rheological parameters (viscosity, shear stress, yield value) of clay suspensions may often reflect particle–particle interactions. The magnitude of the attractive and repulsive forces between clay particles was determined by physical and chemical properties of the bentonite–water systems. The polymers in the bentonite suspensions interact with clay particles according to their ionic or non-ionic character. The ionic polymers induced electrostatic interactions, but the non-ionic polymers were adsorbed on the surface of clay minerals by the steric interactions. Polymer concentration, its molecular weight and hydrolysis groups of polymer, size and shape of clay particle, its surface charge and clay concentration in suspension, pH, and temperature may all affect the clay/polymer interactions.

The rheological parameters of the dispersions were measured in a Brookfield DVIII type low-shear viscometer in laboratory conditions. Increase in PEI concentration led to a decrease in the flocculation of dispersion probably due to the repulsions between positive charges on the clay surface at higher PEI concentrations.

Tapadia and Wang (2006) [39], studied direct visualization of continuous simple shear in non-Newtonian polymeric fluids. A particle tracking velocimetric technique was used to study the rheological properties (10 wt% 1, 4-polybutadiene (PBD) solution).

They showed a direct evidence of nonlinear velocity profiles during simple-shear flow of an entangled polymer solution, offering a new insight into of such characteristics as stress overshoot. They used a particle tracking velocimetry that send a laser beam along the velocity gradient direction through the gap between cone and plate and they video recorded the illuminated moving particles over time with CCD camera facing the gap as shown in figure 2-18.

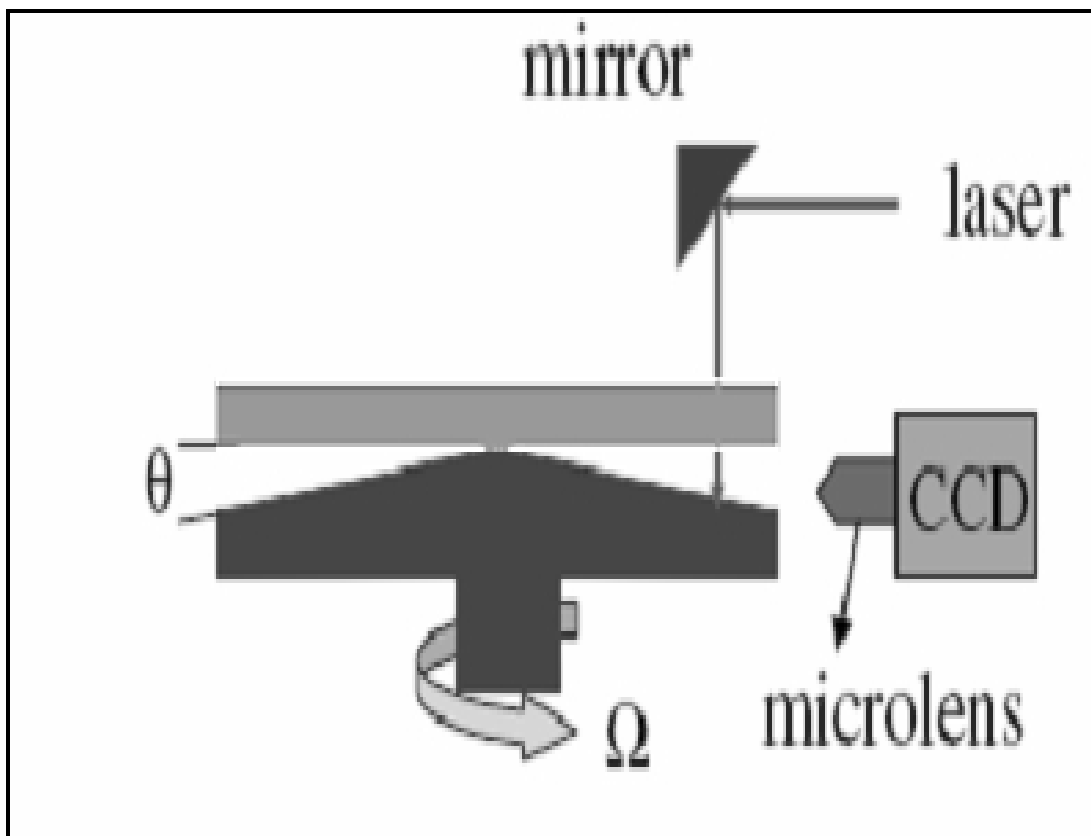


Figure 2-18 The Setup of The Particle Tracking Velocimetry [39].

S. İşçi, et al. (2006) [7], studied the rheology and structure of aqueous bentonite-polyvinyl alcohol dispersions.

The influence of polymer on flow behavior of Balıkesir, Turkey bentonite dispersion (2% w/w) was studied for Non-ionic polymer, polyvinyl alcohol (PVA).

PVA in a range of 3.3×10^{-6} – 3.3×10^{-5} mol/l was added to the bentonite dispersions in different concentrations and its behavior was observed on rheology parameters. The data were interpreted taking into account the interactions of colloidal clay particles, bentonitic clay concentrations, structure, and concentrations of added PVA. The particle size analysis was explained by surface orientation of PVA to the clay particles dispersed in aqueous solution. Zeta potential determination also emphasized that PVA molecules were attached on the face and edge surface of clay particles.

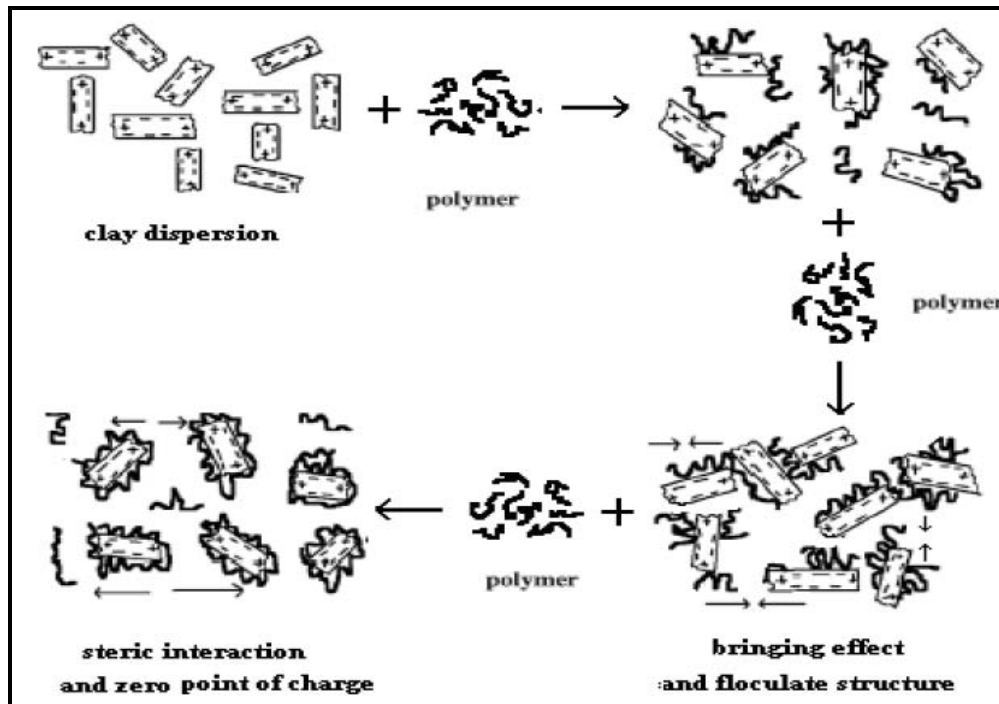


Figure 2-19 Schematic Representation of Adsorption of PVA Polymer on Bentonite Particles as a Function of Concentration of Polymer [7].

Figure 2-19 shows a schematic representation of adsorption of PVA polymer on bentonite particles as a function of concentration of polymer. Increasing concentration of PVA resulted in a decrease in the zeta potential value of the bentonite dispersions. This decrease in the zeta revealed that PVA molecules attached on the net negatively charged clay particles. As the adsorbed amount increased, zeta potential reached zero point, and with further adsorption, zeta potential became a positive.

Song, et al. (2006) [40], studied xanthan gum solutions for oscillatory shear flow behavior.

In this study they used a strain-controlled rheometer [Advanced Rheometric Expansion System (ARES)]. Both the strain amplitude and the concentration dependencies of dynamic viscoelastic behavior were firstly reported at full length from the experimental data obtained from strain tests. Secondly, the linear viscoelastic behavior was explained in detail and the effects of angular frequency and concentration on this behavior were discussed using the well-known power law type. Finally, a fractional derived model originally developed by Ma and Barbosa-Canovas (1996) was employed to make a quantitative description of a linear viscoelastic behavior and then the applicability of this model was examined with brief comment on its limitations.

They concluded that xanthan gum solutions did not form a chemically cross-linked stable (strong) gel but exhibited weak gel-like behavior, regarded as a highly elastic liquid over a wide range of time scale. In addition, they concluded that a fractional derived model might be attractive means for

predicting a linear viscoelastic behavior of concentrated Xanthan gum solutions. However, this model may be classified as a semi-empirical relationship because there existed no real physical meaning for the model parameters.

Sarraf and Havrda (2007) [41], studied rheological behavior of concentrated alumina suspension (effect of electrosteric stabilization).

The aim of this study was to investigate the rheological behavior of highly (43 Vol. %) concentrated sub-micron α -Al₂O₃ aqueous suspensions containing different amounts of electrosteric polyelectrolyte (Dolapix CE64) as dispersant. A concentric cylindrical Rheometer (Thermo HAAKE Ltd., Sensor Z41-DIN measurement system, RV1) was used. The flow curves were automatically recorded via a built-in program at a particular temperature $23 \pm 1^\circ\text{C}$.

It was found that in an aqueous alumina/dispersant system, as the amount of dispersant increased up to its optimum, the viscosity and yield stress of the suspension decreased. The flow curves of alumina suspensions illustrated typical shear-thinning behavior and were fitted satisfactorily to the power law, Herschel-Bulkley and Bingham models. The application of various flow models on the alumina systems confirmed that the optimum dispersant concentration which will impart the minimum viscosity to prepare stable suspensions is 0.4 wt% of Dolapix CE64. Finally, the results obtained from rheological measurements indicated that dispersant Dolapix CE64 had great efficiency in electrosterically dispersing of concentrated alumina suspension and enables the preparation of lower viscous suspensions, suitable for colloidal processing such as slip-casting.

Liu, et al. [2007] [42], studied the rheological behaviors of Polyacrylonitrile /1-Butyl-3-Methylimidazolium Chloride [(PAN)/ ([BMIM] Cl)] concentrated solutions.

One of the room temperature ionic liquids, 1-butyl-3-methylimidazolium chloride ([BMIM] Cl) was chosen to prepare the concentrated solutions of Polyacrylonitrile (PAN).

Steady state rheological measurements were performed on a HAAKE RS150L rotational rheometer using a 35 mm, 1° cone and plate. The shear rate was linearly increased from (0.01 to 1000) s⁻¹ without oscillation. Dynamic rheological measurements were performed on a TA ARES-RFS rotational rheometer. Under different conditions, including temperatures, concentration, and molecular weight of PAN, the solutions exhibited shear-thinning behaviors. The viscosities decreased with the increasing of shear rates according to the so-called power law equation:

$$\tau = K \cdot \dot{\gamma}^n \quad \text{or} \quad \eta_{ap} = K \dot{\gamma}^{n-1}$$

Where K and n are constants. For pseudo plastic liquids the viscosity should decrease nearly linearly with shear rate on the log-log plot and the value of n is less than one. However, the viscosity decreased sharply at high shear rates when the concentration was up to 16 wt%. The dependence of the viscosity on temperature was analyzed through the determination of the apparent activation energy (Arenac equation). Unusually, the viscosity of solutions of higher concentration is lower than that of lower concentration. Similarly, the viscosity of low molecular weight PAN was higher than high molecular weight PAN at high shear rates. The dynamic rheological measurement indicated that the loss modulus was much higher than storage modulus. The trend of complex viscosity was similar with the result of static rheological measurement.

Deosarkar and Ghanta [2008] [43], studied rheological characteristics of solid-liquid suspension—comparison between empirical models and artificial neural network (ANN) model.

The aim of the study was to observe the rheological characteristics of magnetite ore suspension in 1.1 % (by weight) carboxymethyl cellulose (CMC) and guar gum solutions and to find a suitable model for the same.

The suspensions had varied particle size of (50- 74.8) μ m. For magnetite ore slurries in aqueous CMC and guar gum solutions, the viscosity of the slurry increased with increase in particle size and solids concentrations.

Solid concentration of 10% 20% and 30 % (by weight) in aqueous CMC and guar gum solution, exhibited pseudo plastic behavior for any particle size studied. The rheological characteristics were determined by programmable rheometer (Brookfield DV-III +).

Experimental results were tested with well-known two-parameter power law model and Bingham plastic model and three parameter Herschel-Bulkley models. Experimental data were found to fit more satisfactorily the power law model as compared to Bingham and Herschel-Bulkley model. Moreover, an attempt also was made to develop artificial neural network (ANN) model for presenting the rheological behavior of the suspension. It was observed that the ANN model predicted the slurry viscosity more accurately than the empirical models. An ANN model was better than the power law model. In representing the rheological behavior of the slurries.

Erin, et al. (2008) [44], studied shear stress measurements of non-spherical particles in high shear rate flows. The behavior of liquid-solid flows varies greatly depending on fluid viscosity; particle and liquid inertia; and collisions and near-collisions between particles. This study was performed for a range of Reynolds numbers, solid fractions and ratio of particle to fluid densities. With neutrally buoyant particles, the dimensional shear stress exhibited a linear dependence on Reynolds number: the slope was monotonic but a non-linear function of the solid fraction. However, non-neutrally buoyant particles exhibited a similar linear dependence at higher Reynolds numbers. At lower values, the shear stress exhibited a non-linear behavior in which the stress increased with decreasing Reynolds number due to particle settling.

Shear stress measurements were made in a coaxial rheometer with a height to gap ratio (b/r^0) of 11.7 and gap to outer radius ratio (h/b) of 0.166 that was specially designed to minimize the effects of secondary flows as shown figure 2-20.

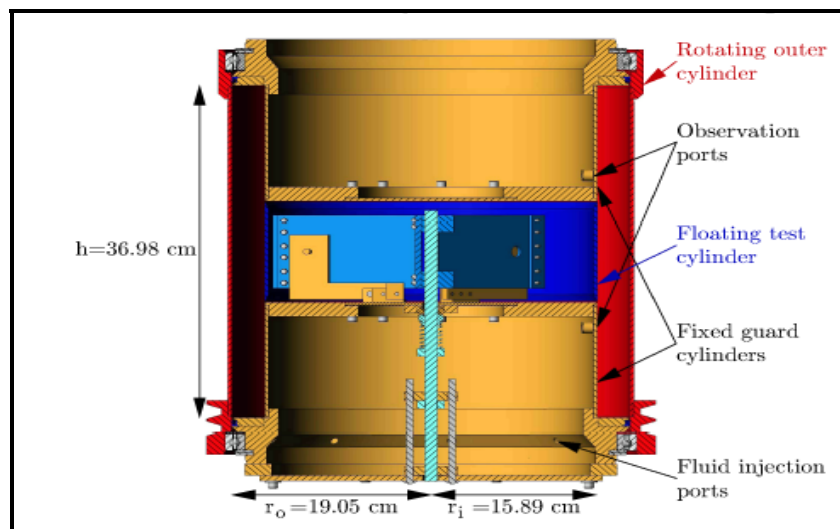


Figure 2-20 Coaxial Rotating Cylinder, Couette Flow Device, the Outer Cylinder (red) Rotates While the Inner Cylinder Remains Fixed [44].

Mohammed and Mohamed, (2008) [45], studied the effect of concentration of water-soluble polymer solutions on rheological properties.

This experimental study of the rheological behavior of polymer solutions. All polymers studied in this work are water soluble and used in industries as rheology control additives (rheology modifiers), these are: XC-polymer, Carboxymethyl cellulose (two types), Hydroxyethyl cellulose and Polyvinyl alcohol. The rheological properties of these polymer solutions was investigated using a Couette coaxial cylinder rotational viscometer (Fann model 35A), by measuring shear stresses versus shear rates (i.e. the flow curve). 55 experiments were performed with different polymer concentrations and at room temperature. By using the Solver Add-in in Microsoft Excel, the power law flow model was found to be the best fits the experimental results. It was found that as polymer concentration increased, the flow behavior index (n) decreased and the consistency index (k) increased. This behavior reflects the fact that as polymer concentration increases, the solution become far from Newtonian. Correlations that describe the effect of polymer concentration on n and k (for each polymer used in this study) was found and presented in a linear and exponential form respectively. In addition, it was found that XC-polymer solutions have a higher viscosity, and its viscosity decreases much more than other polymer solutions used in this study.

Chapter Three

Experimental Work

3.1 Solid Suspension Used.

All solid suspensions studied in this investigation were suspended in distilled water. Three dispersion were used, these are: Bentonite, Graphite and Corn starch as follow:

1. Corn starch used is a commercially available product made by Qingdao Shengda Commercial & Trade Co., Ltd. Specification: Protein< 0.35% , Moisture< 13.5% , pH:5.4 - 6.4.
2. Graphite powder used is a commercially available product in Al Doura refinery (Panzhuhua Panxi Graphite Co., Ltd.). Specification: High purity, low sulphur, low ash, low porosity, low resistivity, high gravity and high carbon content.
3. Bentonite used is a commercially available product made by Comieco Company (Wyoming) (Na⁺ Bentonite Specific gravity equal 2.5).

3.2 Polymers Used.

All polymers studied in this investigation are water soluble and are used in industries as a rheology control additive (rheology modifiers). Four polymers are used in this study, these are: XC-polymer, CMC-Carboxymethyl cellulose, HEC-Hydroxyethyl cellulose and PVA-polyvinyl alcohol, as follow:

1. XC polymer used is a commercially available product supplied from Yongkang Rig china Group Co. (China).
2. HEC used is a commercially available product type Cellosize QP 4400H, supplied from DOW Chemical Company (USA).

3. CMC polymer used is laboratory available product supplied from BDH chemicals Ltd Poole England. Particular size 99.5% passes 60 meshes B.S.
4. The PVA polymer used is Yongan Baohualin Industrial_Development Co., Ltd product.

3.3 Sets of Experiments.

Seventy six experiments were performed to study the rheological properties of the aqueous solutions of polymers and solid suspension used. Experiments were performed at different temperatures. A list of experiments is shown in table 3-1.

Table 3-1 List of all experiments.

Exp.No	Material	Conc.(g/l)	Temp.°C	Exp.No	Material	Conc.(g/l)	Temp.°C
1	CMC	4	20	21	CMC	40	55
2	CMC	7	20	22	XC	4	20
3	CMC	10	20	23	XC	10	20
4	CMC	15	20	24	XC	20	20
5	CMC	20	20	25	XC	30	20
6	CMC	25	20	26	XC	40	20
7	CMC	30	20	27	XC	4	35
8	CMC	35	20	28	XC	10	35
9	CMC	40	20	29	XC	20	35
10	CMC	10	35	30	XC	40	35
11	CMC	15	35	31	XC	4	45
12	CMC	25	35	32	XC	10	45
13	CMC	40	35	33	XC	20	45
14	CMC	10	45	34	XC	40	45
15	CMC	15	45	35	XC	4	55
16	CMC	25	45	36	XC	10	55
17	CMC	40	45	37	XC	20	55
18	CMC	10	55	38	XC	40	55
19	CMC	15	55	39	HEC	4	20
20	CMC	25	55	40	HEC	10	20

Table 3-1 Continued.

Exp. No.	Material	Conc.(g/l)	Temp.°C
41	HEC	20	20
42	HEC	30	20
43	HEC	40	20
44	HEC	10	35
45	HEC	20	35
46	HEC	30	35
47	HEC	40	35
48	HEC	10	45
49	HEC	20	45
50	HEC	30	45
51	HEC	40	45
52	HEC	10	55
53	HEC	20	55
54	HEC	30	55
55	HEC	40	55
56	PVA	2	35
57	PVA	5	35
58	PVA	7	35
59	PVA	10	35
60	Bentonite	50	35
61	Bentonite	80	35
62	Bentonite	120	35
63	Graphite	30	35
64	Graphite	40	35
65	Graphite	70	35
66	Graphite	90	35
67	Corn Starch	300	35
68	Corn Starch	400	35
69	Corn Starch	500	35
70	Corn Starch	600	35
71	Corn Starch	700	35
72	Corn Starch	800	35
73	Bentonite+PVA	40+2	35
74	Bentonite+PVA	40+5	35
75	Bentonite+PVA	40+7	35
76	Bentonite+PVA	40+10	35

3.4 Equipments Used.

The main equipments used in this study are:

1. **Fann VG-viscometer, model 35A figure 3-1.**

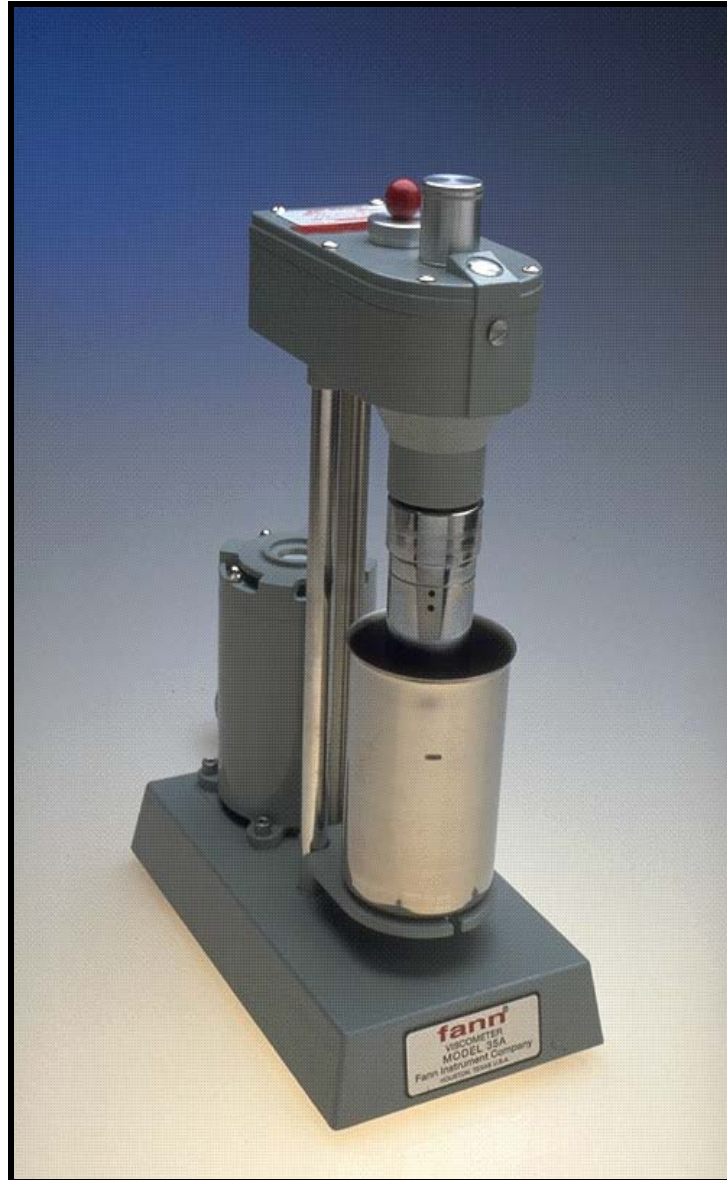


Figure 3-1 Fann VG-Viscometer, Model 35A.

2. **Standard Hamilton Beach Mixer (Specifications):** One spindle, 3 test speeds: (13000, 16000 and 18000) rpm, stainless steel mixing cup and power (supply: 230 V AC / 50 - 60 Hz motor) [46]. Hamilton beach mixer and cup figure 3-2.



Figure 3-3 Hamilton beach mixer and cup.

- 3. Electronic balance.**
- 4. Drying oven.**
- 5. Microwave oven.**
- 6. Hot plate heater.**
- 7. Thermometer (0 – 200 °C)**
- 8. Stop watch.**
- 9. Volumetric flask.**
- 10. Glass beakers (500 ml)**

2.5 Instruments to Measure Rheological Properties.

Most instruments designed to measure viscosity can be classified in two general categories: tube type and rotational type. Figure 3-3 shows the different types of instruments available. The selection of a particular instrument must be based on the type of analysis required and the characteristics of the fluid to be tested. For example, rotational methods are generally more appropriate for non-Newtonian fluids [2].

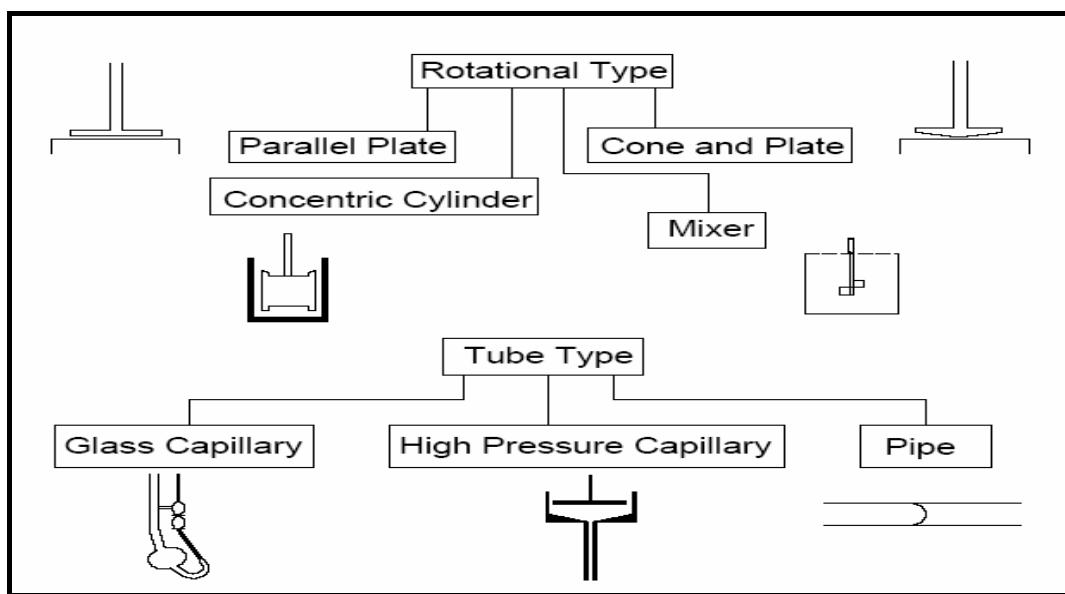


Figure 3-3 Classification of Rheological Instruments [2].

Instruments which measure rheological properties are called rheometers. Viscometer is a more limiting term referring to devices that only measure viscosity. Rotational instruments may be operated in the steady shear (constant angular velocity) or oscillatory (dynamic) mode. Some rotational instruments function in the controlled stress mode facilitating the collection of creep data.

This information is needed to understand the internal structure of materials. The controlled rate mode is most useful in obtaining data required in process engineering calculations [19].

Rotational viscometers consist of two basic parts separated by fluid being tested. The parts may be concentric cylinder (cup and bob), plates, a low angle cone and plate, or a disk paddle or rotor in cylinder. Rotation of one part against the other produces a shearing action on the fluid. The torque required producing a given angular velocity or the angular velocity resulting from a given torque is a measure of the viscosity.

Rotational viscometers are more versatile than other viscometers. They can be used with a wide range of materials because opacity, settling, and non-Newtonian behavior do not cause difficulties. Viscosities over a range of shear rates and as a function of time can be measured. Therefore, they are useful in characterizing shear thinning and time-dependant behavior. Rotational viscometers are considerably more complicated mechanically than most other viscometers [47].

3.6 Viscometer (The Model 35A Viscometer).

Fann model 35A viscometers are versatile instruments for research or production use. They can be used wherever a regulated-frequency power source is available. The model 35A viscometer is widely known as the “**Standard of the Industry**” for drilling fluid viscosity measurements.

In the six-speed models, test speeds of 600, 300, 200, 100, 6 and 3 rpm are available via synchronous motor driving through precision gearing. Any test speed can be selected without stopping rotation. The shear stress is displayed continuously on the calibrated scale.

Specifications of viscometer: operating temperature 0-55 °C, Max. Sample temperature 92 °C and power supply 115 V AC / 60 Hz motor. This instrument has been designed so that viscosity in centipoises of a Newtonian fluid is indicated on the dial with the standard rotor, bob, and torsion spring operating at 300 rpm. Viscosities at other test speeds may be measured by using multipliers of the dial reading [48, 49].

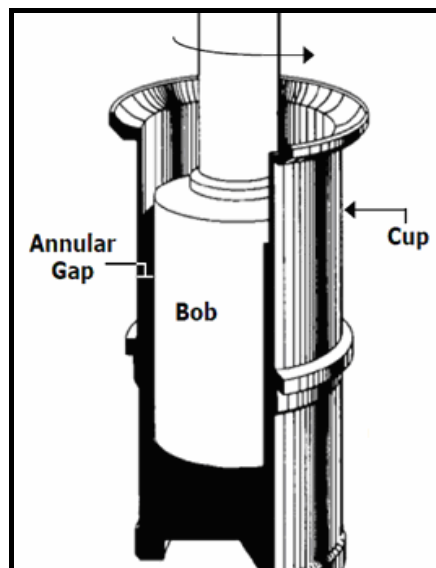


Figure 3-4 The Essential Elements of Rotational Viscometer [49].

3.7 Calibration of Viscometer.

This procedure is used for calibration using only Newtonian certified calibration fluids. Fann calibration fluids are available in nominal 20, 50, 100, 200 and 500 cP. All are traceable to ASTM standards and each bottle of fluid is furnished with a viscosity temperature chart [50].

- a) The instrument must be cleaned before immersing the rotor and bob into the calibration fluid. If necessary the rotor is removed and the bob, bob shaft, and rotor are thoroughly cleaned.
- b) The sample cup was filled to the scribed line with the calibration fluid and placed on the instrument stage. The stage was elevated so that the rotor was immersed to the proper immersion depth.

- c) A thermometer was placed into the sample until the bob touches the bottom and then secured to the side of the viscometer to prevent breakage.
- d) The instrument was operated at 300 rpm for three minutes. This will equalize the temperature of the bob, rotor and the fluid.
- e) The dial was read at 300 rpm and 600 rpm. These numbers were recorded, and the temperatures from the thermometer to the nearest 0.1°C were recorded.

The above steps are standard calibration viscometer; in my work the calibration of viscometer used water (Newtonian Fluid) because the certified calibration fluids are not available in the laboratory. The figure 3-5 as shown the shear stress versus shear rate, it is clear that linear and through the origin point.

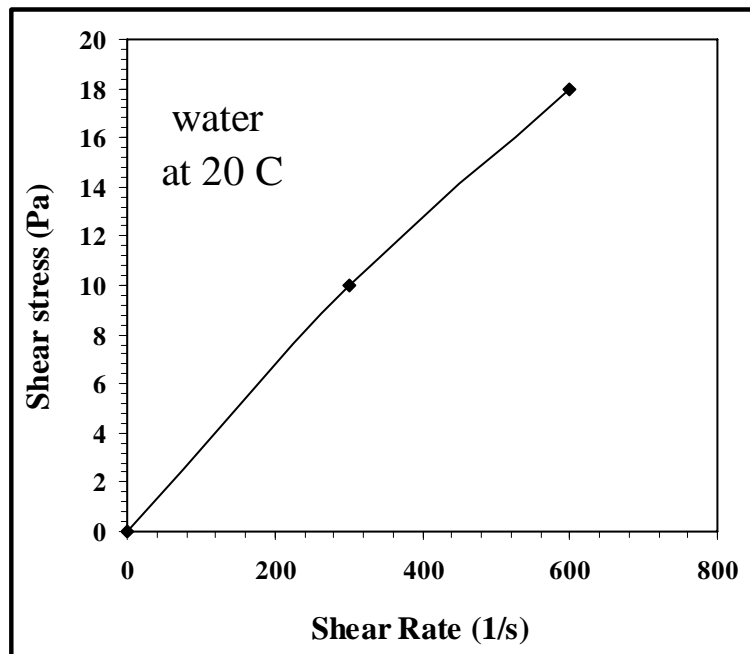


Figure 3-5 Shear Stresses versus Shear Rate for Water at 20 °C

3.8 Solid Suspension.

Suspension, in chemistry, mixture of two substances. Common suspensions include sand in water, fine soot or dust in air, and droplets of oil in air. A suspension, or perhaps more broadly dispersion, consists of discrete particles randomly distributed in a fluid medium. Generally, we divide suspensions into three categories [51]: Solid particles in a liquid medium (often the word suspension is restricted to this meaning). Liquid droplets in a liquid medium (or an emulsion). Gas in a liquid (or foam).

Solid suspensions in this work include:

3.8.1 Bentonite Suspension.

Sodium bentonite (also known as western or wyoming bentonite) is smectite clay with sodium as the dominant exchangeable ion. Small amounts of bentonite are also used as a catalyst in the refining of petroleum [52, 53].

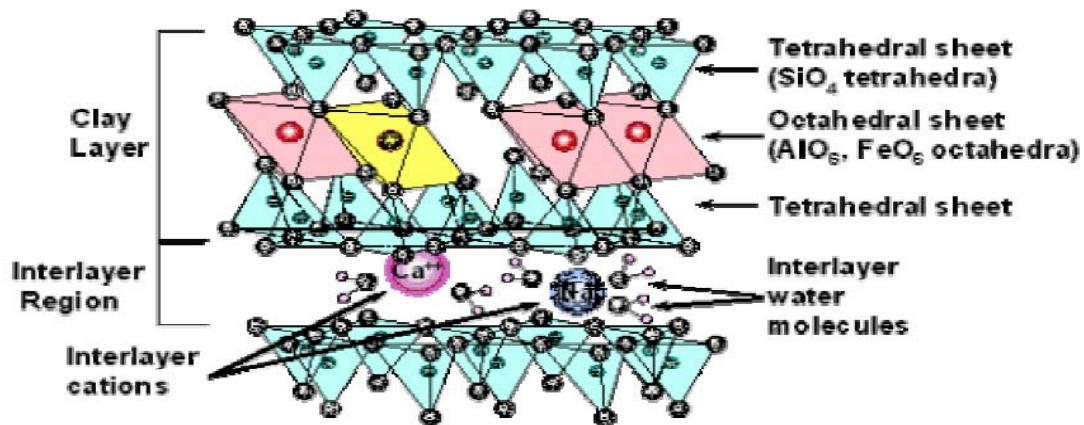


Figure 3-6 Molecular Structure of Bentonite Slurry.

3.8.2 Corn Starch Suspension.

Starch is a complex carbohydrate composed of chains of glucose molecules. Basic consumer necessities such as paper and textiles are examples of its use in major industrial applications [54].

2.8.3 Graphite Suspension.

The word “graphite” is derived from the Greek word graphein. Other common names for graphite include plumbago and mineral carbon. The basic structure of graphite consists of a hexagonal arrangement of carbon atoms which form stable planar lattices with only weak inter-layer bonding (Van der Waals forces) [55].

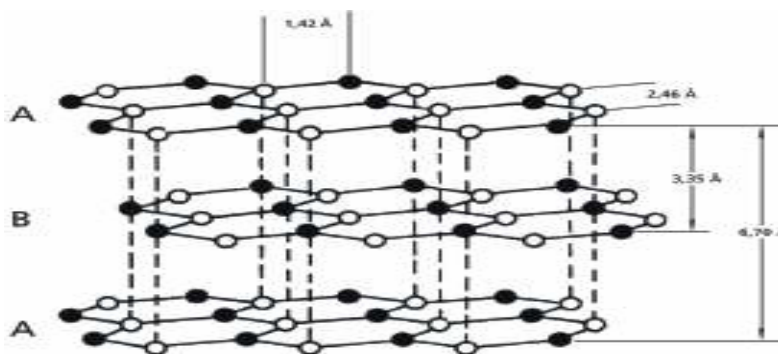


Figure 3-7 Molecular Structure of Graphite.

3.9 Polymer Definition.

The term polymer is devised from the Greek “ploys” meaning many and “meros” meaning part or units. The simple molecules from which polymers are formed are called monomer (mono meaning one) i.e., a single unite to function as a monomers, a compound must have at least two reactive sites at which other monomer units can be joined [56]. The most important kinds of chemically modified cellulose are:

2.9.1.1 Sodium Carboxymethyl Cellulose (CMC).

CMC is prepared by the reaction of cellulose with chloroacetic acid in the presence of sodium hydroxide. It is contains strong carboxyl groups which place it in the anionic polyelectrolyte category [57]. The molecular structure of CMC is shown in figure 3-8.

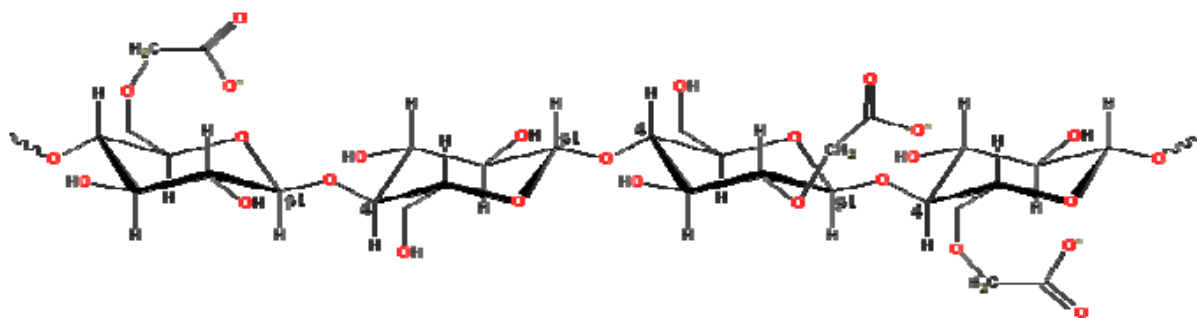


Figure 2-8 Molecular Structure of CMC.

3.9.1.2 Hydroxyethyl Cellulose (HEC)

HEC is prepared by reaction of alkali cellulose with ethylene oxide in the presence of isopropyl alcohol. HEC is used in industry as agent of dispersing, thickening, film forming etc [39].

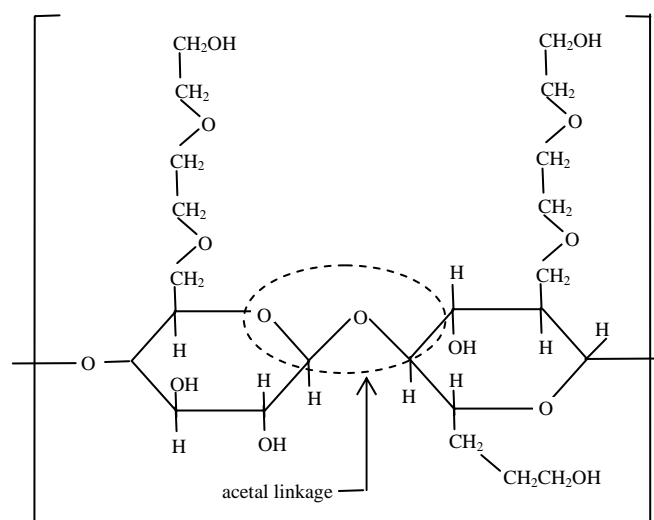


Figure 3-9 Molecular Structure of HEC.

3.9.2 XC Polymer (Xanthan Gum)

XC polymer, also known as Xanthan gum, is an anionic polysaccharide derived from the fermentation of the plant bacteria *Xanthomonas campestris*. It is soluble in hot or cold water and gives visually hazy and neutral pH solution [29].

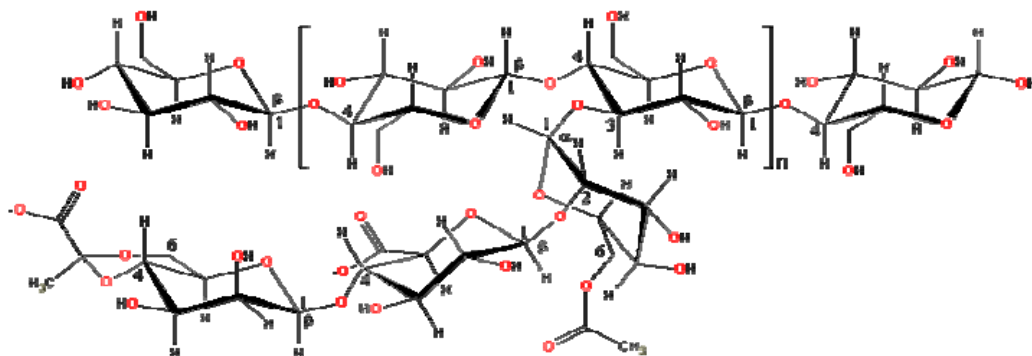


Figure 2-10 Molecular Structure of XC Polymer [59].

3.9.3 Polyvinyl Alcohol (PVA).

Unlike most vinyl polymers, PVA is not prepared by polymerization of the corresponding monomer. PVA instead is prepared by partial or complete hydrolysis of polyvinyl acetate to remove acetate group [60, 27]. The molecular structure of PVA is shown in figure 3-11.

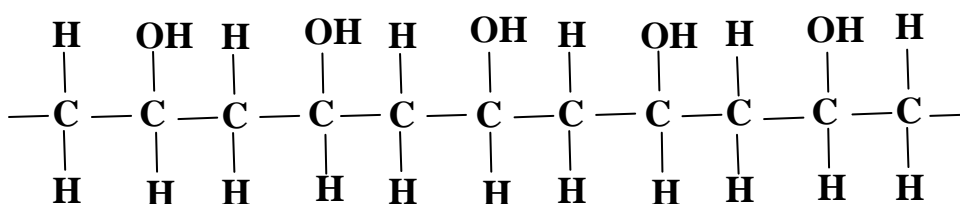


Figure 2-11 Molecular Structure of PVA.

3.10 Preparation of CMC, HEC and XC Polymer Solutions.

The method for preparing a sample of polymeric solution at a certain concentration was as follows:

1. 500 ml of distilled water was measured in a volumetric flask and placed in the Hamilton Beach cup.
2. A previously dried polymer powder was weighted to the nearest mg using electronic balance.

3. The polymer was lightly sprinkled into the water while stirring continued. Stirring continued for 30 min. to ensure complete polymer dissolution.
4. The prepared solution was poured into a properly labeled bottle and sealed.
5. The prepared solution was kept at rest at room temperature for 24 hr prior to conducting the rheological measurements.

3.11 Preparation of PVA Solution.

There are two methods for preparing aqueous solution of polyvinyl alcohol, the conventional heating method and the microwave heating method. The microwave oven method is the preferred method for preparing the PVA solution [58, 61], so it was considered in this investigation as follow:

- a) Dry PVA powder was weighted to the nearest mg using electronic balance.
- b) The polymer was added to 500 ml of distilled water in a Pyrex beaker with stirring.
- c) The beaker was covered with microwave plastic wrap and placed in a microwave oven.
- d) The microwave was turned on high for three minutes. The solution was stirred and heated for an additional three minutes.
- e) The prepared solution was allowed to cool, and then poured into a properly labeled bottle and sealed.
- f) The prepared solution was kept at rest at room temperature for 24 h. prior to conducting the rheological measurements.

3.12 Rheological Measurements.

The procedure for measuring the rheological properties of polymer solutions, using the Fann viscometer model 35 was as follows:

1. The instrument was cleaned using distilled water before immersing the rotor and bob into the polymer solution. If necessary, the rotor was removed and the bob, bob shaft, and the rotor were cleaned thoroughly.
2. The sample cup was filled with polymer solution to the scribed line, and the cup was placed on the instrument stage. The instrument stage was elevated so that the rotor was immersed to the proper immersion depth.
3. The instrument was operated at 300 rpm for three minutes to equalize the temperature of the bob, rotor and polymer solution.
4. The instrument speed was switched to 600 rpm and the dial reading was recorded.

[Step 4 was repeated for 300, 200, 100, 6 and 3 rpm].

3.13 Preparation and Measuring of Rheological Properties of Solid Suspension (Bentonite, Graphite and Corn Starch).

The test procedure for the Fann VG-Viscometer, Model 35A to prepare and calculate the rheological properties of solid suspension is as follows:

1. 500 ml of tap water (bentonite) and distilled water (graphite and corn starch) were measured in a volumetric flask and placed in the Hamilton Beach cup.
2. A previously dried dispersion powder was weighted to the nearest mg using electronic balance.
3. The powder was lightly sprinkled into the water while stirring
4. Stirring continued for 30 min. to ensure complete dispersion.

5. The viscometer was cleaned before immersing the rotor and bob into the solid suspension.
6. The cup was filled to the scribed line with the solid suspension and placed on the platform of the instrument. The platform was raised so that the surface of the solid suspension was level with the scribed line on the rotor.
7. The instrument was set to rotate at 600 rpm until a steady reading was obtained (3 min.). This reading was recorded as the 600 rpm reading to equalize the temperature of the bob, rotor and solid suspension and stopped the viscometer.
8. Step 9 was repeated for 300, 200, 100, 6 and 3 rpm.

3.14 Preparation of Add PVA to Bentonite Suspensions.

1. After aging, prepared bentonite slurry at the concentration 40g/0.5L was poured into a properly labeled jug.
2. The PVA polymer was added, at different concentrations 2, 5, 7, and 10 g/0.5L.
3. The PVA polymer was added drop by drop during 5 minutes.
4. The samples were stirred for an additional 20 minutes use the Hamilton Beach mixer after PVA addition, interrupting briefly at 5 and 10 minutes to scrape any adhering material on the sides of the cup into the fluid.
5. The samples were placed in closed containers (covered Hamilton Beach cups or equivalent) and were allowed to static age for 2 hours at room temperature.
6. After all concentrations were prepared (Bentonite-PVA), the rheological properties were measured.

Chapter Four

Results and Discussion

4.1 Introduction.

A total of 76 runs were performed to study the rheological properties using Fann VG-Viscometer, Model 35A. This includes 59 Runs for polymers: CMC, HEC, PVA and XC, at different concentration and temperatures, 13 runs for solid suspension: Graphite, Bentonite and Corn starch and 4 runs for adding polymer to solid suspension (PVA to Bentonite)

First, the flow curve of each experimental was studied using the power law model. Secondly, the effect of concentration polymer solution, solid suspension on flow model parameter and solution viscosity was investigated. Thirdly, the effect of temperature on viscosity of polymer solution and comparison between different polymer solution system used in this work was examined. Finally, the effect of adding polymer (PVA) to solid suspension (Bentonite) was examined.

The fann, model type 35A, viscometer has been designed so that the shear rate is measured in rpm and shear stress in dial reading unit. To convert the shear rate and shear stress to SI unite, the following conversion equations were used [50]:

$$\gamma = 1.7023 N \quad \dots (4.1)$$

$$\tau = 0.1 k_1 k_2 \theta \quad \dots (4.2)$$

In which:

N is the bob speed (rpm), θ is the dial reading. $k_1 = 386$, the torsion constant in (dyne .cm)/degree deflection. $k_2 = 0.01323$, the shear stress constant for the effect in bob surface, cm^3 .

The power law is widely used as a model for non-Newtonian fluid. It holds for many solutions and can describe Newtonian, shear thinning, and shear thickening behavior, depending on the power factor, n , also called the flow behavior index. For a Newtonian fluid, n equals 1 and the equation reduces to the Newtonian model. If n is less than 1, the fluid is shear thinning, if it is greater than 1, the fluid is shear thickening. A test of whether the power law applies and a means of determining n is to plot the log shear stress vs. log shear rate. If the plot is linear, the power law applies. The value of n , which is the reciprocal of the slope of the line, can be used as a measure of the degree of shear thinning or shear thickening.

$$\tau = K \gamma^n \quad \dots (4.3)$$

Where τ is shear stress (Pa), γ is shear rate (s^{-1}), K is the power law constant (consistency index), n is constant (flow behavior index). Dividing the power law equation through by gives an expression in terms of viscosity [62].

$$\eta = k \gamma^{n-1} \quad \dots (4.4)$$

4.2 Results of Polymer Solution.

4.2.1 Study Shear Flow Behavior.

Sample of the experimental results are shown in figures 4-1, 4-2 and 4-3, which are plot of shear stress versus shear rate. Figure 4-1 presents the CMC polymer at concentration 20 g/l, figure 4-2 presents the XC polymer at concentration 20 g/l and figure 4-3 presents the HEC polymer at concentration 20 g/l. The figures are plotted using the Fann viscometer instrument. The flow curves of all experiments are shown in appendix (A). As shown in these figures the shear stress increase with increasing shear rate in a non linear shape.

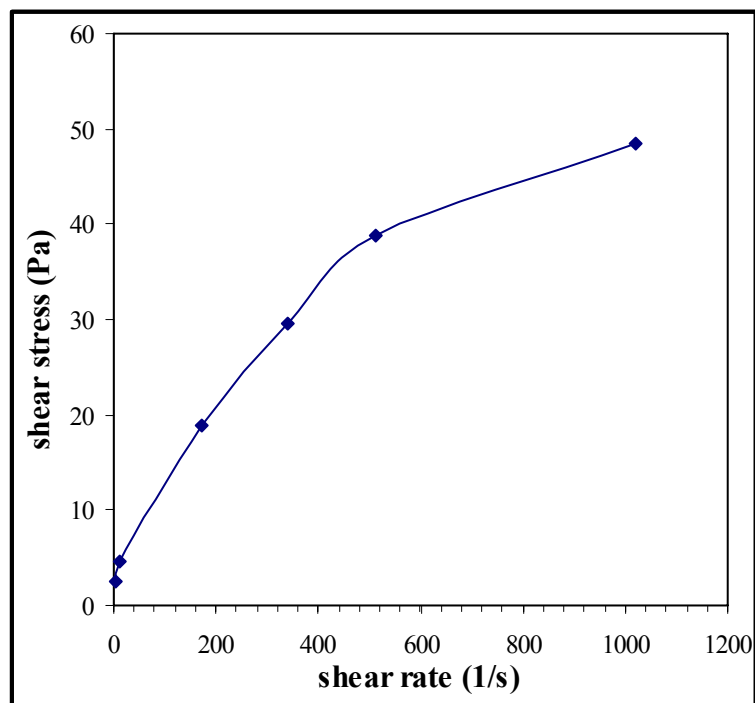


Figure 4-1 Flow Curve for CMC Polymer Solution at Concentration 20 g/l at 20 °C.

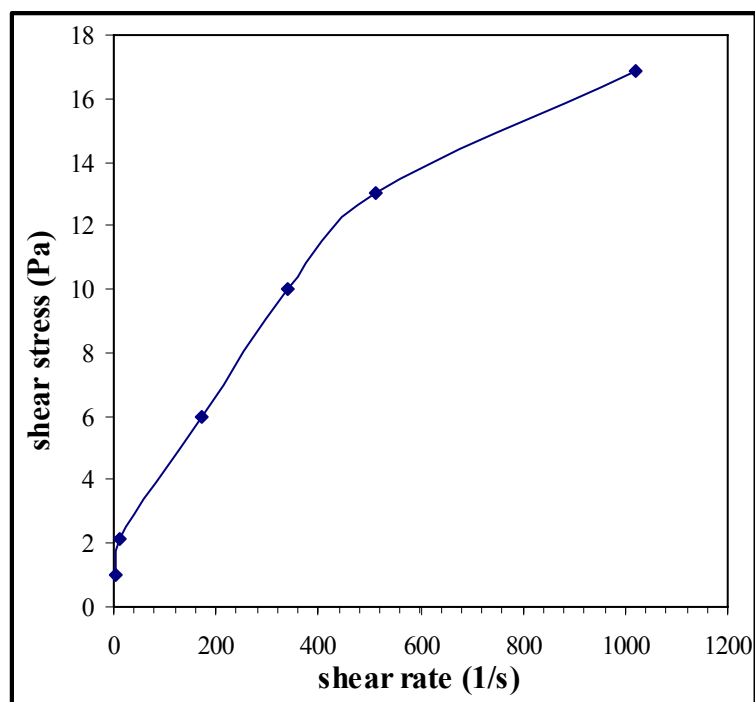


Figure 4-2 Flow Curve for HEC Polymer Solution at Concentration 20 g/l at 20° C.

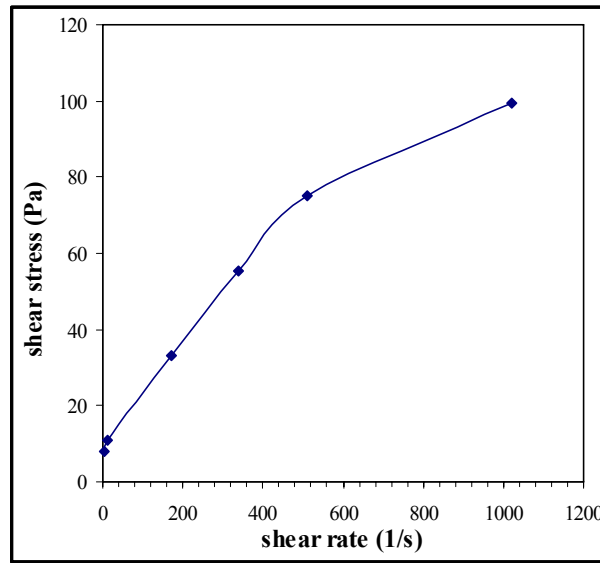


Figure 4-3 Flow Curve for XC Polymer Solution at Concentration 20 g/l at 20 °C.

The power index (n) is the slope of the line. For the CMC, XC and HEC polymers on logarithmic scale are shown in figures 4-4, 4-5 and 4-6. The values of n and k , with the correlation coefficients of the best fit line (R^2) for all experiments are presented in table 4-1.

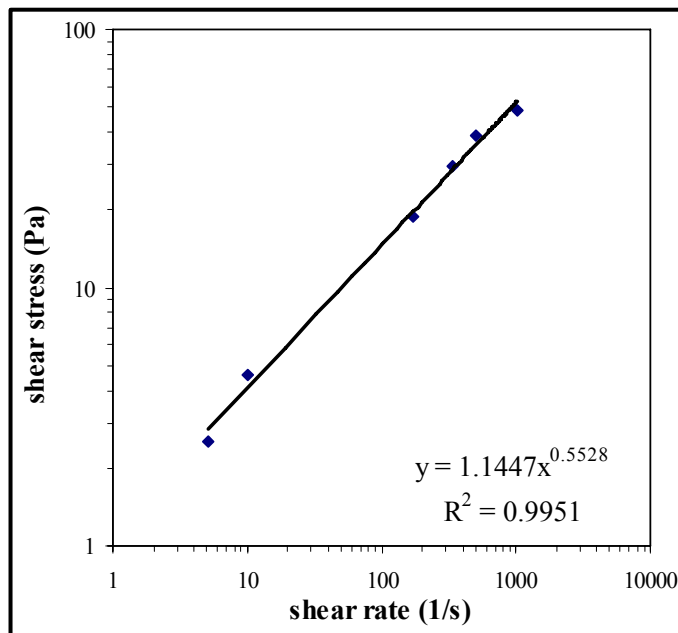


Figure 4-4 Flow Curve for CMC Polymer Solution at Concentration 20 g/l at 20 °C.

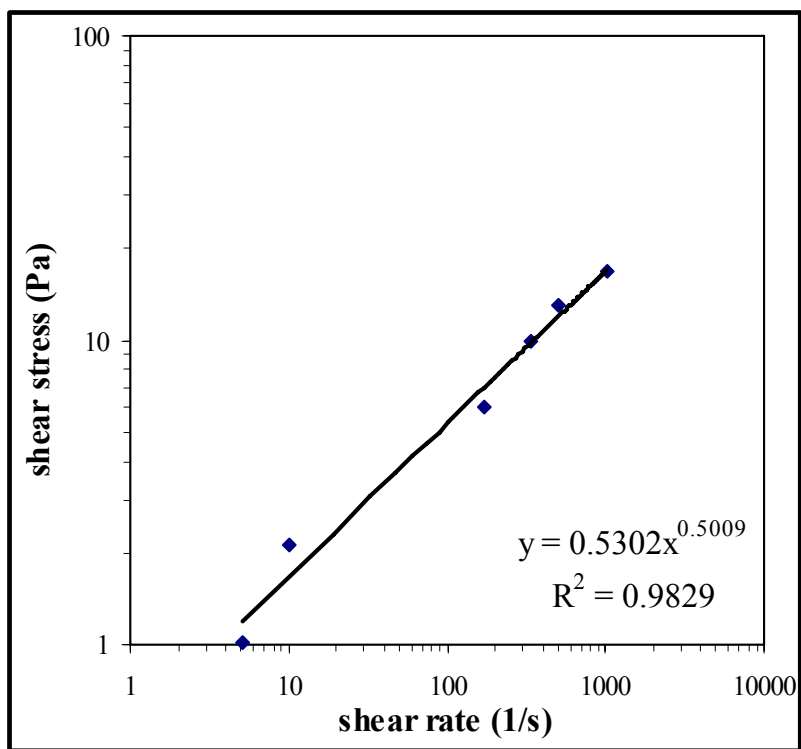


Figure 4-5 Flow Curve for HEC Polymer Solution at Concentration 20 g/l at 20 °C.

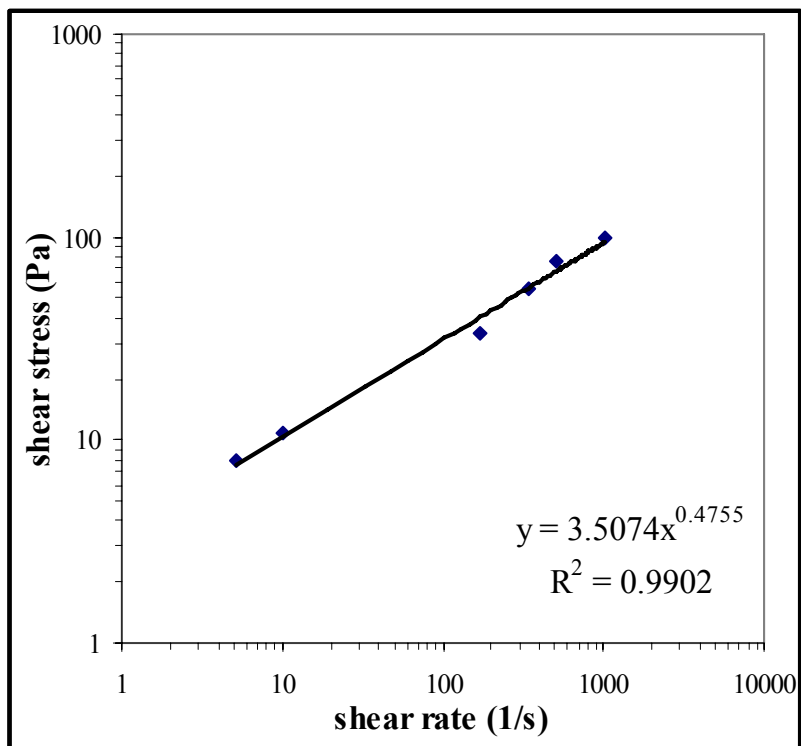


Figure 4-6 Flow Curve for XC Polymer Solution at Concentration 20 g/l at 20 °C.

Table 4-1 Flow Behavior Index (n) and Consistency Index (k) at 20°C.

Material	Conc. (g/l)	n	k	R ²
CMC	4	0.6814	0.1910	0.9330
CMC	7	0.6415	0.2554	0.9969
CMC	10	0.6031	0.3401	0.9799
CMC	15	0.5995	0.5286	0.9903
CMC	20	0.5529	1.1434	0.9951
CMC	25	0.5469	2.4407	0.9915
CMC	30	0.4709	6.6378	0.9901
CMC	35	0.4605	7.7493	0.9837
CMC	40	0.4537	9.4716	0.9750
HEC	4	0.5387	0.2977	0.9935
HEC	10	0.5316	0.3675	0.9918
HEC	20	0.5010	0.5247	0.9829
HEC	30	0.4826	0.8525	0.9954
HEC	40	0.4664	1.4048	0.9826
XC	4	0.5519	0.2939	0.9918
XC	10	0.4845	1.0531	0.9928
XC	20	0.4756	3.5040	0.9902
XC	30	0.4605	7.7493	0.9837
XC	40	0.4552	7.9553	0.9966

4.2.2 Effect of Polymer Concentration on Flow Behavior Index (n).

The effects of polymer concentration on the flow behavior index (n) for all polymer solutions used are shown in figures 4-7, 4-8 and 4-9.

The flow behavior index (n) measured for all polymer was found to be less than 1, thus in the range of concentrations considered they behave as pseudo plastic (shear thinning) fluid, for $n < 1$ the slope will be negative. It is evident that with the increase in the concentration of polymer solutions the flow behavior index (n) decreases. The range of n is between (0.7- 0.4).

Equations that describe the effect of polymer concentration on the flow behavior index can be presented in a linear form as shown in the equations below:

The range concentration between 4-40 g/L.

$$n_{cmc} = - 0.0063 C_{cmc} + 0.6935 \quad R^2 = 0.9584 \quad \dots (4.5)$$

$$n_{xc} = - 0.021 C_{xc} + 0.5318 \quad R^2 = 0.6841 \quad \dots (4.6)$$

$$n_{hec} = - 0.0021 C_{hec} + 0.5479 \quad R^2 = 0.9849 \quad \dots (4.7)$$

From the above equations and from figure 4-7 it deduce that n for XC polymer is more affected by concentration than other polymer used in this study because the molecular weight is higher than other polymer used.

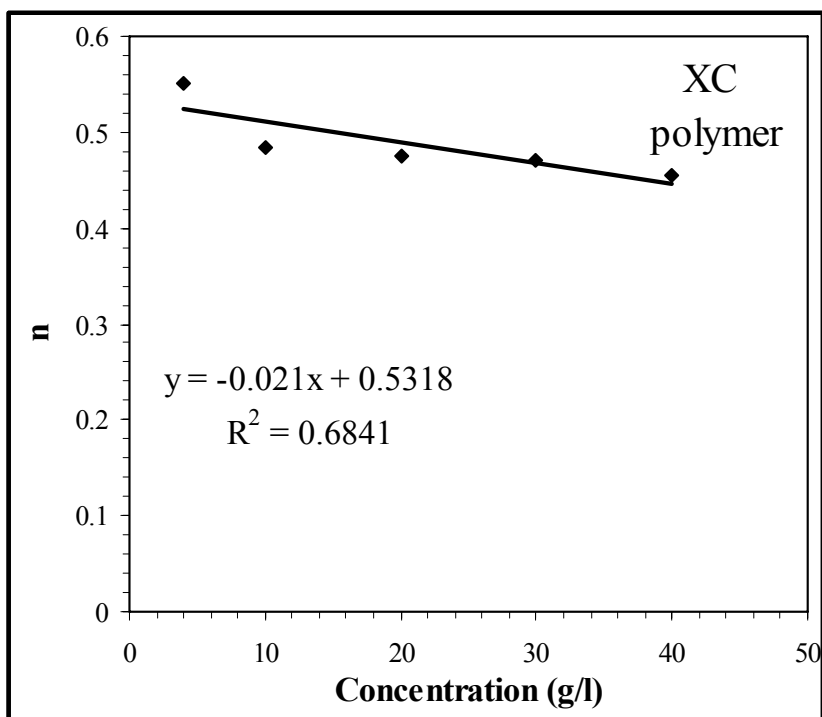


Figure 4-7 Effect of XC Polymer Concentration on Flow Behavior Index at 20°C.

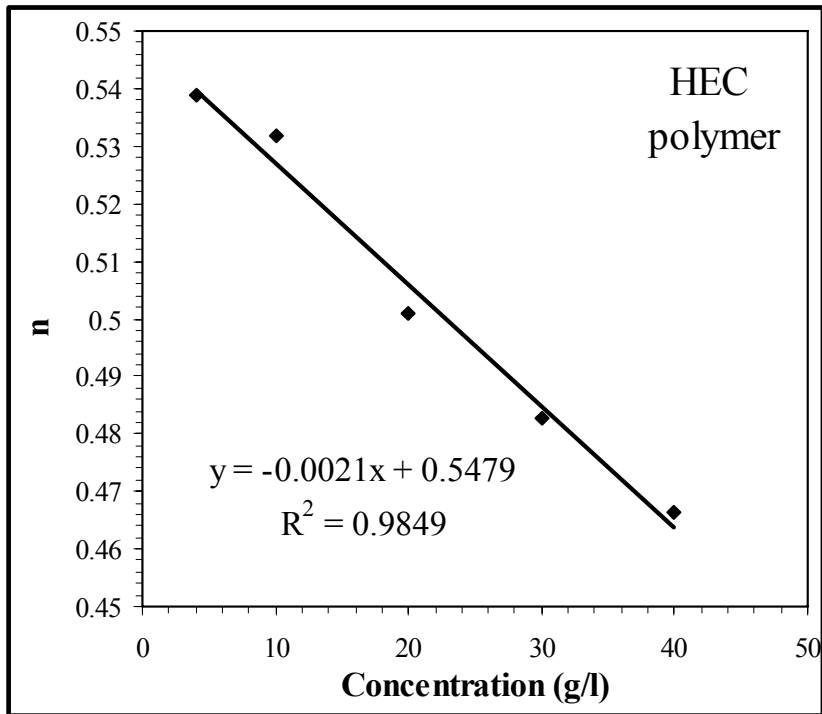


Figure 4-8 Effect of HEC Polymer Concentration on Flow Behavior Index at 20°C.

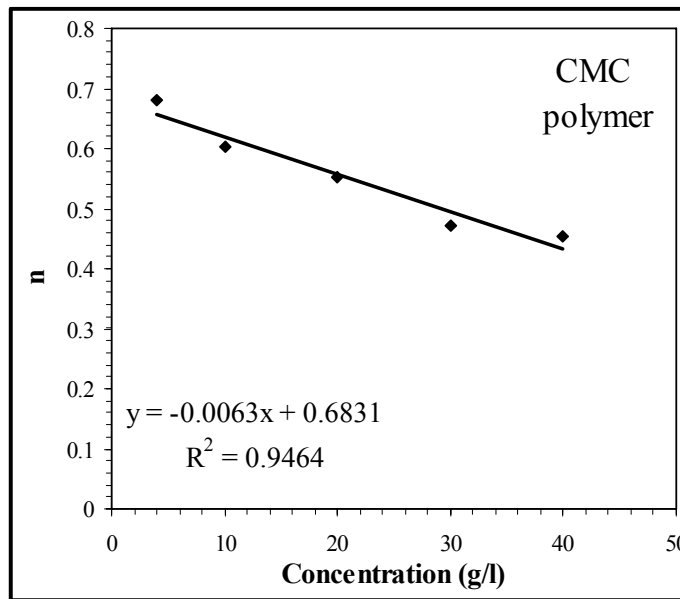


Figure 4-9 Effect of CMC Polymer Concentration on Flow Behavior Index at 20°C.

4.2.3 Effect of Polymer Concentration on Flow Curves.

Figures 4-10, 4-11, and 4-12 shows effect of polymer concentration on flow curve. These figures indicate that the shear stress increase with the increase in the shear rate . The fluid has been observed non linear (non-Newtonian behavior).

At low concentration the flow curve of polymer solutions is approximately linear and the flow curves are close to each other. At high concentration the flow curves of polymer solution bends down and the flow curves are far from to each other.

Choi S. K. [63] concluded that, the increased numbers of polymer molecules result in more interaction between polymer chains, which cause more friction effects to increase the shear stress. At very low concentrations there is no strong interaction between polymer molecules. In this region, the effect of concentration is not appreciable.

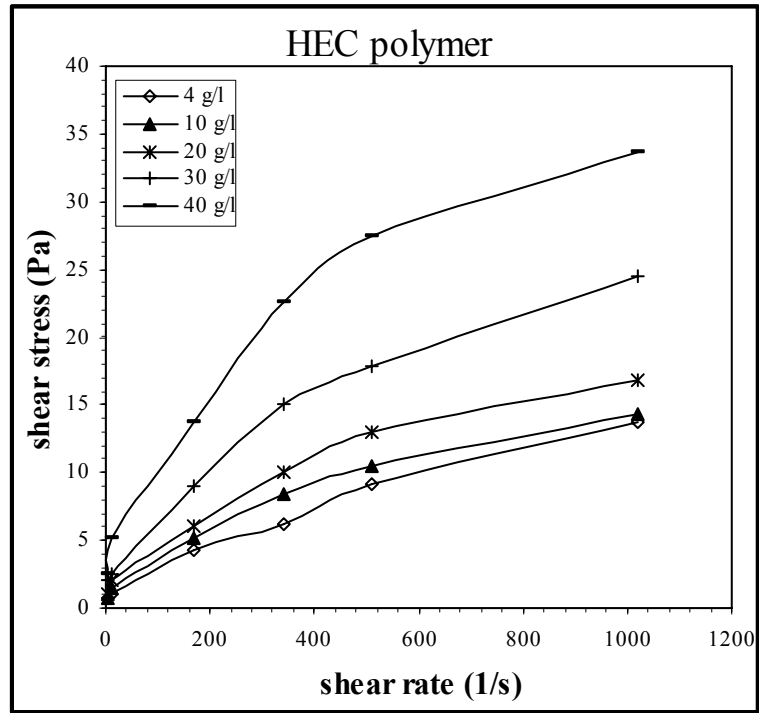


Figure 4-10 Effect of HEC Polymer Concentration on Flow Curves at 20°C.

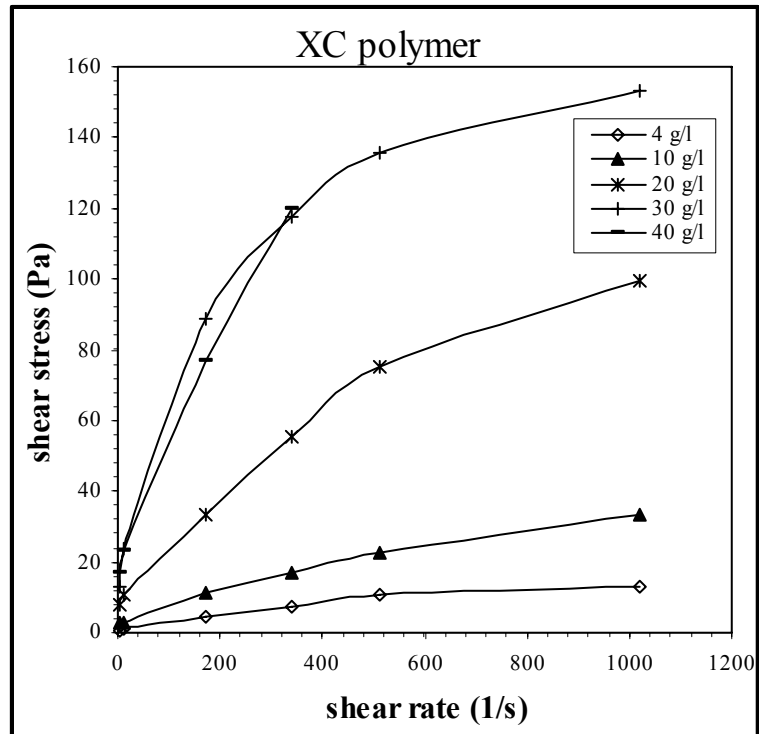


Figure 4-11 Effect of XC Polymer Concentration on Flow Curves at 20°C.

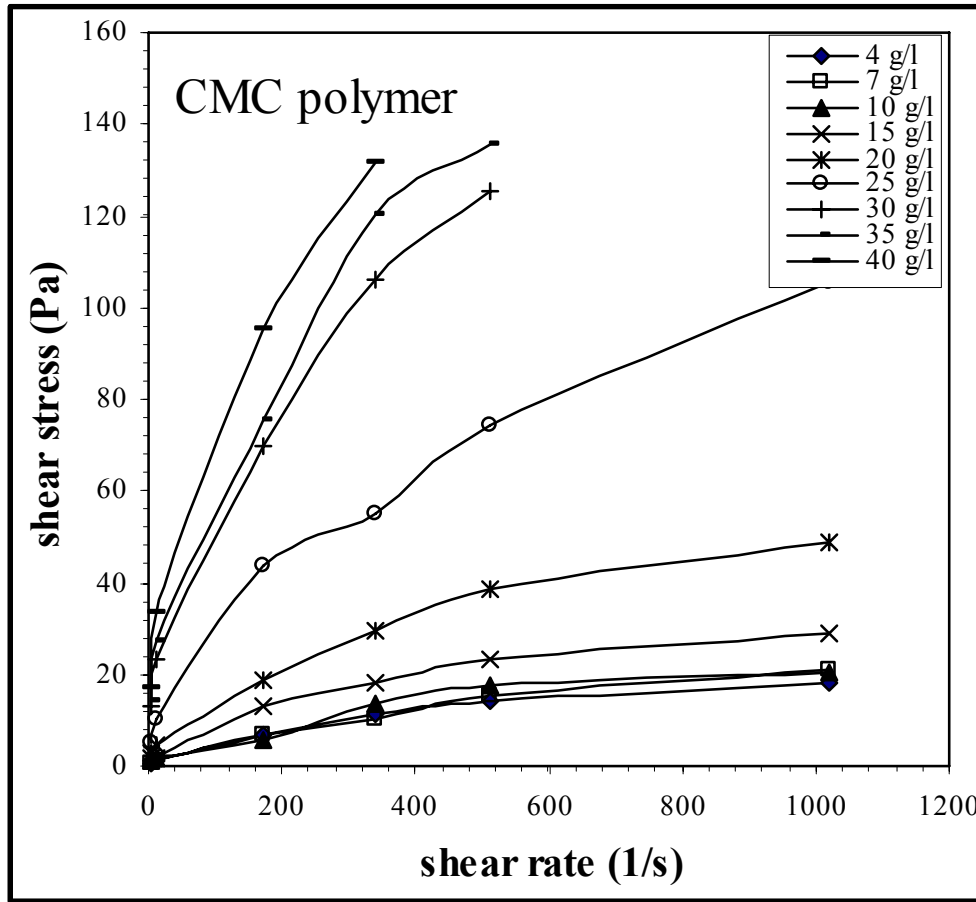


Figure 4-12 Effect of CMC Polymer Concentration on Flow Curves at 20°C.

Increasing the polymer concentration decreases the distance between polymer particles and the slopes of the lines increase with increased polymer concentration. The apparent viscosity increases with increasing the concentration since the polymer solution with higher concentration has stronger intermolecular force.

Figures 4-13 , 4-14 and 4-15 present the shear stress versus shear rate at logarithmic scale in varies concentration.

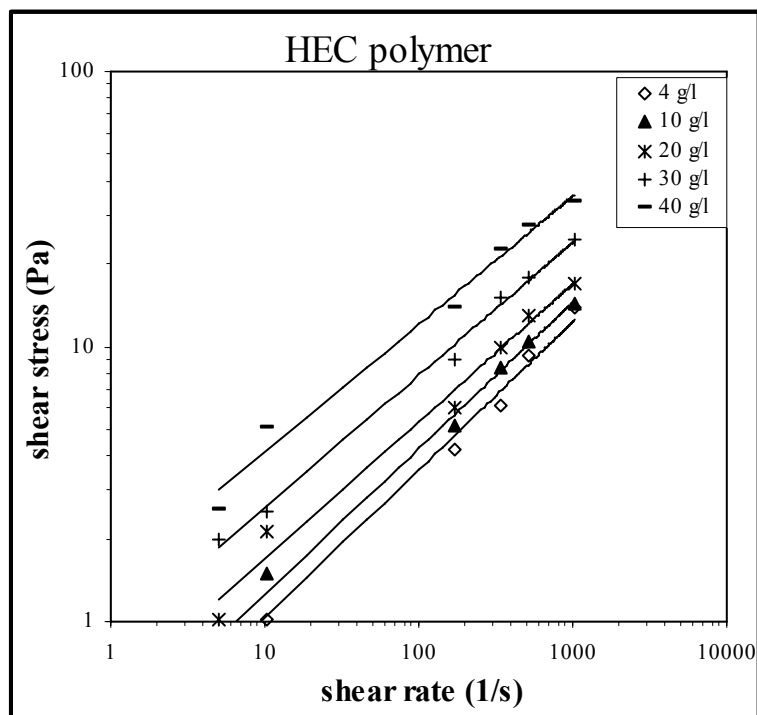


Figure 4-13 Effect of HEC Polymer Concentration on Flow Curves at 20°C.

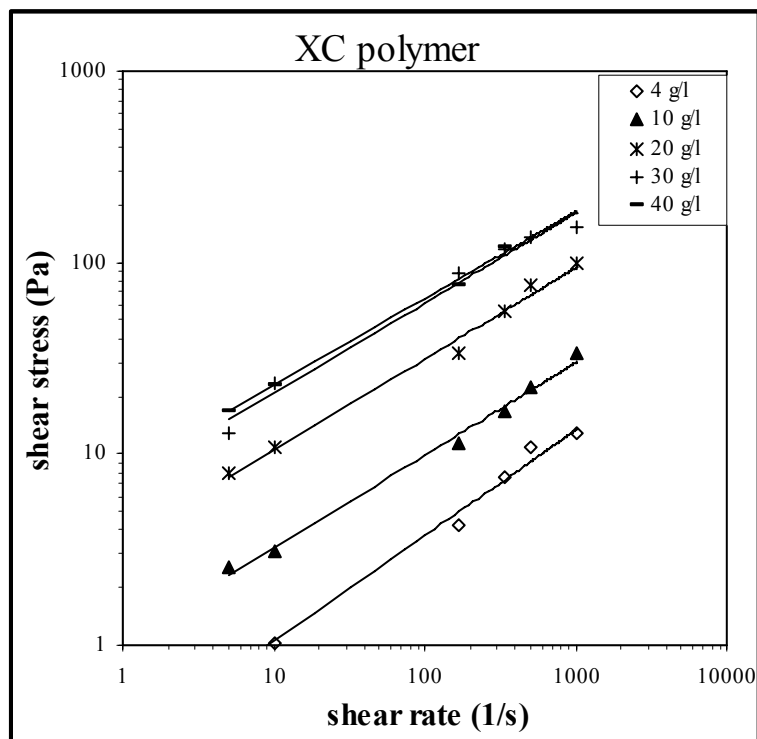


Figure 4-14 Effect of XC Polymer Concentration on Flow Curves at 20°C.

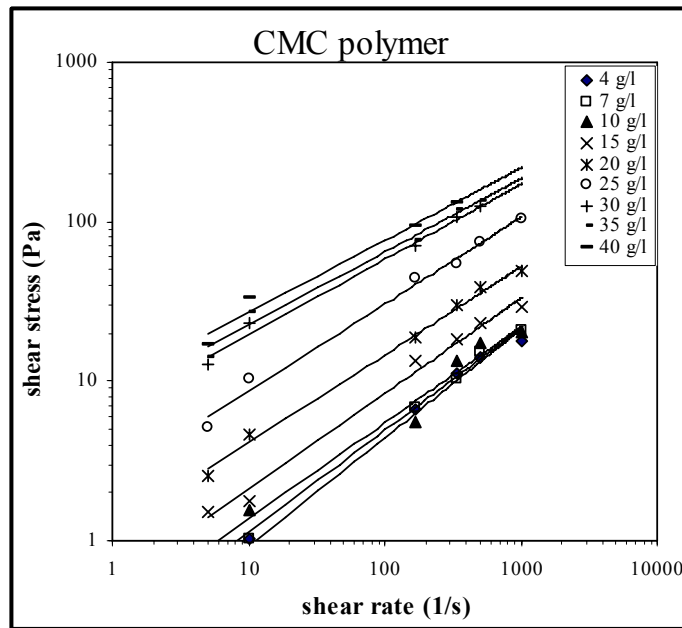


Figure 4-15 Effect of CMC Polymer Concentration on Flow Curves at 20°C.

4.2.4 Apparent Viscosity of Polymer Solution.

The apparent viscosity effect in polymer solutions is shown in figures 4-16, 4-17 and 4-18. It is clear that the apparent viscosity decreases as the shear rate increases and the XC polymer viscosity has a higher value than other polymers.

The most common viscosity model describing the non-Newtonian relationship between viscosity and shear rate is the power law model (the Oswald models).

$$\eta_a = k \dot{\gamma}^{n-1} \quad \dots (4.8)$$

Viscosity is an important parameter to characterize the flow of polymer solution. The polymer solution has random-coil macromolecular structure and present typical pseudo plastic or shear thinning behavior.

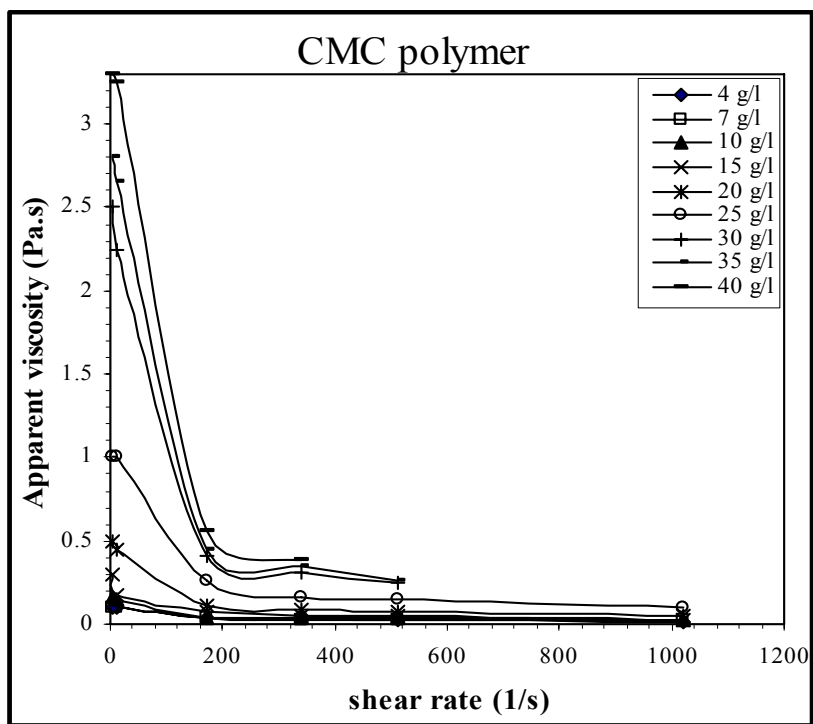


Figure 4-16 Apparent Viscosity of CMC Polymer Solutions at Different Concentration at 20°C.

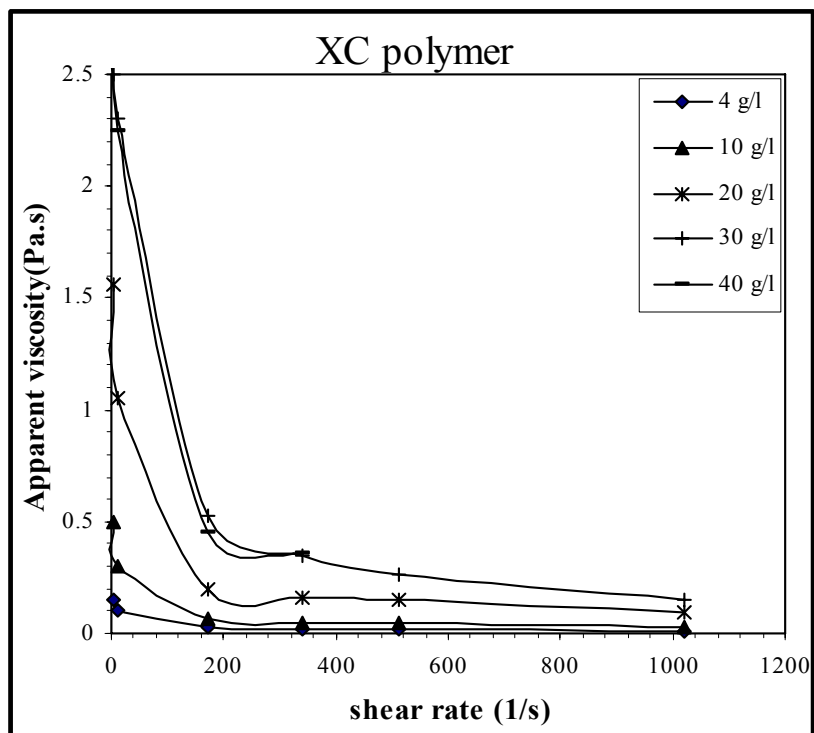


Figure 4-17 Apparent Viscosity of XC Polymer Solutions at Different Concentration at 20°C.

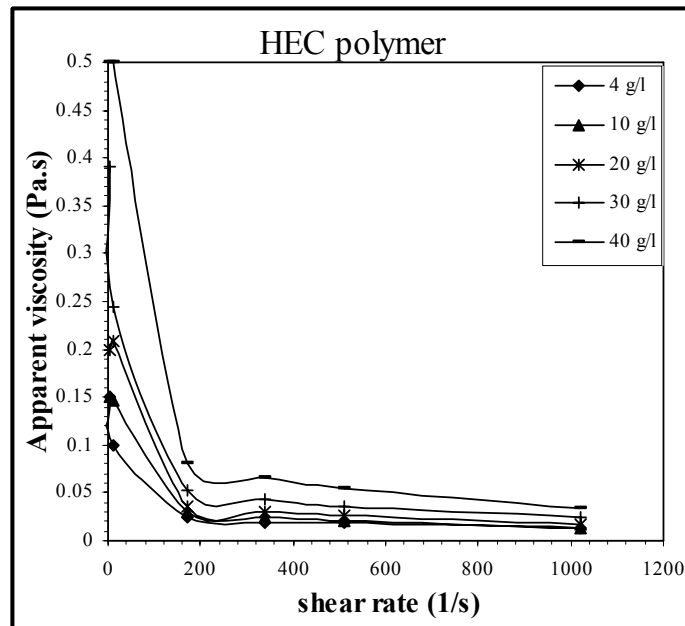


Figure 4-18 Apparent Viscosity of HEC Polymer Solutions at Different Concentration at 20°C.

4.2.5 Effect of Temperature on Polymer Solution Viscosity.

The effects of temperature on polymer solution viscosity are shown in figures 4-19, 4-20 and 4-21.

The results show that the viscosities of the three polymers (CMC, XC and HEC) decreased with increasing shear rate and with increasing temperature, as expected. However, temperature effect was more significant at higher concentrations.

Liu, et al., [42] concluded that, the viscosity of materials decrease as temperature increases. This is due to increase in the distances between particles of polymer causes low attraction forces. The increase in temperature destroys the bonding between particles.

Practically, plot of $\text{Log } \eta$ vs. T tend to be straight line over a considerable range of values.

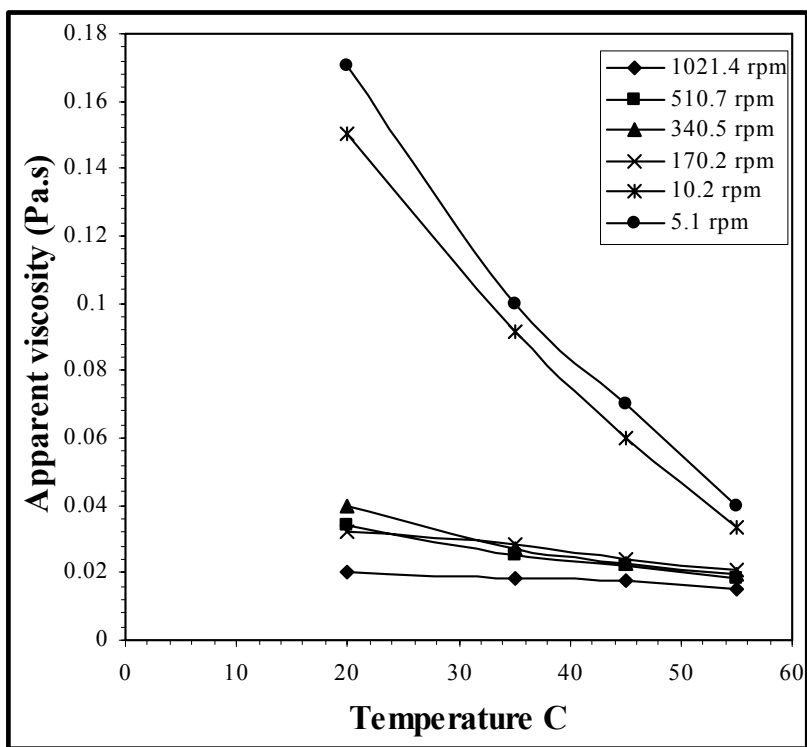


Figure 4-19 Effect of Temperature in CMC Polymer Viscosity at Concentration 10g/l at 20°C.

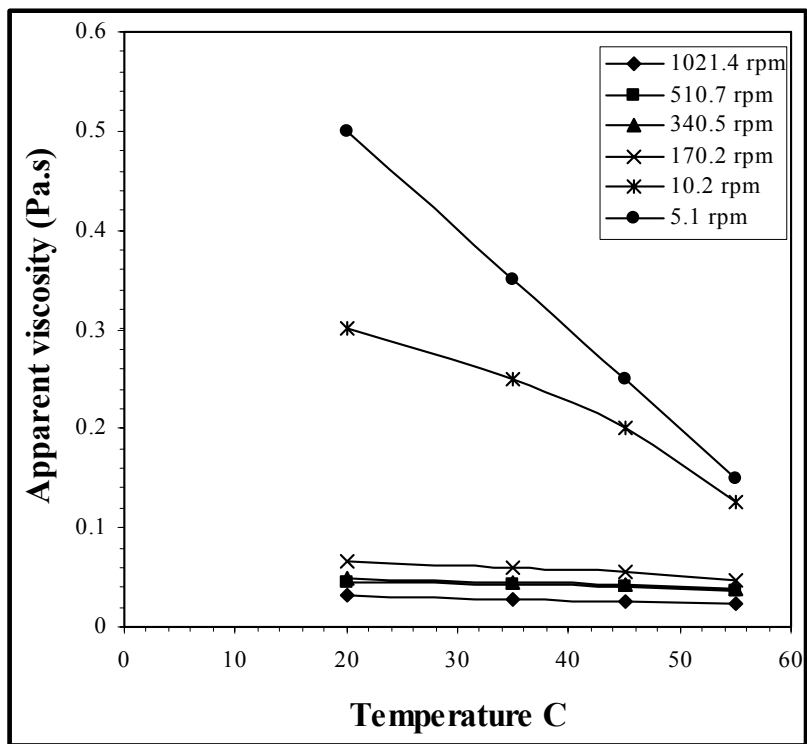


Figure 4-20 Effect of Temperature in XC Polymer Viscosity at Concentration 10g/l at 20°C.

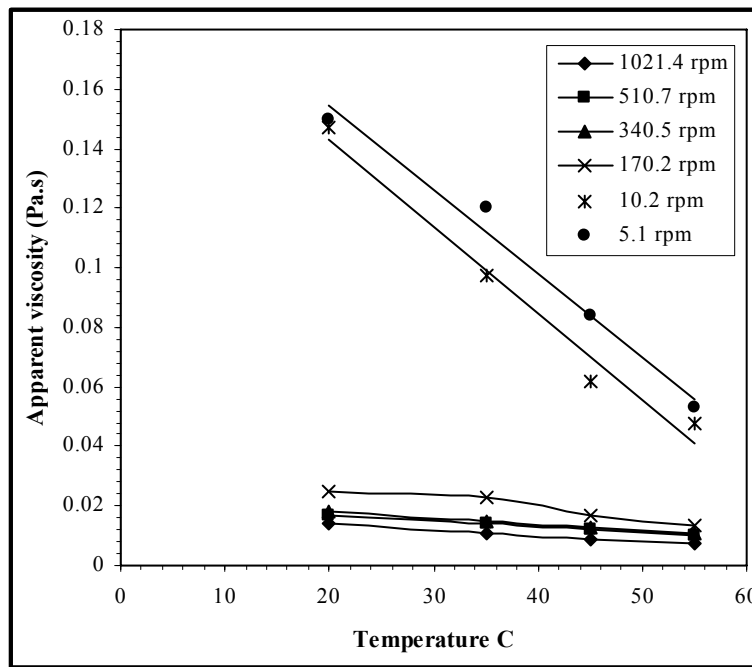


Figure 4-21 Effect of Temperature in HEC Polymer Viscosity at Concentration 10g/l at 20°C

The variations in temperature influence the value of n and k . The increases in temperature cause an increase in n and decrease in k . Table 4-2 shows the influence of the temperature on the values of n and k .

Table 4-2 The Influence of The Temperature on The values of n and k for Polymer Solutions at 10 g/l.

-A- CMC			-B- HEC			-C- XC		
Temp.°C	N	K	Temp.°C	N	K	Temp.°C	n	K
20	0.6031	0.3401	20	0.5316	0.3675	20	0.4845	1.0531
35	0.6721	0.1789	35	0.5232	0.2716	35	0.5262	0.7452
45	0.7335	0.1078	45	0.5726	0.1643	45	0.5764	0.5132
55	0.8259	0.0520	55	0.6140	0.1060	55	0.6674	0.2656

4.2.6 Effect of Polymer Type on Viscosity.

The effects of polymer type on viscosity at the same concentration of 10 and 20 g/l are shown in figures 4-22 and 4-23.

The deduce information about from this effect the concentration of XC polymer solution have higher viscosities than other polymer solution used in this work.

Barnes, [14] concluded that, the polymer that higher in molecular weight exhibits more pronounced viscoelastic behavior than the polymer which is lower in molecular weight. We can conclude that, in the range of polymer concentration used in this study, the apparent viscosity can be ordered as:

$$\eta_{XC} > \eta_{CMC} > \eta_{HEC}$$

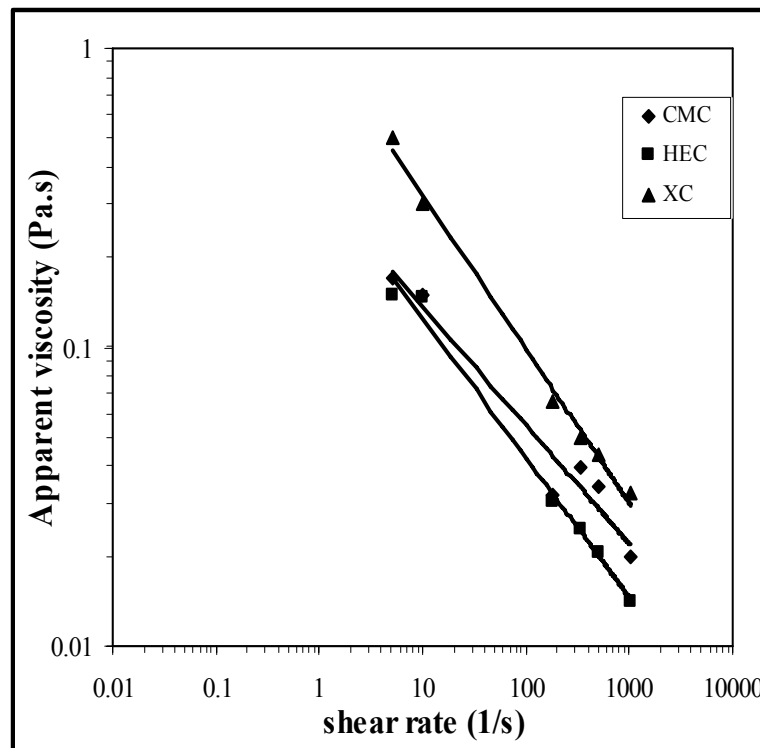


Figure 4-22 Effect of Polymer Type on Viscosity at Polymer Concentration of 10g/l at 20°C

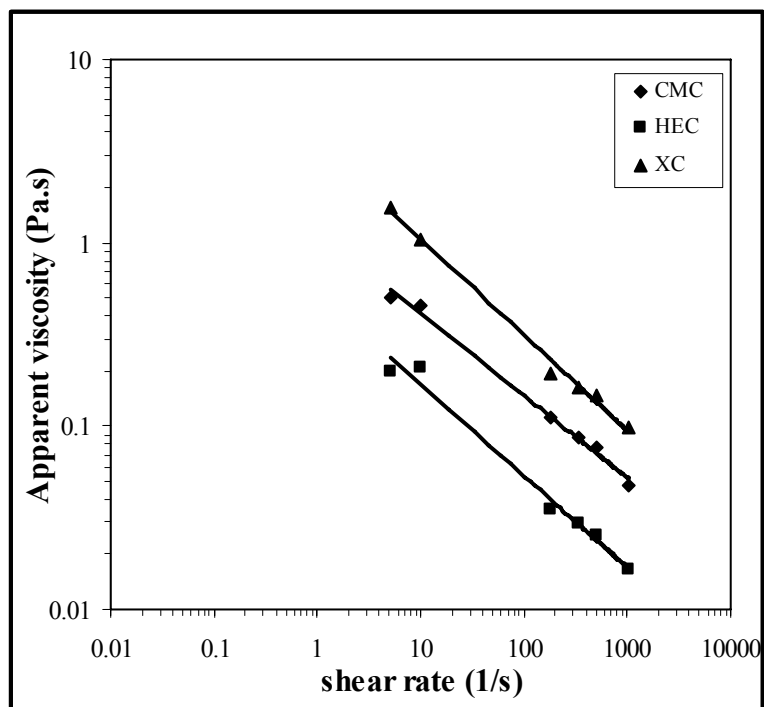


Figure 4-23 Effect of Polymer Type on Viscosity at Polymer Concentration of 20g/l at 20°C

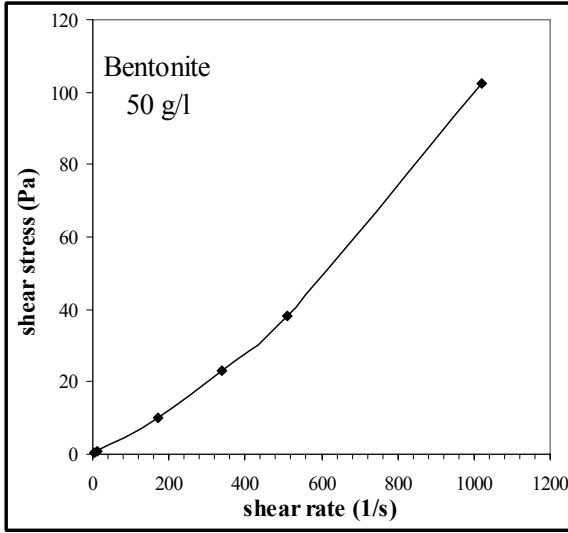
4.3 Results of Solid Suspension.

4.3.1 Shear Flow Behavior.

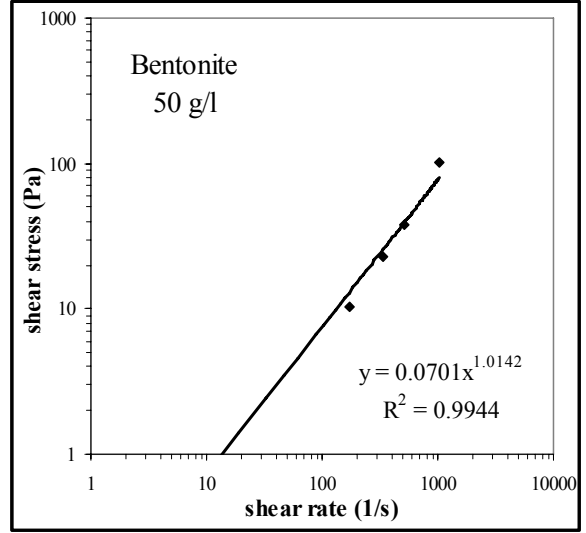
The flow curves are used for a plot of shear stress versus shear rate. Figures 4-24, 4-25 and 4-26 show a sample of flow curves for different solid suspensions and different concentrations at temperature 35°C. It is indicated that the shear rate increases with an increase in the shear stress for all solid suspensions.

The flow curve starts as a straight line ($n = 1$) at very low shear rates. As the shear rate increases the flow curve bends up ($n > 1$) and it behaves as a shear thickening (dilatants).

The Flow curve of all experiments are shown in appendix (A) (plots of shear stress versus shear rate).

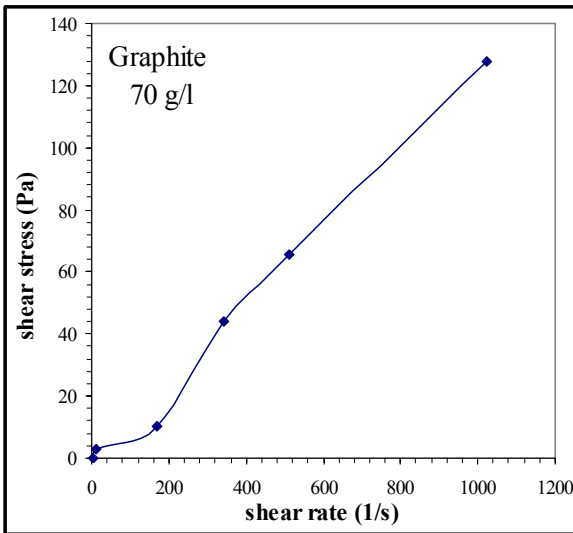


(A)

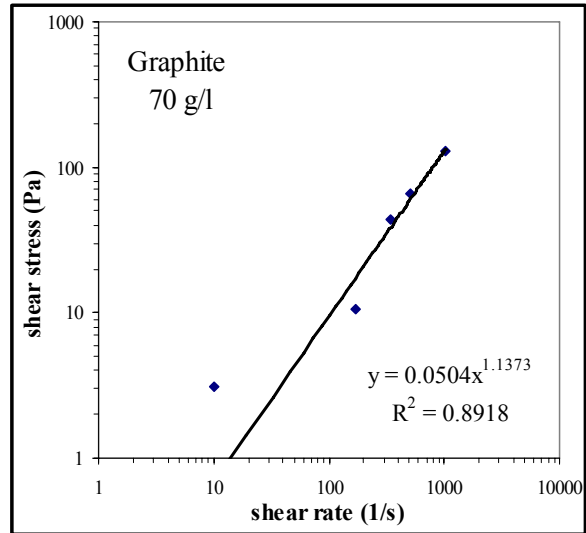


(B)

Figure 4-24 Flow Curve for Bentonite Suspension at Concentration 50g/L at 35°C.



(A)



(B)

Figure 4-25 Flow Curve for Graphite at Concentration 70 g/L at 35°C.

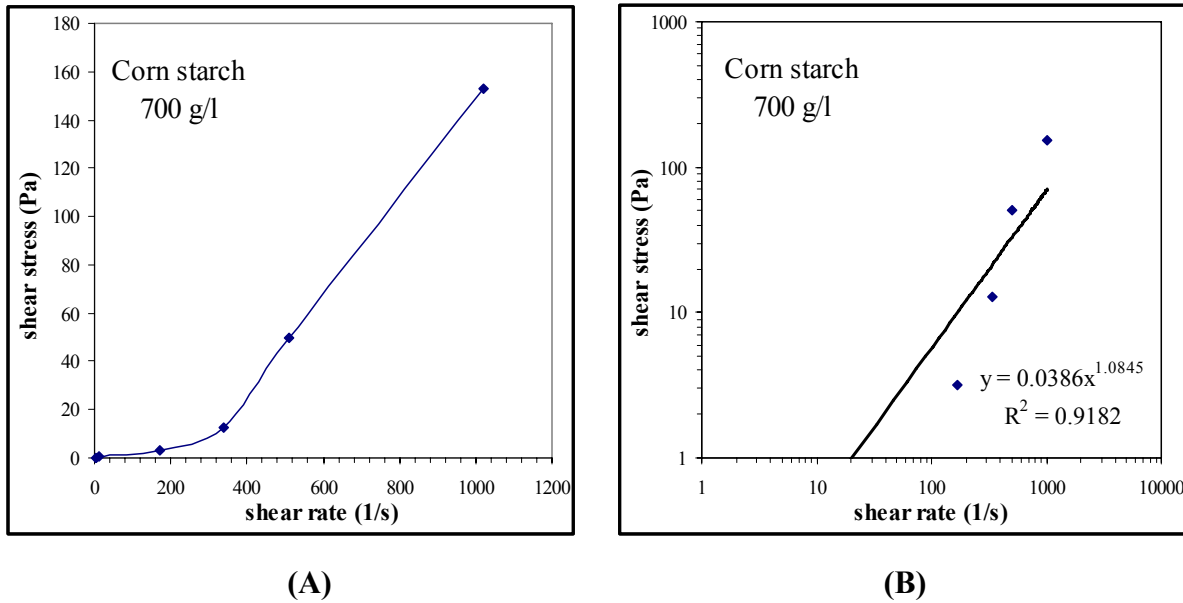


Figure 4-26 Flow Curve for Corn Starch at Concentration 700 g/L at 35°C..

4.3.2 Effect of Solid Suspension Concentration on Flow Curves.

The effects of suspension concentration on flow curve are shown in figures 4-27, 4-28 and 4-29. From these figures one can see that with increase in solid suspension content the shear stress gradually increase.

Leuven, et. al., [64] concluded that suspension rheology at low solids concentration is primarily dictated by the particle liquid interfacial interactions. Under shear, there is enough liquid phase between particles to lubricate them and the interaction between particles is mainly conducted by the liquid. With increasing solids content, however, the mean distance between particles decreases and drastic interactions such as particle-particle and hydrodynamic effects influence the flow.

Nick Triantafillopoulos, [49] concluded that increasing the volume fraction seems to universally increase the tendency for shear thickening, where by the gradual shear thickening appears at lower volume fractions than the sudden variety. With increasing volume fraction the critical shear rate decreases and the subsequent viscosity increase becomes steeper and larger.

As shown in figure 4-28 (the flow curve of corn starch suspension), at low shear rate the flow curve behavior is shear thinning and the increasing gradually in shear rate cause the flow curve to become shear thickening.

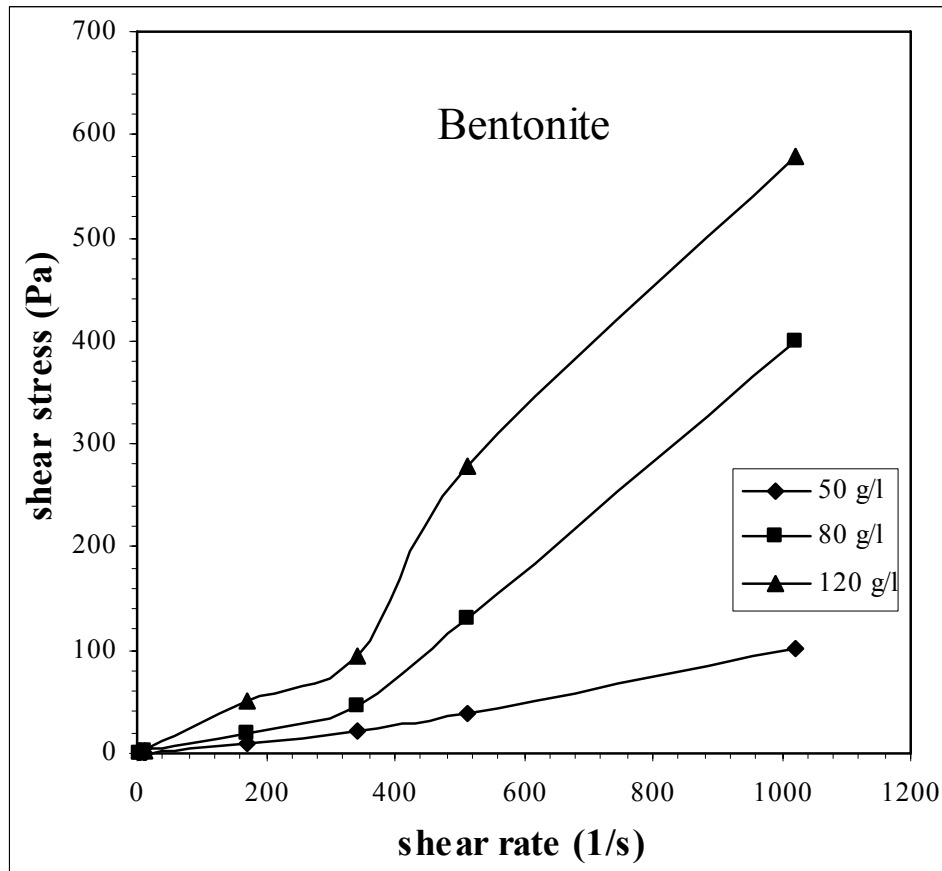


Figure 4-27 Effect of Bentonite Concentration on Flow Curves at 35°C..

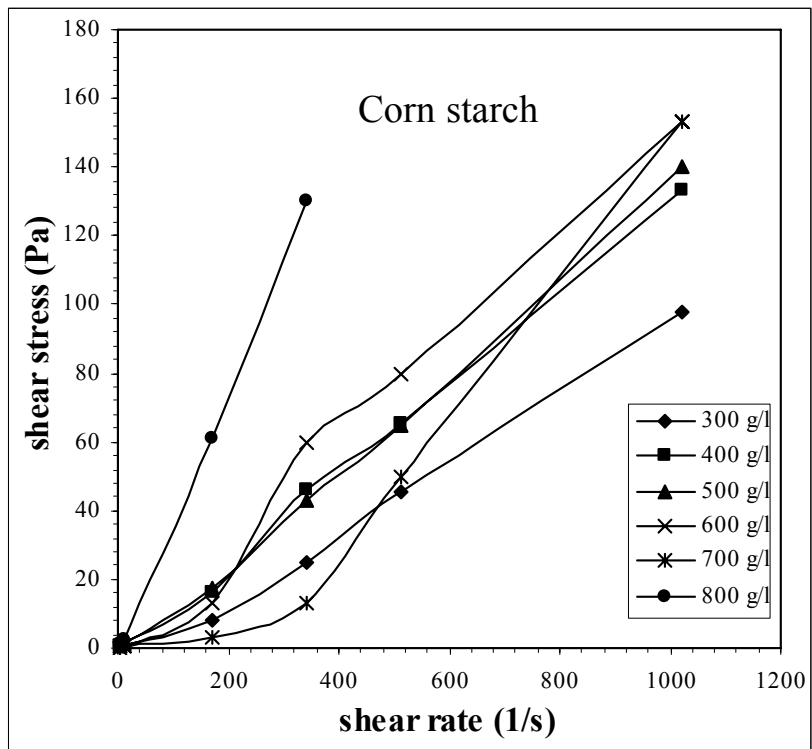


Figure 4-28 Effect of Graphite Concentration on Flow Curves at 35°C..

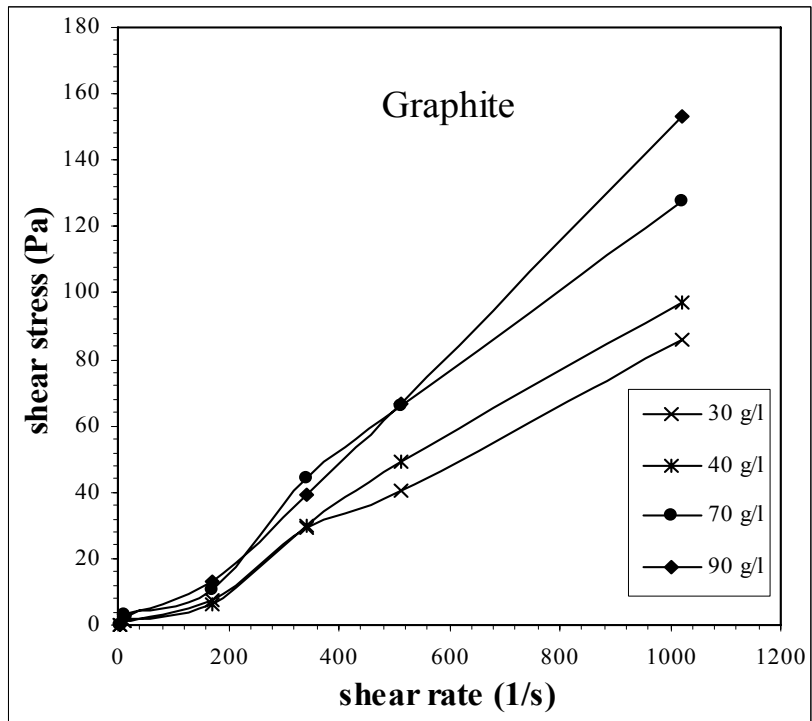


Figure 4-29 Effect of Corn Starch Concentration on Flow Curve at 35°C..

4.3.3 Effect of Solid Suspension on Flow Behavior Index (n).

The effects of solid suspension concentration on the flow behavior index (n) for all solid suspensions used are shown in figures 4-30, 4-31 and 4-32.

The flow behavior index (n) calculated for all solid suspension was found to be greater than 1, thus in the range of concentrations considered they behave as shear thickening fluid.

The flow behavior index (n) represent the slopes of the flow curves that varies with the increase of the solid suspension concentration. It is evident the increase in the concentration of solid suspension increase the flow behavior index (n), the range between (1-1.3).

Equations that describe the effect of solid suspension concentration on the flow behavior index can presented in a linear form as shown in the equations below:

The range concentration between 50-120 g/L

$$n_{\text{Bentonite}} = 0.0012 C_{\text{Bentonite}} + 0.9549 \quad R^2 = 0.9584 \quad \dots (4.11)$$

The range concentration between 30-90 g/L.

$$n_{\text{Graphite}} = 0.0036 C_{\text{Graphite}} + 0.9136 \quad R^2 = 0.6841 \quad \dots (4.12)$$

The range concentration between 300-800 g/L.

$$n_{\text{Corn starch}} = 0.0001 C_{\text{Corn starch}} + 0.9869 \quad R^2 = 0.9849 \quad \dots (4.13)$$

From the above equations and from figure 4-32 it reveal that n for Graphite suspension is more affected by concentration that other solid suspensions used in this study.

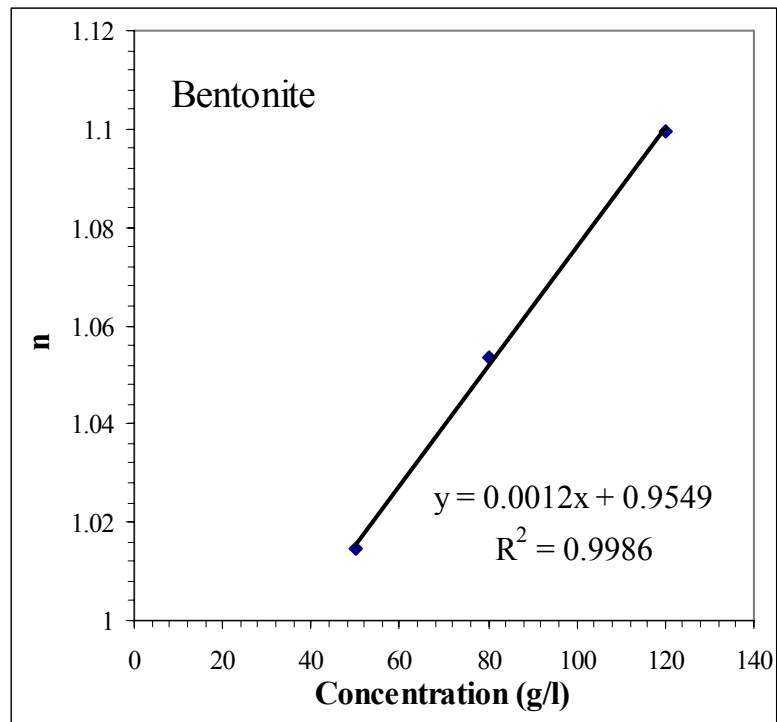


Figure 4-30 Effect the Bentonite Suspension on Flow Behavior Index at 35°C..

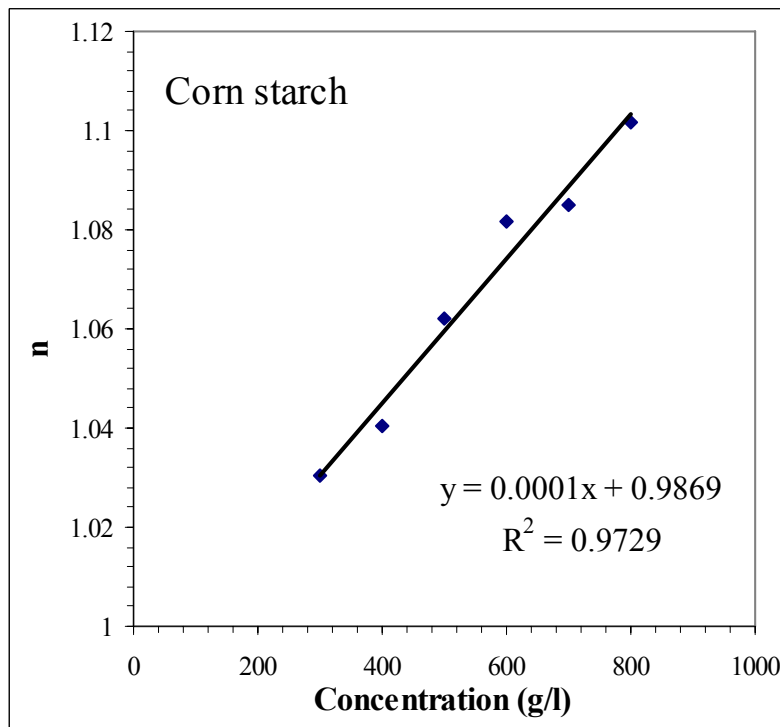


Figure 4-31 Effect the Corn Starch on Flow Behavior Index at 35°C..

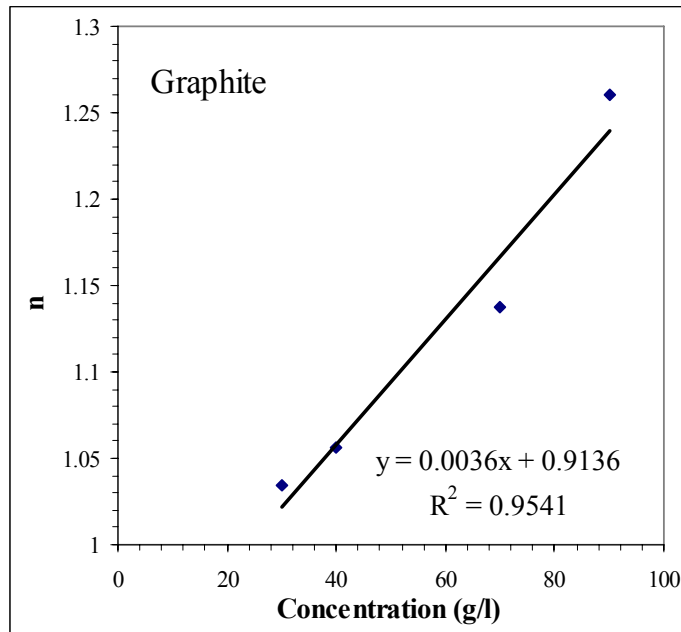


Figure 4-32 Effect the Graphite on Flow Behavior Index at 35°C..

The values of n and k , with the correlation coefficients of the best fit line (R^2) for all experiments are presented in table 4-2.

Table 4-3 Flow behavior index (n) and Consistency Index (k) at 35°C.

Material	Conc. g/l	n	k	R^2
Bentonite	50	1.0142	0.0701	0.9944
Bentonite	80	1.0537	0.1535	0.9673
Bentonite	120	1.0996	0.2262	0.9887
Graphite	30	1.0340	0.0605	0.9810
Graphite	40	1.0566	0.0561	0.9720
Graphite	70	1.1373	0.0502	0.8918
Graphite	90	1.2602	0.0256	0.8889
Corn starch	300	1.0306	0.0628	0.9800
Corn starch	400	1.0404	0.0955	0.9969
Corn starch	500	1.0620	0.0851	0.9992
Corn starch	600	1.0818	0.0825	0.9814
Corn starch	700	1.0846	0.0385	0.9541
Corn starch	800	1.1018	0.2117	1

4.3.4 Viscosity of Solid Suspension.

In figures 4-33, 4-34 and 4-35 the shear rate variation with apparent viscosity are shown for Bentonite, Graphite and Corn starch suspension. The apparent viscosity of a shear thickening solid suspensions increases as the shear rate increases.

At low shear-rates, slight shear-thinning can be observed because Antiparticles repulsion forces delay shear thickening. The low level of viscosity at these shear rates reflects the non flocculated nature of the system. At a gradually increase shear rate the viscosity begins to increase steeply. The viscosity rise by nearly an order of magnitude in the process.

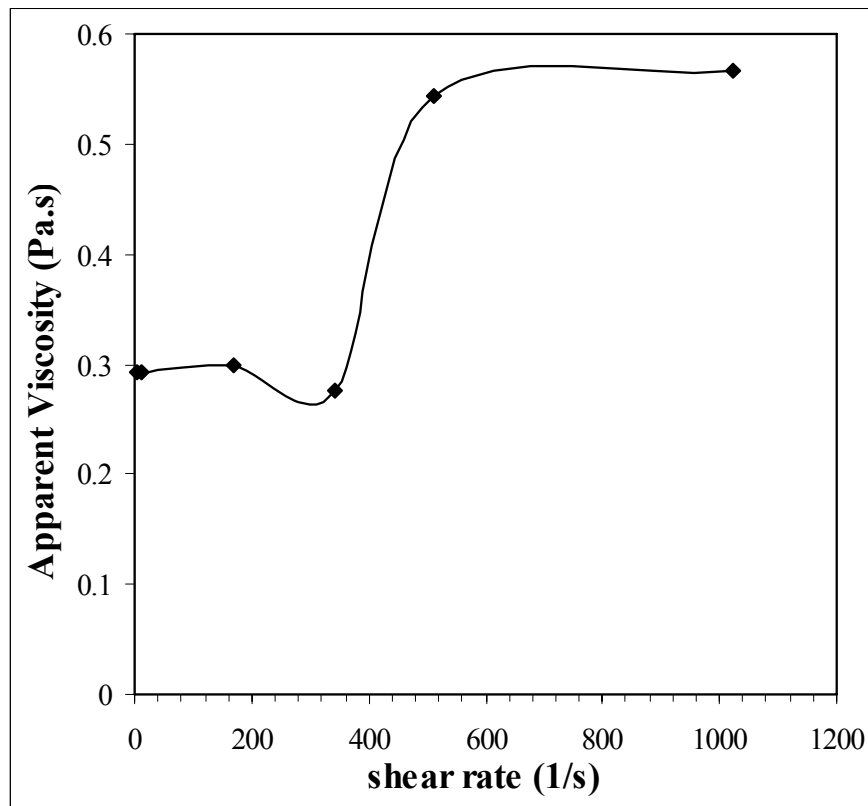


Figure 4-33 Apparent Viscosity of Bentonite Suspension at Concentration 120 g/l at 35°C.

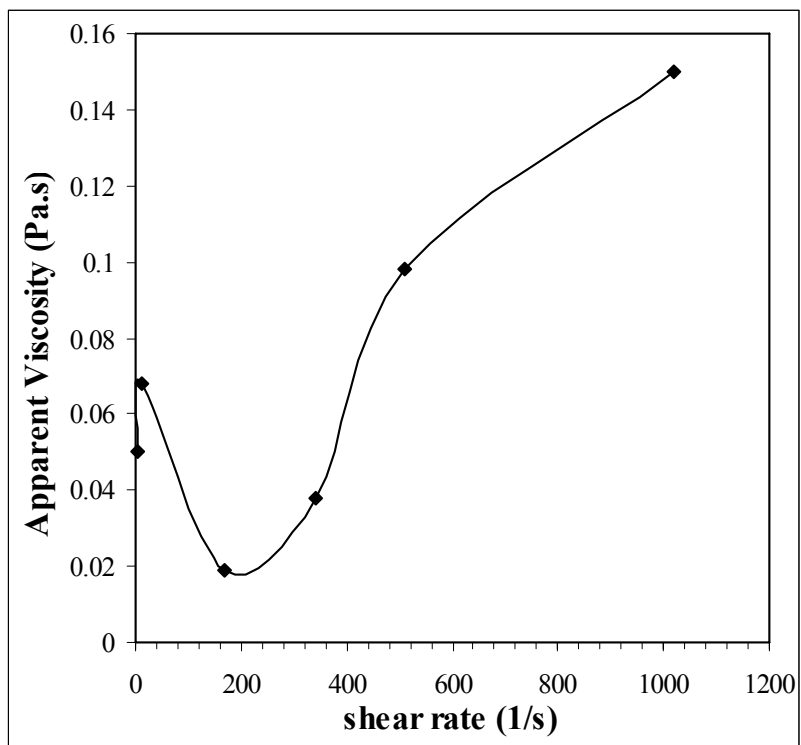


Figure 4-34 Apparent Viscosity of Corn Starch at Concentration 700g/l at 35°C

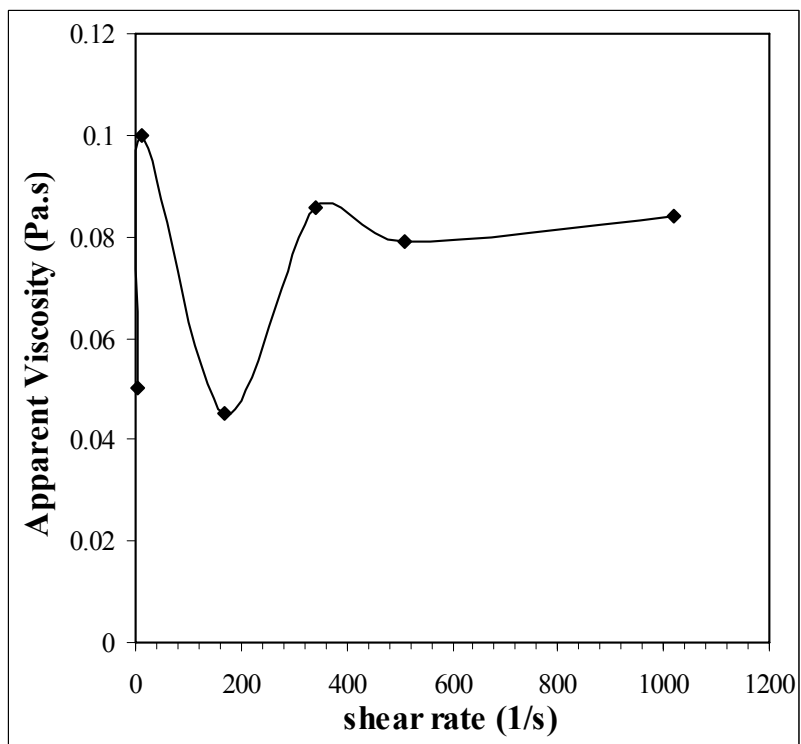


Figure 4-35 Apparent Viscosity of Graphite at Concentration 30 g/l at 35°C

4.4 Steady the Effect of Adding PVA to Bentonite.

4.4.1 General of Rheological Properties.

Figures 4-36, 4-37, 4-38, and 4-39 show the effect of adding PVA to bentonite suspension. The determination of rheological properties of Bentonite slurry (Bentonite/fresh water) systems is very important for its characterization. Bentonite dispersions have colloid structure. The control of the rheological properties of these systems is not only important from a technological but also from a scientific point of view.

The rheological properties of the Bentonite in water is shear thickening (dilatants) and the apparent viscosity increases with increased shear rate as shown that in figure 4-31. This characteristic properties are not desired technological but can be changed to gain the desired properties with the addition of various polymers.

PVA is a polymer with non-ionic structure, which is dissoluble in water. Non-ionic polymer does not interact electrostatically with charged bentonite particles. The polymer molecules can attach or anchor on the particle surfaces and into the interlayer. Adsorption of the polymer on charged surface of the clay particles leads to significant modification of the charge distribution in the electrical double layer.

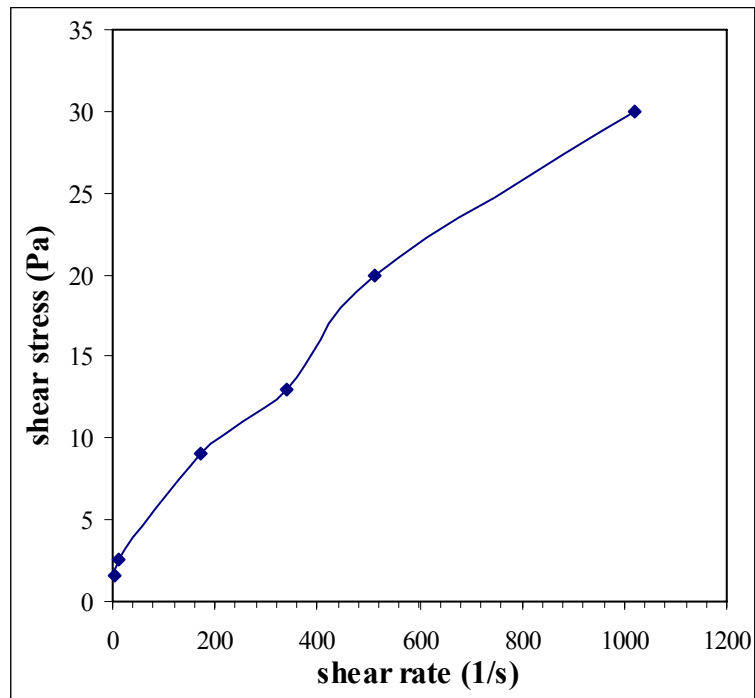


Figure 4-36 Changing Result From The Shape in Flow Curve Caused by Adding 2g/0.5L PVA Polymer to Bentonite Slurry at 35°C..

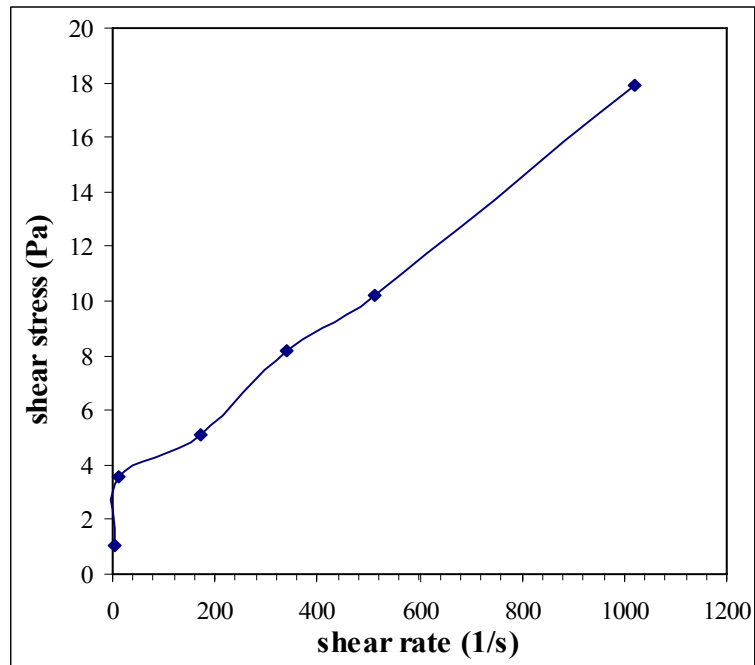


Figure 4-37 Changing Result From The Shape in Flow Curve Caused by Adding 5 g/0.5L PVA Polymer to Bentonite Slurry at 35°C..

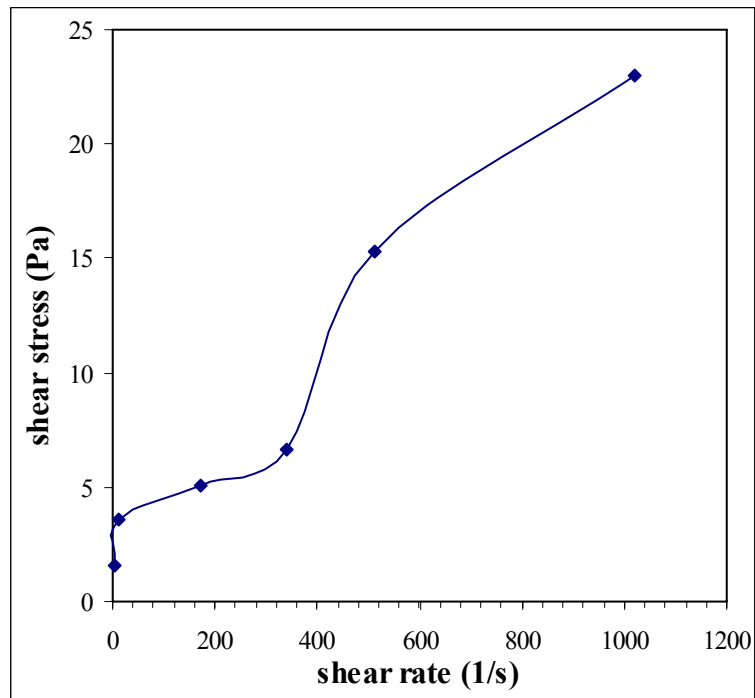


Figure 4-38 Changing Result From The Shape in Flow Curve Caused by Adding 7 g/0.5L PVA Polymer to Bentonite Slurry at 35°C..

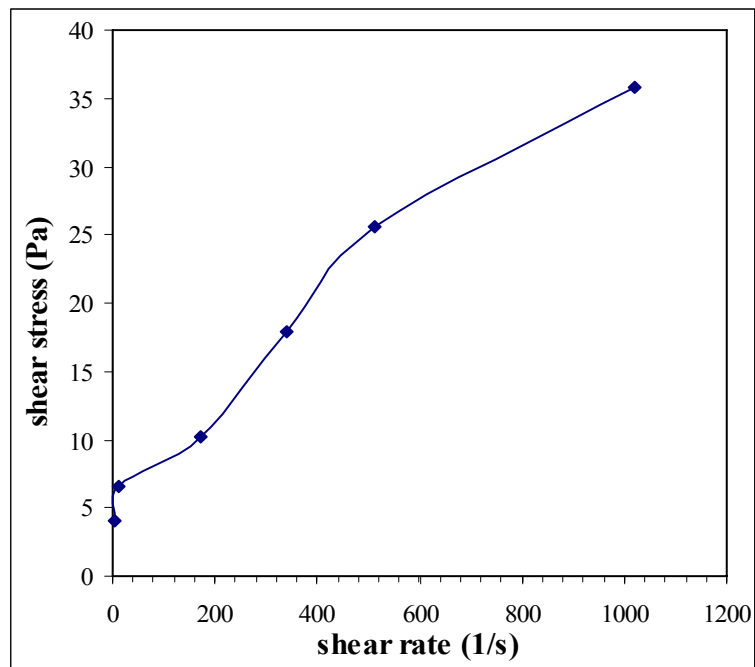


Figure 4-39 Changing Result From The Shape in Flow Curve Caused by Adding 10g/0.5L PVA Polymer to Bentonite Slurry at 35°C..

4.4.2 Flow Model Selection.

The selection of the flow model that best fit the rheological behavior is useful for treating experimental data or for describing flow behavior. In this work a new method is used, which is proposed by Morrison (2005). This method uses the Solver Add-in in Microsoft Excel to optimize the solution.

The basic outlines of this method include [65]:

1. begin by arranging the experimental data in the excel spreadsheet. will use two columns, one for shear rate and one for shear stress.
2. create a column that has a predicted value of shear stress calculated from a considered flow model. Since we do not know the values of any of our model parameters, we will start with some guesses.
3. now need to create a new column for the square of the deviation between the actual shear stress and the predicted value. add up all the values in the error column and put that value in a cell.
4. The solver function in the excel is set up to minimize the error cell mentioned above. Solver will replace our initial guesses with optimized values.

The solver allow us to put constrains on the ways in which it manipulate the cells it is changing. For our work we know that none of the model parameters may be negative, so we put this as a constraint.

The results for using the add-in in Microsoft excel for the Bentonite/PVA are shown in table 4-4. From this table, one can conclude that the Bingham plastic model best fits the experimental results (lower value in sum of square error). So this model will be considered in the following sections.

Figures 4-40 to 4-43 illustrate the results of using the solver add-in in Microsoft Excel for adding different concentration of PVA (2, 5, 7 and 10) g/0.5l to Bentonite at 40 g/0.5l respectively.

Of the models listed in table 4-5 use the solver Add-in in Microsoft Excel to optimize the solution. the Newtonian is the simplest. It fits water, solvents and many polymer solutions over a wide strain rate range. The plastic or Bingham body model predicts constant plastic viscosity above a yield stress. This model works for a number of dispersions including some pigment pastes. Yield stress, τ_o , and plastic (Bingham) viscosity, $\eta_p = (\tau - \tau_o) / \dot{\gamma}$, may be determined from the intercept and the slope beyond the intercept, respectively, of a shear stress versus shear rate plot [5].

The power law, $\tau = k\dot{\gamma}^n$, is widely used as a model for non-Newtonian fluids. It holds many solutions and can describe Newtonian, shear-thinning, and shear-thickening behavior, depending on the power factor, n, also called the flow behavior index.

The power model can be extended by including the yield value $\tau - \tau_o = k\dot{\gamma}^n$ and the Robertson- stiff model is the last using in the Solver Add-in in Microsoft Excel program. The equation of model $\tau = A(\dot{\gamma} + C)^B$, A, B and C is the variable parameter

Table4-4 Model Selection for (Bentonite/PVA) Using Add-in Solver Microsoft Excel.

Exp. No.	Conc. (g /l)	Sum of Square Error				
		Newtonian	Bingham	Power Law	With Yield	Robertson
74	(2+40)	1.911	0.172	0.403	0.224	0.483
75	(5+40)	1.858	0.489	0.500	0.859	0.856
76	(7+40)	1.850	0.377	1.283	1.977	1.450
77	(10+40)	1.928	0.131	0.298	0.440	0.383

Table 4-5 Flow Equations for Flow Models [5].

Flow model	Flow equation	Equ. no.
Newtonian	$\tau = \eta \dot{\gamma}$...(4.8)
Bingham plastic	$\tau - \tau_o = \eta \dot{\gamma}$...(4.9)
Power law	$\tau = k \dot{\gamma}^n$...(4.10)
Modified power law	$\tau - \tau_o = k \dot{\gamma}^n$...(4.11)
Robertson – Stiff	$\tau = A (\dot{\gamma} + C)^B$...(4.13)

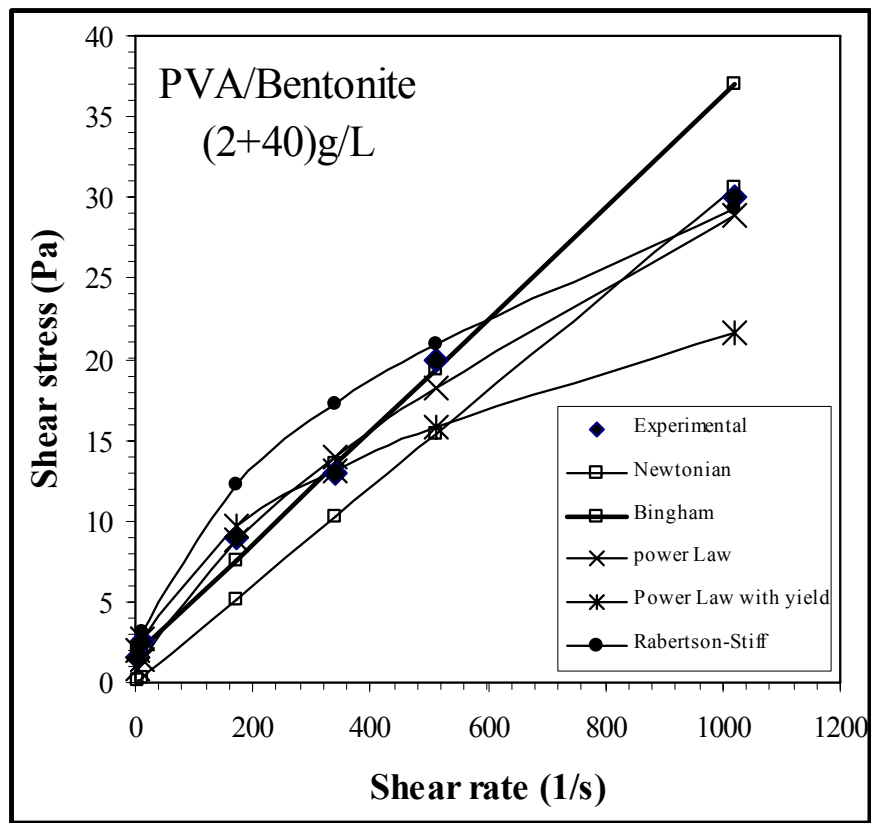


Figure 4-40 Experimental Results and Flow Models Representation For PVA/ Bentonite Suspension at Concentration (2+40) g/l at 35°C.

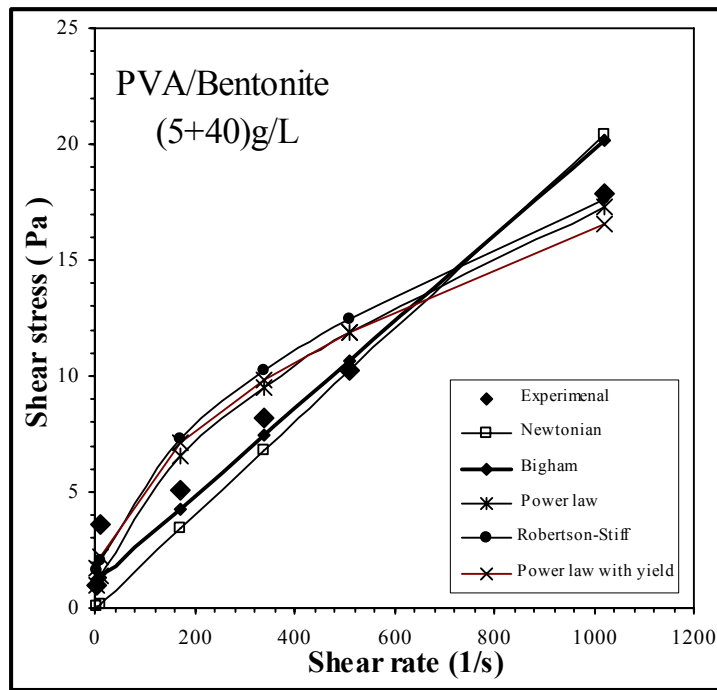


Figure 4-41 Experimental Results and Flow Models Representation For PVA/ Bentonite Suspension at Concentration (5+40) g/l at 35°C.

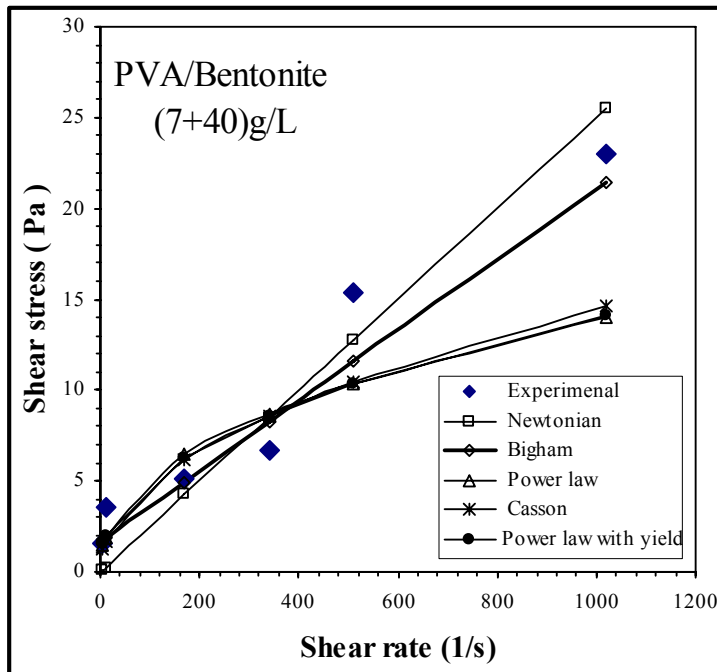


Figure 4-42 Experimental Results and Flow Models Representation For PVA/ Bentonite Suspension at Concentration (7+40) g/l at 35°C.

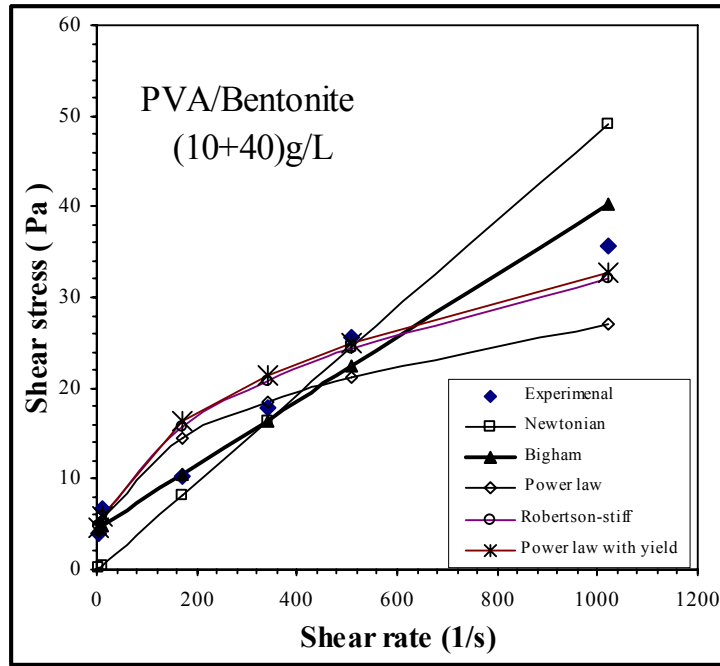


Figure 4-43 Experimental Results and Flow Models Representation For PVA/ Bentonite Suspension at Concentration (10+40) g/l at 35°C.

4.4.3 Bingham Model.

The Bingham model is widely used as a model for describing viscoplastic fluids exhibiting a yield response. Also Bingham model can describe Newtonian fluid, shear thinning and shear thickening behavior.

The ideal Bingham material is an elastic solid at low shear stress values and a Newtonian fluid above a critical value called the Bingham yield stress, τ_B . The plastic viscosity region exhibits a linear relationship between shear stress and shear rate, with a constant differential viscosity equal to the plastic viscosity, η_p . If subjected to shear stress smaller than the yield stress, they retain a rigid structure and do not flow. It is only at stresses in excess of the yield value that flow occurs. In the case of a Bingham plastic model, the shear rate is proportional to shear stress in excess of the yield stress.

$$\tau = \tau_B + \eta_p \cdot \dot{\gamma} \quad \dots (4.14)$$

The experimental results are shown in figures 4-44 to 4-47. Which are plot of shear stress versus shear rate in Bingham plastic model at concentration (2, 5, 7 and 10) g/0.5L adding 40 g/0.5L Bentonite slurry.

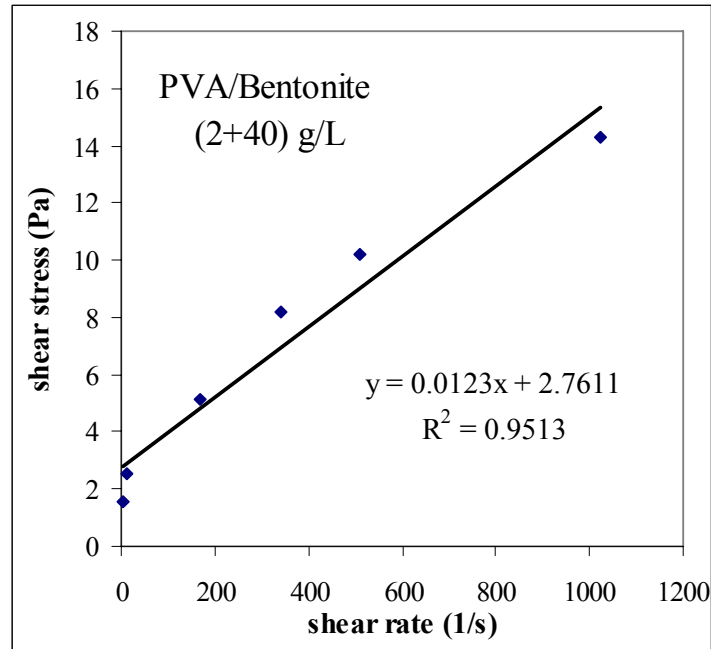


Figure 4-44 Rheogram for PVA/Bentonite Suspension at Concentration (2 in 40) g/L at 35°C.

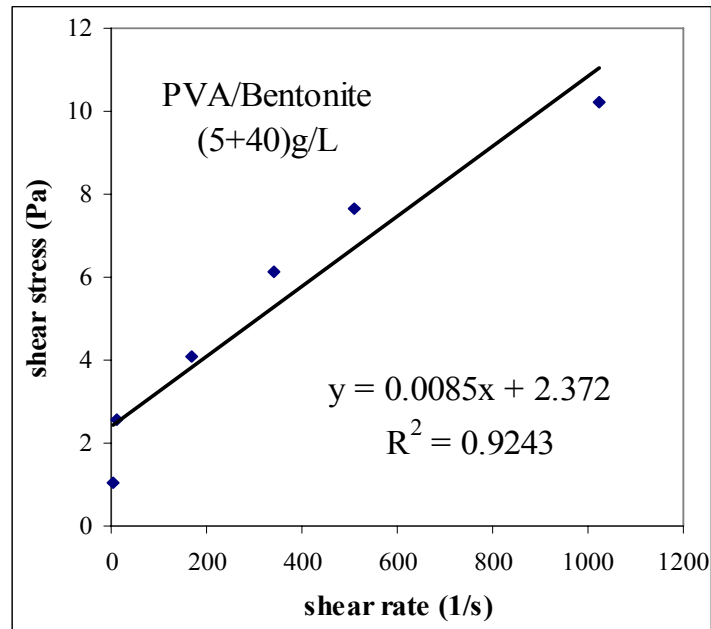


Figure 4-45 Rheogram for PVA/Bentonite Suspension at Concentration (5 in 40) g/L at 35°C.

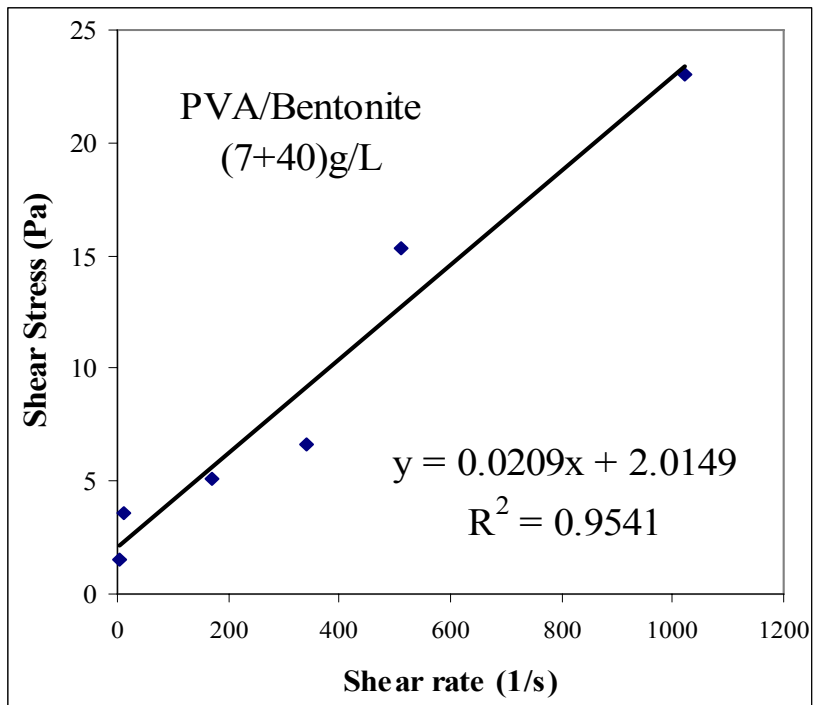


Figure 4-46 Rheogram for PVA/Bentonite Suspension at Concentration (7 in 40)g/L at 35°C.

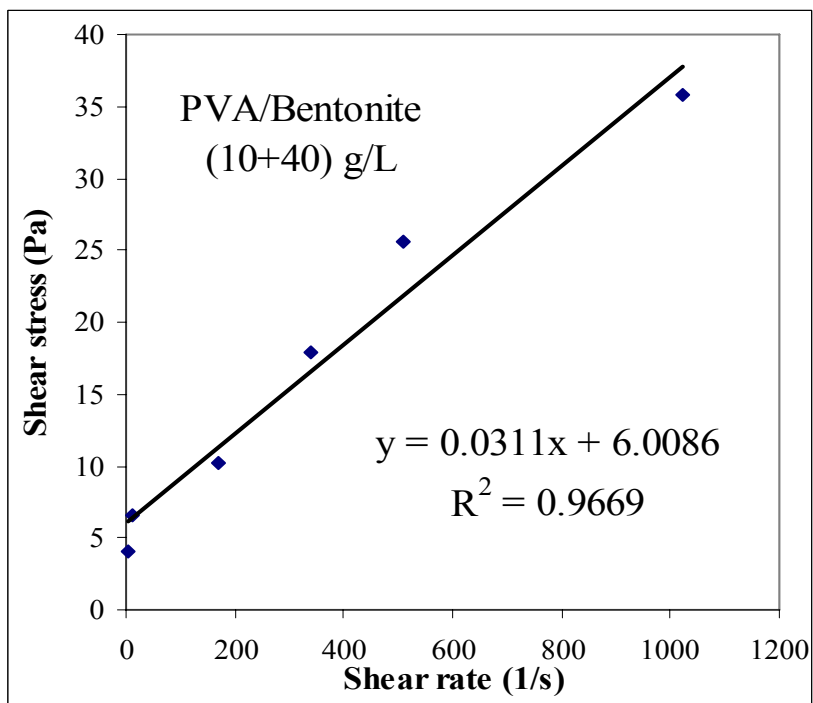


Figure 4-47 Rheogram for PVA/Bentonite Suspension at Concentration (10 in 40)g/L at 35°C.

4.4.4 Effect Concentration PVA Polymer on Bingham Yield Stress.

The effects of concentration of PVA polymer on the Bingham yield stress is shown in figure 4-48. It is clear from figure 4-48, that the Bingham yield stress decreases when adding PVA polymer, when the concentration reaches 14-15g/l the yield stress start to increase.

The polymer molecules can attach or anchor on the particle surfaces and into the interlayer. Adsorption of the polymer on charged surface of the clay particles leads to significant modification of the charge distribution in the electrical double layer.

When PVA was added to the dispersions, a decrease in initial yield value was observed, showing an interaction between polymer molecules and Bentonite particles. PVA behaved like a salt and decreased the double layer thickness of thin particles. This caused a decrease in electro viscous effect and yield values of dispersions decreased to a minimum (14-15) g/l polymer concentrations. An increase was observed after addition of more concentration of PVA polymer.

Rossi, et. al., [35] concluded that the reason was that the bridge flocculation made by two Bentonite particles with their surrounding polymer extensions when they approached each other. The entanglement of adsorbed polymer chains may also occur and result in high system viscosity. The increase of yield value was an indicator of a net structure formed in the dispersions. This decrease was related to the steric push that occurred between PVA covered clay particles.

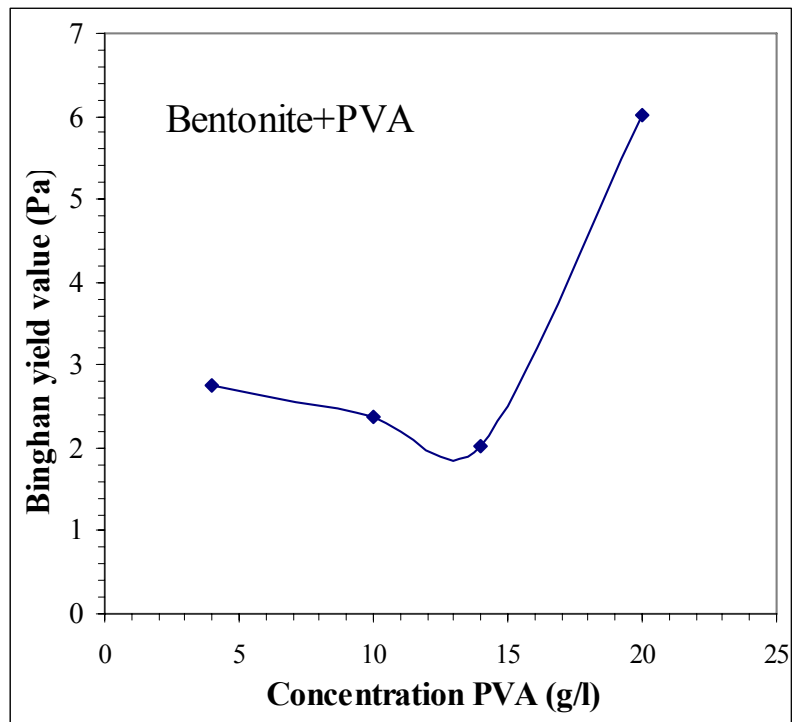


Figure 4-48 The Influence of PVA on The Bingham Yield Value of 8% (w/w) Bentonite Water System at 35°C..

4.4.5 Apparent Viscosity of PVA/Bentonite.

The change of apparent viscosity as a function of shear rate are shown in figure 4-49 to 4-52 . The effect of PVA polymer on the rheological properties of the Bentonite slurry was modifier the data for apparent viscosity. This experimental evidence shows that the apparent viscosity of Bentonite/PVA decreases with increasing shear rate, while the experimental data for Bentonite/water (with out polymer) show that increase of apparent viscosity with increase in shear rate, see figure 4-33 . Kadaster, et. al., [66] concluded that at low concentration of added PVA polymer chains bridge Bentonite particles resulting, apparent viscosity is slightly increase and at high concentration of

PVA polymer, however enough polymer chains are adsorbed on the clay surface to leave few free surface site for a single polymer chain to bridge two particles.

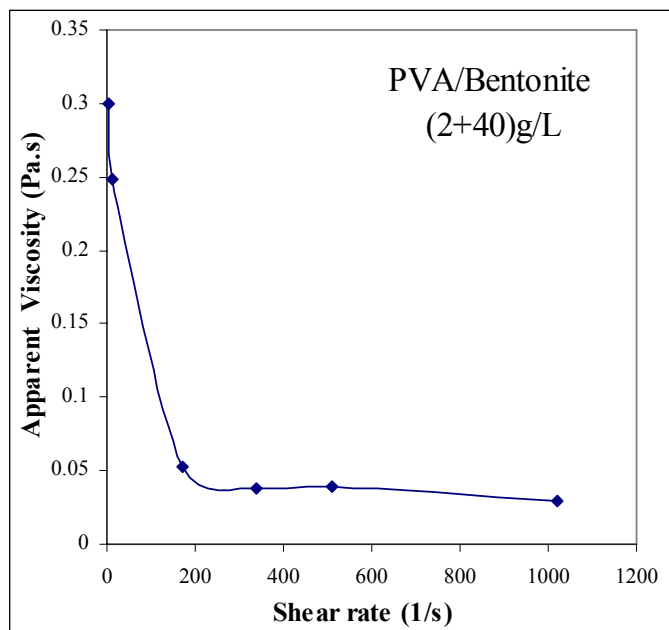


Figure 4 -49 Viscosity as a Function of Shear Rate for Bentonite/ PVA Polymer at Concentration (2 in 40) g/L at 35°C.

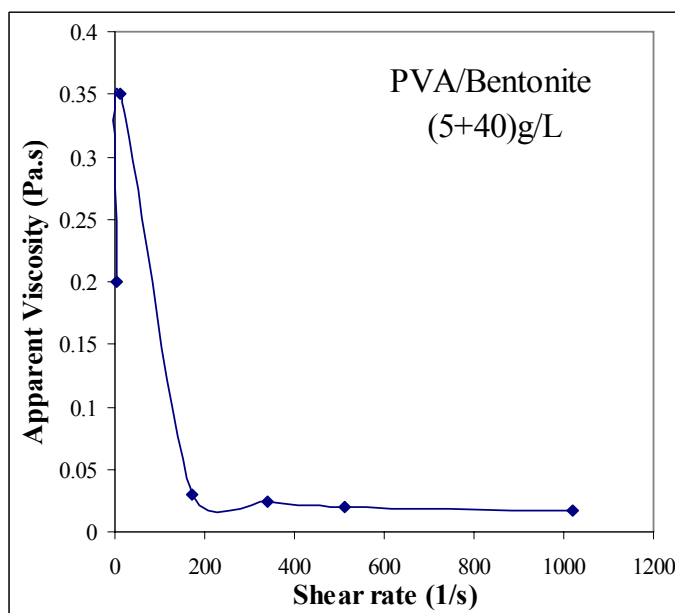


Figure 4 -50 Viscosity as a Function of Shear Rate for Bentonite/ PVA Polymer at Concentration (5 in 40) g/L at 35°C.

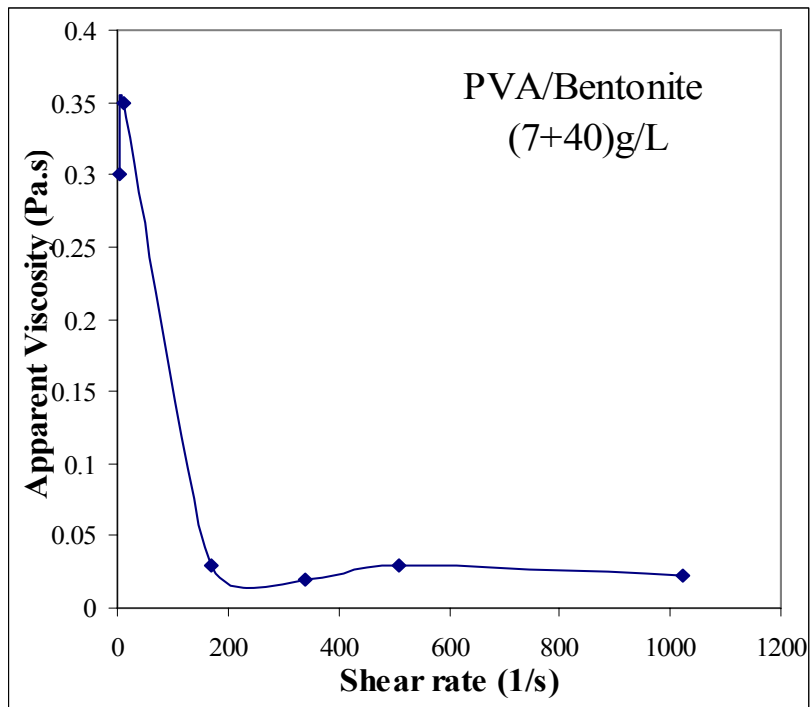


Figure 4 -51 Viscosity as a Function of Shear Rate for Bentonite/ PVA Polymer at Concentration (7 in 40) g/L at 35°C.

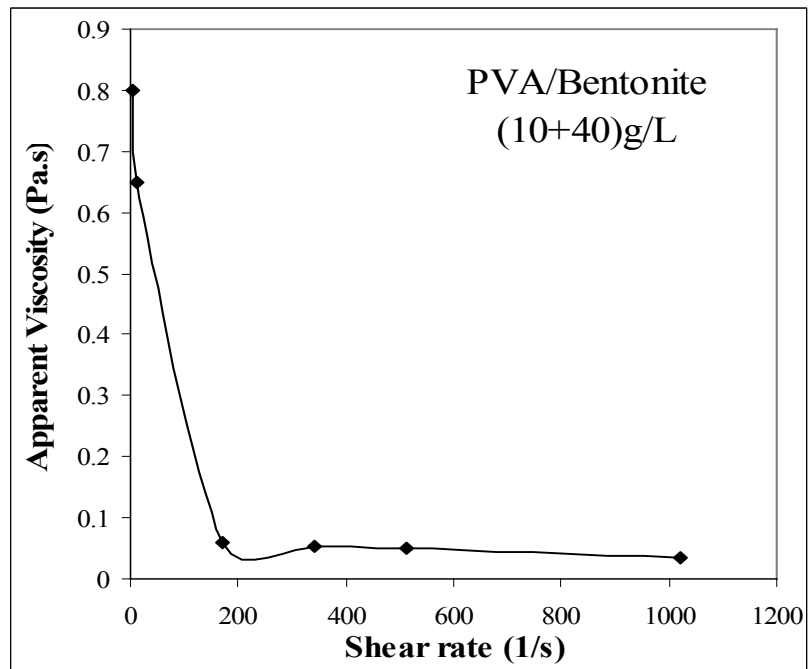


Figure 4 -52 Viscosity as a Function of Shear Rate for Bentonite/ PVA Polymer at Concentration (10 in 40) g/L at 35°C.

Chapter Five

Conclusions and Recommendations for Future Work.

5.1 Conclusions.

From the present study, one can conclude the followings:

1. All polymer solutions used in this work (XC-polymer, Carboxymethyl cellulose and Hydroxyethyl cellulose) behave as shear-thinning fluid, in which the viscosity decrease as the shear rate increase and all solid suspensions used in this work (Bentonite, Graphite and Corn starch) behave as shear-thickening fluid, in which the viscosity increase as the shear rate increase.
2. As the polymer and solid suspension concentrations are increased, the flow behavior index (n) are decreased and increased respectively. This behavior reflects the fact that as the polymer concentration increases the solution become far from Newtonian behavior. New correlations were developed, which describe the effect of polymer and solid suspensions concentration on the flow behavior index (n) for each polymer and solid used in this study.
3. XC-polymer solutions have a higher viscosity, and its viscosity decreases much more than other polymer solutions used in this study.
4. By using the Solver Add-in in Microsoft Excel, the Bingham plastic flow model was found to be the best fit to the experimental results of added Bentonite/PVA.
5. By adding PVA to bentonite suspension, the suspension turned from shear thickening behavior to shear thinning behavior.

6. The Bingham yield point is found firstly decreases and suddenly increase with increasing PVA concentration, while the plastic viscosity decreased.

5.2 Recommendations for Future Works.

1. Studying the rheological properties at different (lower or higher) shear rates used in this work, this may have useful industrial applications.
2. Using other methods (rather than standard rheometric techniques), such as particle tracking method to study the rheological properties of polymer solutions.
3. Studying the effect of temperature on the rheological properties of Bentonite/polymer solutions.
4. Studying the effect of adding (rather than PVA) to bentonite suspension.

References

- 1 Dalwadi, D. H., Ch. Ganet, N. Roye and K. Hedman, “Rheology: an Important Tool in Ink Development”, American Laboratory, November (2005).
- 2 Chhabra, R. P. and Richardson, J. F., “Non-Newtonian Flow in the Process”, (1999).
- 3 Zou L. and C. Hunt, “Rheology Testing of Solder Pastes and Conductive Adhesives-A Guide”, Centre for Materials Measurement and Technology National Physical Laboratory, (2002) pp.3.
- 4 Harrison, G., V. Franks, V. Tirtaatmadj, and D. Boger, “Suspensions and Polymers – Common Links in Rheology”, Korea-Australia Rheology Journal, Vol. 11, No. 3 (1999) pp. 197-218.
- 5 Kirk-Othemer, “Encyclopedia of Chemical Technology”, 4th edition, Vol. 21, John Wiley and Sons (1998).
- 6 Tadros T. F., “Control of Stability/Flocculation and Rheology of Concentrated Suspensions”, Pure and Appli. Chem., vol. 64, No. 11 (1992) pp. 1715-1720.
- 7 İşçi, S., C. Unlu, O. Atici, and N. Gungor, “Rheology and Structure of Bentonite-Polyvinyl Alcohol Dispersion”, Bull. Mater. Sci., Vol. 29, No.5 (2006).
- 8 Achimescu, D., M.Sc., “Rheology of Quick Sand and Polyethylene Oxide”, Department of Chemical Engineering, University of Amsterdam, (2004).
- 9 Cunningham, N., Brookfield Engineering,
<http://www.rheologyschool.com>

- 10 Steffe, J. F., “Rheological Methods in Food Process Engineering”, 2nd Edition, Freeman press (1996).
- 11 Mazzeo, F., “Characterizing Pressure Sensitive a Phesives Using Rheology”. <http://www.Pstc.org/papers/pdfs/mazzeo.PDF>
- 12 Rheology of Concentrated Lamellar Dispersions.
<http://dissertations.ub.rug.nl/files/faculties/science/1998/j.kevelan/C5.pdf>
- 13 Perry, R. H. and D. W. Green, “Perry s Chemical Engineers Hand Book”, seven editions, Mc Graw Hill, New York, (1997).
- 14 Barnes, H. A., “An Introduction to Rheology”, Elsevier Science Publisher B. V., First Edition, (1989).
- 15 Barnes, H. A., “A Hand Book of Elementary Rheology”, Published by the University of Wales Institute of Non-Newtonian Fluid Mechanics, Department of Mathematics, First edition, (2000).
- 16 Leblanc, G. E., R. A. Secco and M. Kostic, “Viscosity Measurement”, Crc. Press Llc, (1999) pp. 1-24.
- 17 Tihminlioğlu, “Viscosity of Newtonian and Non-Newtonian Fluids”, Izmir Institute of Technology, Chemical Engineering Laboratory I, Spring Semester (2008-2009).
- 18 Holland, F. A. and R. Bragg, “Fluid Flow for Chemical Engineers”, 2nd Edition, Arnold Inc. (1995).
- 19 Tuomo, M.Sc, “Dispersing of Kaolin Slurry in a Laboratory Environment”, May (2007) pp.7-47.
- 20 R. Shankar Subramanian, “Non-Newtonian Flows”.
<http://web2.clarkson.edu/projects/subramanian/ch301/notes/nonnewtonian.pdf>

- 21 Viswanath, D. S., D. H. L. Prasad, N. K. Dutt, K. Y. Rani, T. K. Ghosh, “Viscosity of Liquids Theory, Estimation, Experiment, and Data”, Published by Springer, (2007).
- 22 Xia, S. S., M.Sc. “The Rheology of Gel Formed During the California Mastitis Test”, Department of Engineering the University of Waikato Hamilton, New Zealand August (2006).
- 23 Ryan D. Welsh, B. S., “Viscoelastic Free Surface Instabilities During Exponential Stretching”, the Massachusetts Institute of Technology, Mechanical Engineering University of Cincinnati, December (2001).
- 24 Fluid characterization using Viscometers and Rheometers.
http://infohost.nmt.edu/~mecheng/Fluids_LAB_Website/lab6and7.pdf
- 25 rheology of a shear thickening wormlike micellar system.
<http://www.ucl.ac.uk/euromech492/presentations/fischer.pdf>
- 26 Rashaida, A. A., Ph.D., “Flow of a Non-Newtonian Bingham Plastic Fluid over a Rotating Disk”, University of Saskatchewan the Department of Mechanical Engineering, August (2005).
- 27 Gowariker, V. R., N. V. Viswanathan and J. Sreedhar, “Polymer Science”, John Wiley and sons (1986).
- 28 Lauzon, R., “Water-Soluble Polymer for drilling Fluids”, Oil and Gas Journal, April (1982).
- 29 Vanderbilt Company, Inc., “Rheology Control Additive”.
<http://www.rtvanderbilt.com/wwwprd/No920CD.pdf>
- 30 Gray, G. R. and H. C. H. Darley, “Composition and Properties of Oil Well Drilling Fluids”, Fourth Edition, Gulf Publishing Co., Houston (1981).

- 31 Grassino, S. B., "Polymer Gels and solutions", University of Southern Mississippi. <http://www.pslc.ws/macrog/property/solpol/ps1.htm>
- 32 Alloncle, M., J. Lefebvre, G. Llamas and J. L. Doublier, "A Rheological Characterization of Cereal Starch-Galactomannan Mixtures", American Association of Cereal Chemists, Inc., Vol. 66, No. 2, (1989) pp. 90-93.
- 33 Hassan, B. H., "Viscometric Behavior of Single Strength and Concentrated Date-Water Extracts", J. King Saud Univ., vol. 4, Agric. Sci. (1), (1992) pp. 3-13.
- 34 Petrov, G. and G. Denkovski, "The Power Law for Some Polyacrylonitrile Solutions", Bulletin of the Chemists and Technology of Macedonia, Vol. 14, No. 1, (1995) pp.1-6.
- 35 Rossi, S., P. F. Luckham, S. Zhu, B. J. Briscoe and TH. F. Tadros, "Influence of Low Molecular Weight Polymers on the Rheology of Bentonite Suspension", Revue De L' Institute François Du PÉtrole, VOL. 52, No. 2, Mars-April, (1997) pp. 199-206.
- 36 Heller, H. and R. Keren, "Anionic Polyacrylamide Polymers Effect on Rheological Behavior of Sodium-Montmorillonite Suspensions", SOIL SCI. SOC. AM. J., Vol. 66, 2002 pp 19–25.
- 37 James, D. F. and Brian C. Blakey, "Comparison of the Rheologies of Laterite and Goethite Suspension", Korea- Australia Rheology Journal, Vol. 16, No. 3, (2004) pp. 109-115.
- 38 Alemdar A., N. Öztekin, F. B. Erim, Ö. I. Ece and N. Güngör, "Effects of Polyethylene Mine Adsorption on Rheology of Bentonite Suspensions", Indian Academy of Sciences, Vol. 28, No. 3, June (2005), pp. 287–291.

- 39 Tapadia, P. and Wang, “Direct Visualization of Continuous Simple Shear in Non-Newtonian Polymeric Fluids”, The American Physics Society, Vol. 96 (2006).
- 40 Song, K., H. Kuk, and G. Chang, “Rheology of Concentrated Xanthan Gum Solutions: Oscillatory Shear Flow Behavior”, Korea-Australia Rheology Journal, Vol. 18, No. 2 (2006) pp. 67-81.
- 41 Sarraf H., J. Havrda “Rheological Behavior of Concentrated Alumina Suspension (Effect of Electrosteric Stabilization)”, Department of Glass and Ceramics, Institute of Chemical Technology Prague, Vol. 51, No. 3, (2007) pp. 147-152.
- 42 Liu W., L. Cheng, H. Zhang, Y. Zhang, H. Wang and Yu. Mingfang “Rheological Behaviors of Polyacrylonitrile /1-Butyl-3 Methylimidazolium Chloride Concentrated Solutions”, International Journal of Molecular Sciences Issn 1422-0067, Vol. 8, (2007) pp. 180-188.
- 43 Deosarkar, M. P. and K. C. Ghanta, “Rheological Characteristics of Solid-liquid Suspension–Comparison Between Empirical Models and Artificial Neural Network (ANN) Model”, IE(I) Journal-CH, Vol. 88, March (2008) pp. 33-38.
- 44 Koos E., M. L. Hunt and Ch. E. Brennen, “Shear Stress Measurements of Non-Spherical Particles in High Shear Rate Flows”, American Institute of Physics, Vol.19, Jul (2008) pp.740-742.
- 45 Dr. Muhanned A. R. Mohammed and Areej J. Mohamed, Thesis M.Sc., “Effect of Concentration of Water-Soluble Polymer Solutions on Rheological Properties”, Al- Nahrain University, Chemical Engineering, (2008).

- 46 Measuring Instruments for Testing Drilling Mud, Cement Slurries and Fracturing Fluids, Friedrich Leutert GmbH and Co. KG.
Internet: www.Leutert.com. E mail: info@Leutert.com.
- 47 Miller, E., Ph.D., “The Dynamic and Rheology of Shear Bending Wormlike Micelles and Other Non-Newtonian Fluids”, Mechanical and Industrial Engineering, May (2007).
- 48 “Sheridan Vilt, “Rheology Its Importance Today”.
http://www.fann.com/public1/pubsdata/Brochures/Viscometer_Info2.pdf
- 49 Nick Triantafillopoulos, “Measurement of Fluid Rheology and Interpretation of Rheograms”, Kaltec Scientific, Inc., Second Edition Paper Trade J. 126, Vol. 23, 1948 pp. 60-66.
- 50 Fann Viscometer, Model 35A Manual.
<http://www.expotechusa.com/manuals/fann/35496.pdf>
- 51 Macosko, Ch.W., “Rheology Principles, Measurements and Applications”, Published Simultaneously in Canada, (1994).
- 52 Ball, D. J., M. T. Hutchinson, S. A. Jefferis, P. G. Shotton, L. Satisfied (Chairman) and A. J. Wills, “ Bentonite Support Fluids”, Federation of Piling Specialists, 2nd edition, January (2006).
- 53 Adamis Z., f. Jozse and R. B. Williams, “Bentonite, Kaolin and Selected Clay Minerals”, American of the World Health Organization, (2005).
- 54 Refined Corn Products. <http://www.corn.org>
- 55 Kalyoncu, R. S. “Graphite”, V. S. Geological Surrey Professional, (1998) pp.820.
- 56 Chattergi, J. and J. K. Borchardt, “Applications of Water-Soluble Polymers in the Oil Field”, Journal of Petroleum technology, November (1981).

- 57 “Aqualon Sodium Carboxymethyl Cellulose”, Hercules Incorporated (1999). http://www.herc.com/aqualon/product_data/brochures/250_10.pdf.
- 58 Vanderbilt Company, Inc., “Rheology Control Additive”. <http://www.rtvanderbilt.com/wwwprd/No920CD.pdf>
- 59 Xanthan Gum.
http://en.wikipedia.org/wiki/Xanthan_gum
- 60 Vanzan Xanthan Gum (2007).
<http://www.rtvanderbilt.com/vanzan.pdf>
- 61 Grillet, A. M. and Shaqfeh E. S. G., “Observations of viscoelastic instabilities in recirculation flows of Boger fluids”, Journal of Non-Newtonian Fluid Mechanics, Vol. 64, (1996) pp. 141-155.
- 62 Malkin, A. Y., “Rheology Fundamentals”, Chem. Tec Publishing, (1994) pp.87.
- 63 Choi, S. K., M.Sc., “pH Sensitive Polymer for Novel Conformance Control and Polymer Flooding Applications”, The University of Texas at Austin, August (2008).
- 64 Leuven, k. U. and Belgium, “Shear Thickening Effects in Concentrated”, Dept. Chemical Engineering, pp. 1-21.
- 65 Morrison, F. A., “Using the Solver add-in in Microsoft Excel”, Michigan Technological University (2005).
http://www.chem.mtu.edu/~fmorriso/cm4650/Using_Solver_in_Excel.pdf
- 66 Kadaster, A. G., Gullid, G. J., Hannl, C. L. and Schmidt, D. D., “Field Application of PHPA Muds” SPE Drilling Engineering, September (1992).

Appendix A:

The Flow Curves of the Experiments (Shear Stress versus Shear Rate).

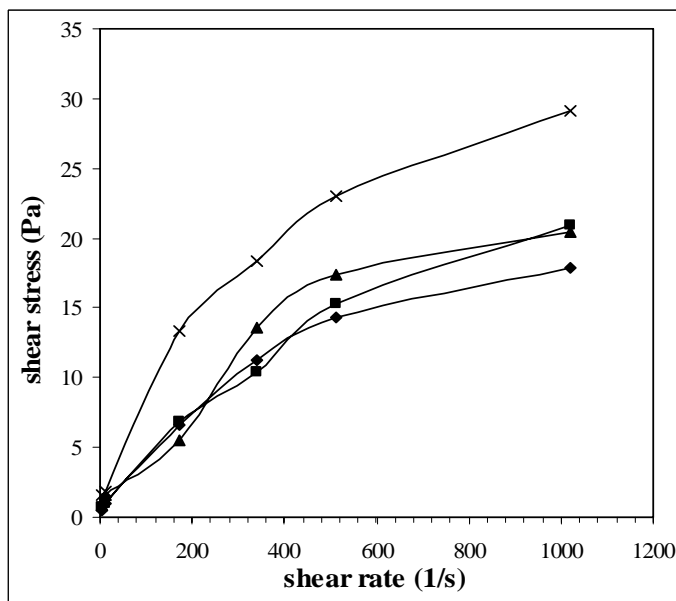


Figure A-1 Shear Stress versus Shear Rate for CMC Polymer at 4, 7, 10 and 15 g/l.

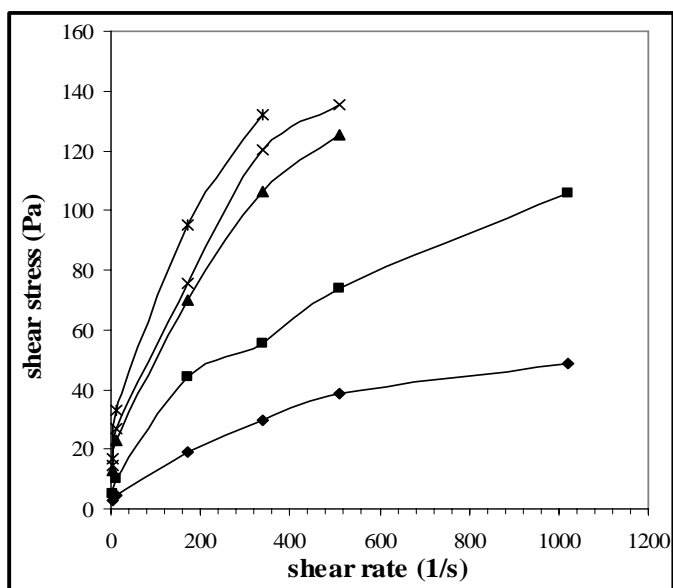


Figure A-2 Shear Stress versus Shear Rate for CMC Polymer at 20, 25, 30, 35 and 40 g/l.

The Flow Curves of the Experiments (Shear Stress versus Shear Rate).

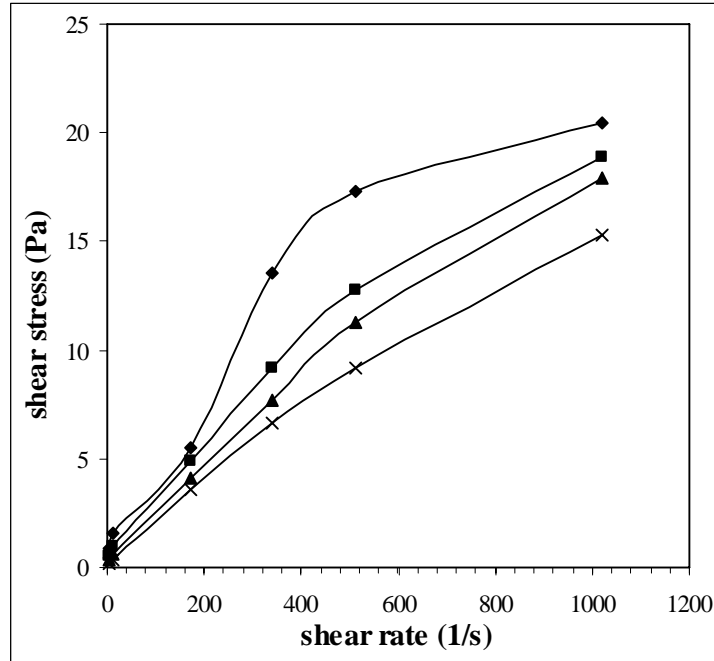


Figure A-3 Shear Stress versus Shear Rate for CMC Polymer in 10 g/l at 20, 35 45 and 55°C.

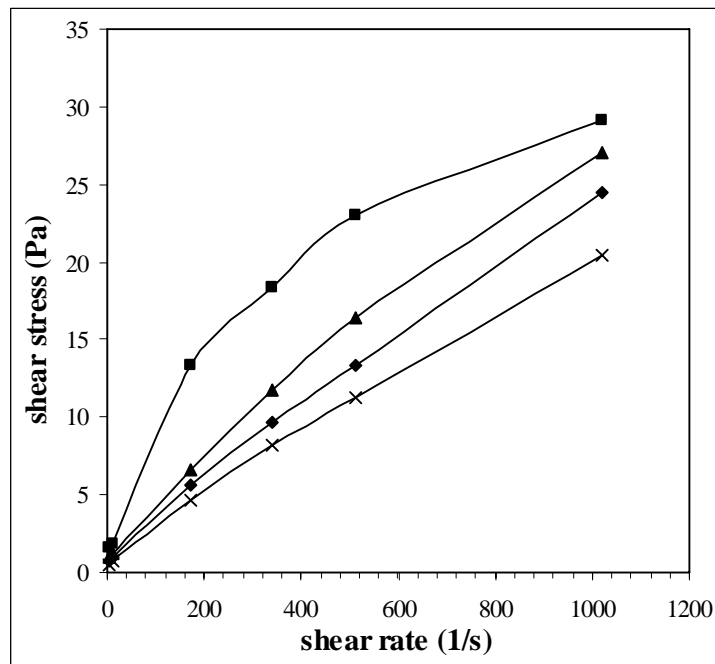


Figure A-4 Shear Stress versus Shear Rate for CMC Polymer in 15 g/l at 20, 35 45 and 55°C.

The Flow Curves of the Experiments (Shear Stress versus Shear Rate).

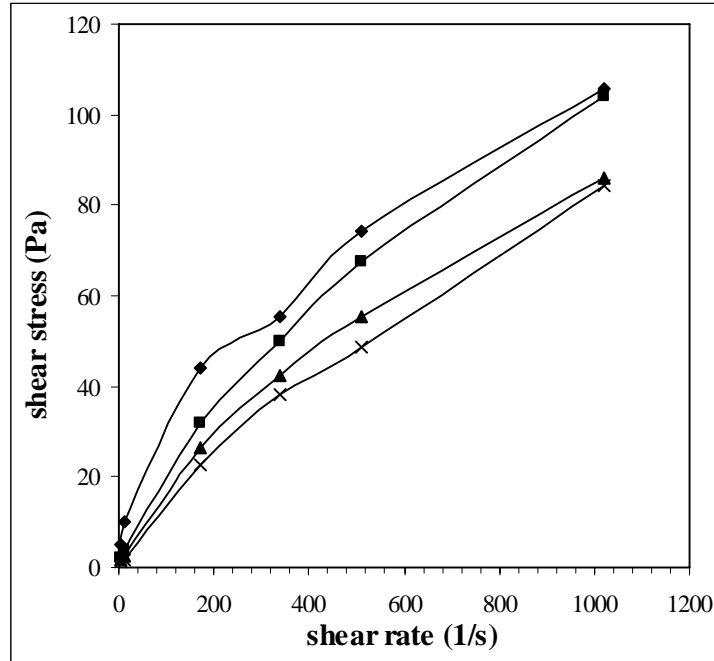


Figure A-5 Shear Stress versus Shear Rate for CMC Polymer in 25 g/l at 20, 35 45 and 55°C.

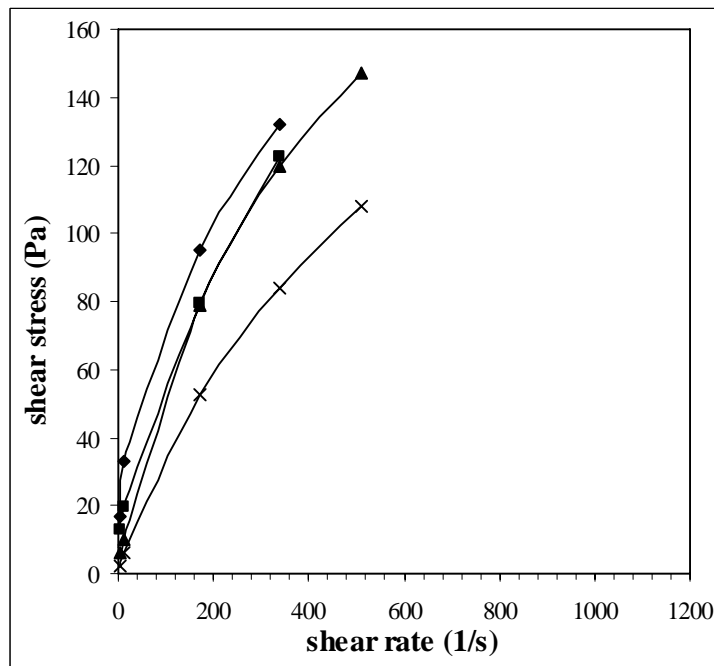


Figure A-6 Shear Stress versus Shear Rate for CMC Polymer in 40 g/l at 20, 35 45 and 55°C.

The Flow Curves of the Experiments (Shear Stress versus Shear Rate).

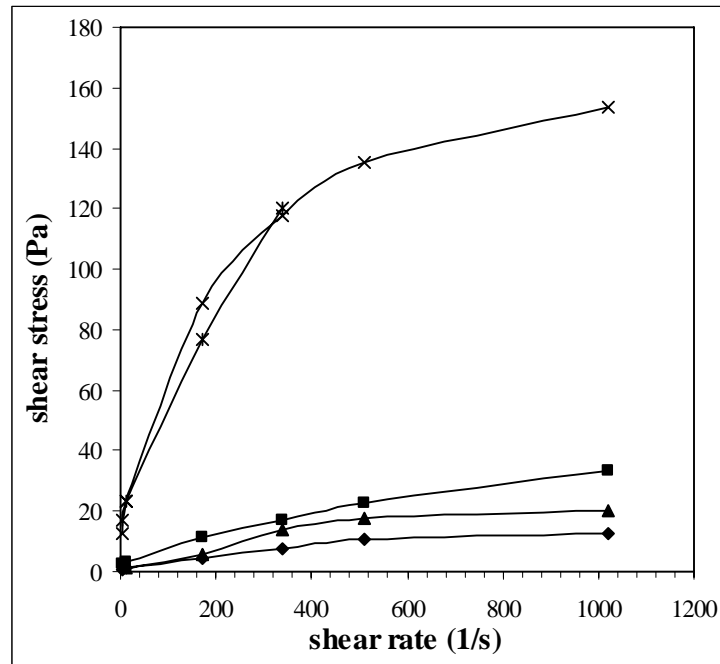


Figure A-7 Shear Stress versus Shear Rate for XC Polymer at 4, 10, 20, 30 and 40 g/l.

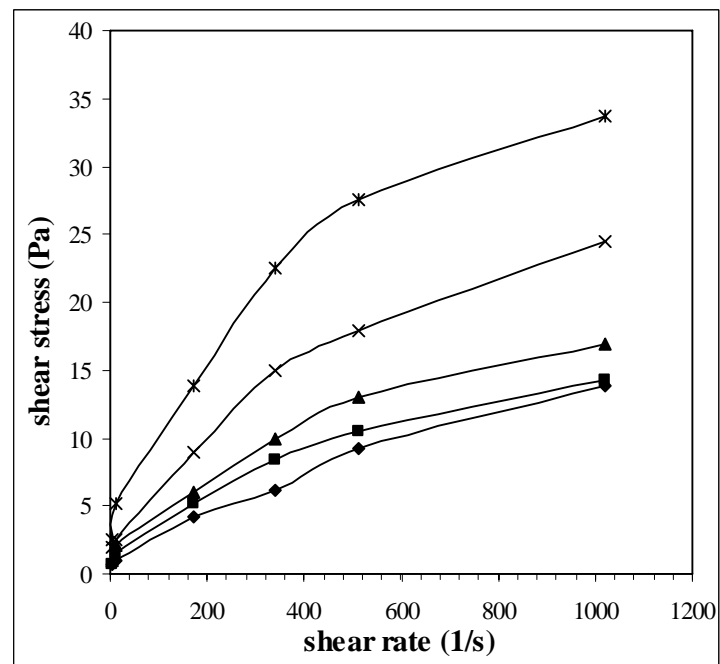


Figure A-8 Shear Stress versus Shear Rate for HEC Polymer at 4, 10, 20, 30 and 40 g/l.

The Flow Curves of the Experiments (Shear Stress versus Shear Rate).

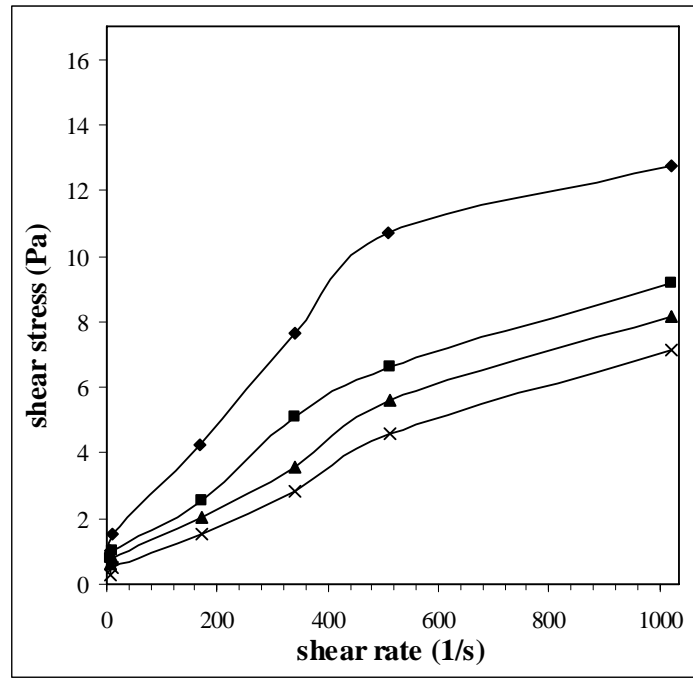


Figure A-9 Shear Stress versus Shear Rate for XC Polymer in 4 g/l at 20, 35 45 and 55°C.

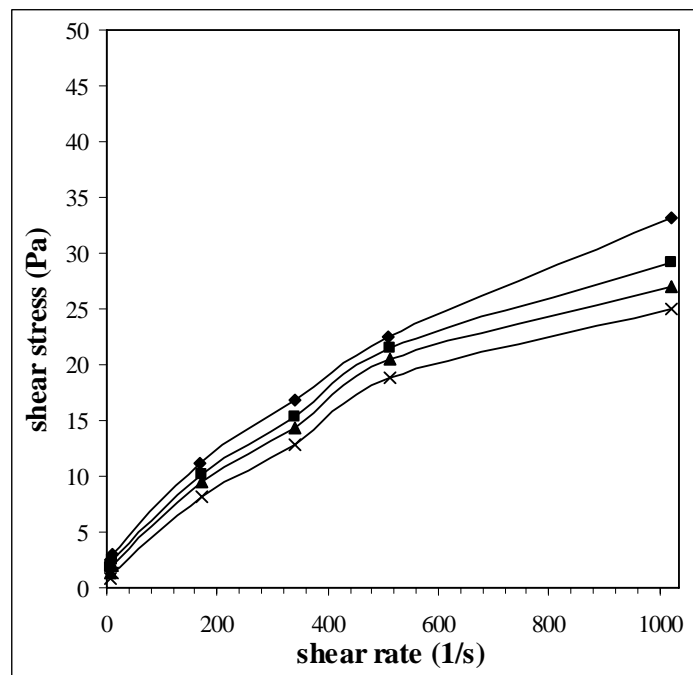


Figure A-10 Shear Stress versus Shear Rate for XC Polymer in 10 g/l at 20, 35 45 and 55°C.

The Flow Curves of the Experiments (Shear Stress versus Shear Rate).

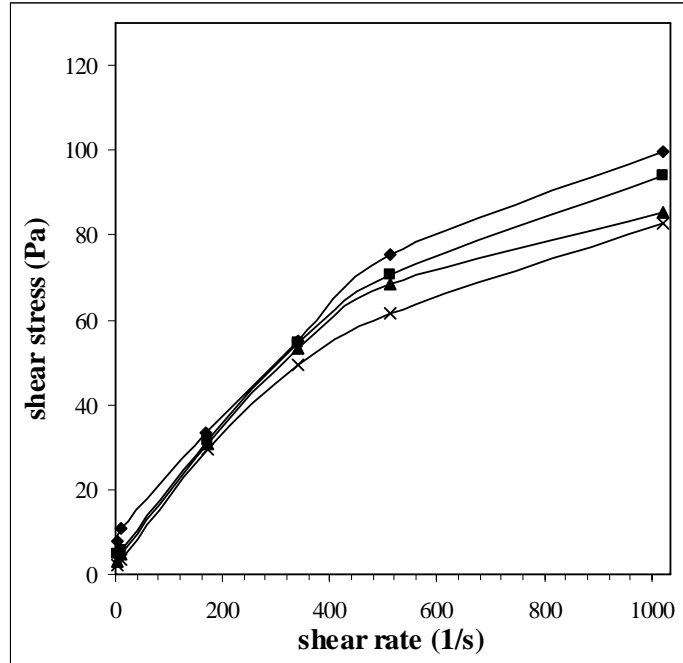


Figure A-11 Shear Stress versus Shear Rate for XC Polymer in 30 g/l at 20, 35 45 and 55°C.

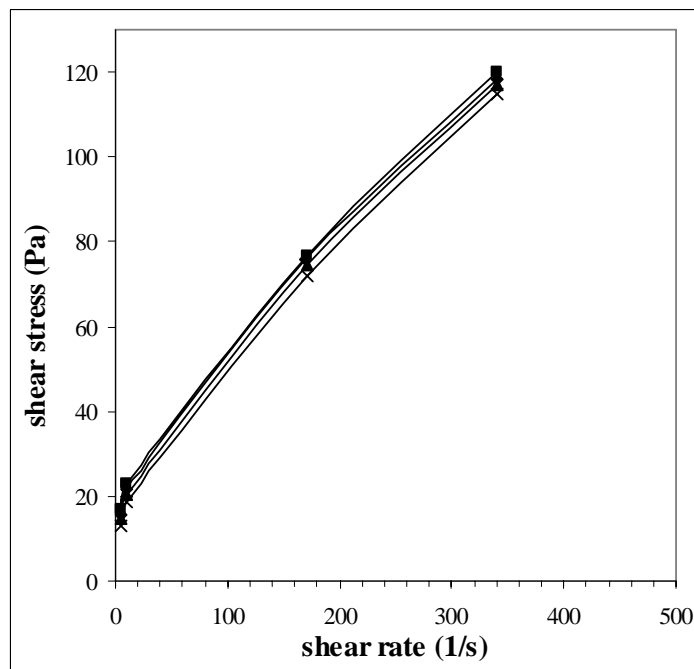


Figure A-12 Shear Stress versus Shear Rate for XC Polymer in 40 g/l at 20, 35 45 and 55°C.

The Flow Curves of the Experiments (Shear Stress versus Shear Rate).

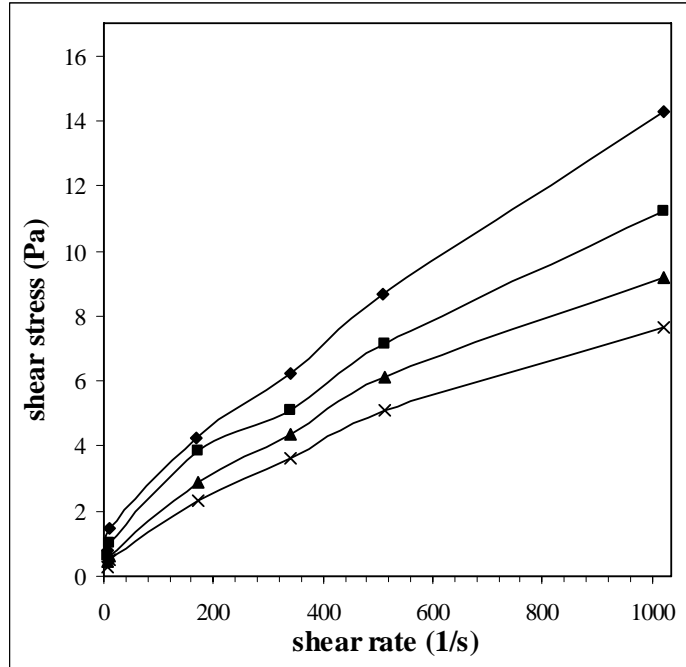


Figure A-13 Shear Stress versus Shear Rate for HEC Polymer in 10 g/l at 20, 35 45 and 55°C.

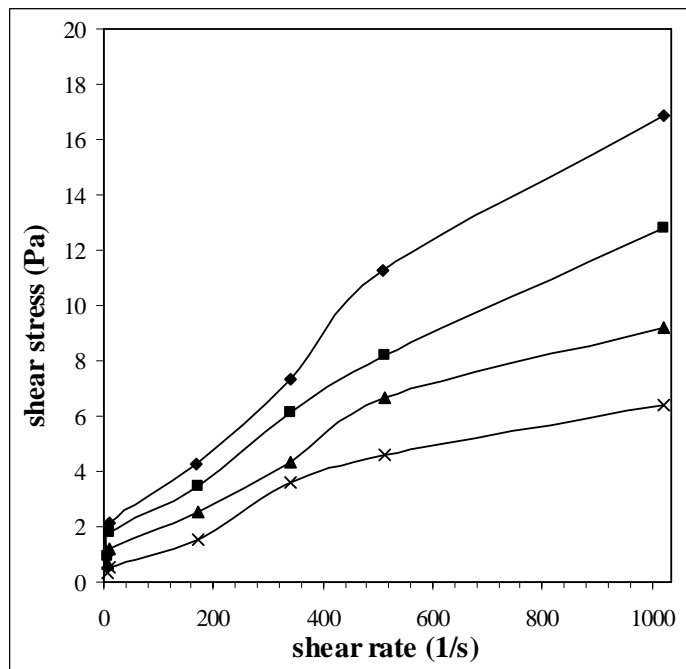


Figure A-14 Shear Stress versus Shear Rate for HEC Polymer in 20 g/l at 20, 35 45 and 55°C.

The Flow Curves of the Experiments (Shear Stress versus Shear Rate).

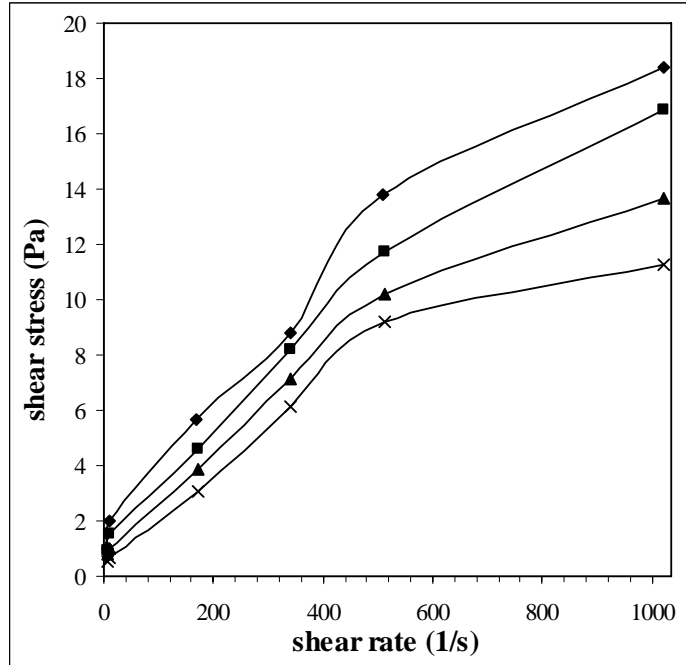


Figure A-15 Shear Stress versus Shear Rate for HEC Polymer in 30 g/l at 20, 35 45 and 55°C.

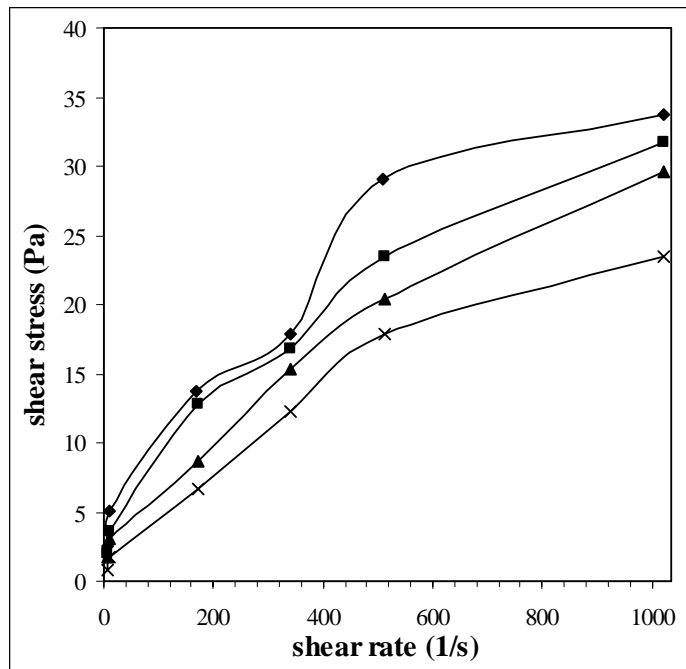


Figure A-16 Shear Stress versus Shear Rate for HEC Polymer in 40 g/l at 20, 35 45 and 55°C.

The Flow Curves of the Experiments (Shear Stress versus Shear Rate).

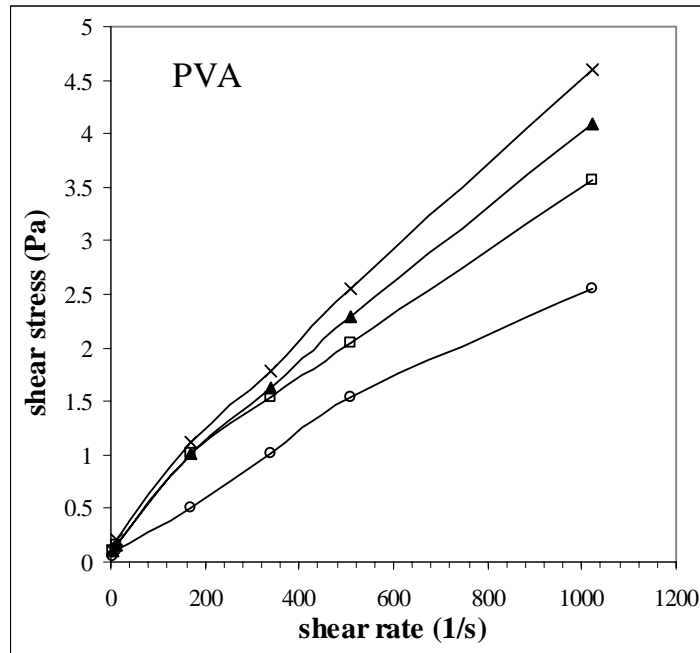


Figure A-17 Shear Stress versus Shear Rate for PVA Polymer at 2, 5, 7 and 10 g/0.5L.

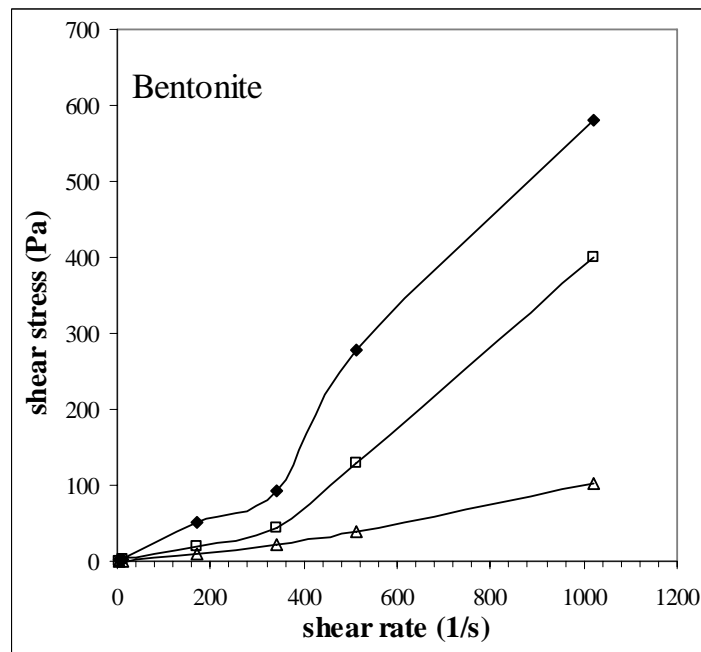


Figure A-18 Shear Stress versus Shear Rate for Bentonite Suspension at 50, 80 and 120 g/l.

The Flow Curves of the Experiments (Shear Stress versus Shear Rate).

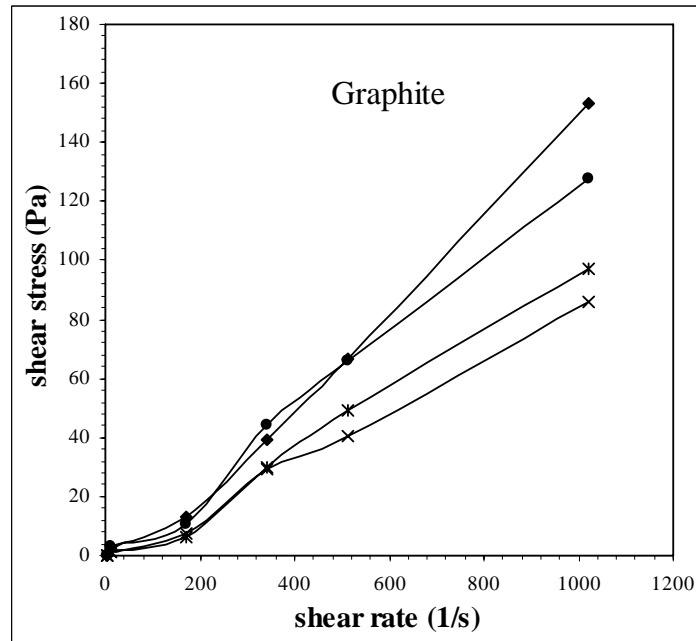


Figure A-19 Shear Stress versus Shear Rate for Graphite Suspension at 30, 40, 70 and 90 g/l.

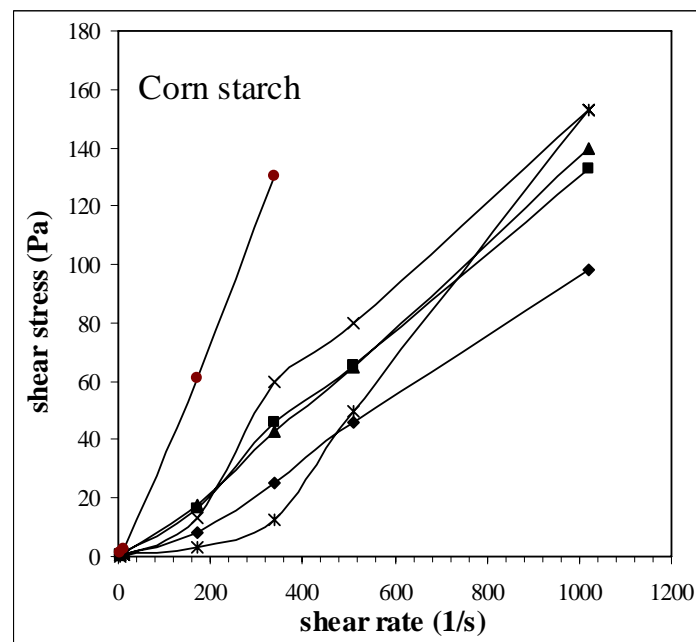


Figure A-20 Shear Stress versus Shear Rate for Corn Starch Suspension at 300, 400, 500, 600, 700 and 800 g/l.

The Flow Curves of the Experiments (Shear Stress versus Shear Rate).

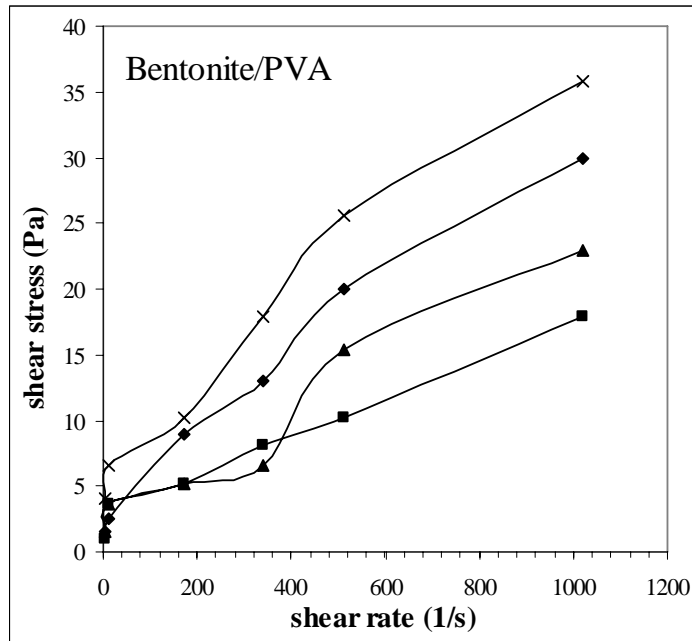


Figure A-21 Shear Stress versus Shear Rate for PVA to Bentonite Suspension at Concentration 2, 5, 7 and 10 g/0.5L to 40 g/0.5L.

Appendix -B-

Experimental Data: Shear Stress versus Shear Rate.

Table B-1 Shear Stress versus Shear Rate for CMC Polymer at concentration 4, 10, 20, 30 and 40 g/L.

θ (1/s)	Shear stress (Pa)				
	4 g/l	10 g/l	20 g/l	30 g/l	40 g/l
1021.4	17.885	20.44	48.545		
510.7	14.308	17.3288	38.836	125.195	
340.5	11.242	13.54	29.638	106.288	131.838
170.2	6.643	5.4821	18.907	70.007	95.046
10.2	1.022	1.5372	4.599	22.995	33.215
5.1	0.511	0.8721	2.555	12.775	16.863

Table B-2 Shear Stress versus Shear Rate for CMC Polymer at Concentration 7, 15, 25 and 35 g/L.

θ (1/s)	Shear stress (Pa)			
	7 g/l	15 g/l	25 g/l	35 g/l
1021.4	20.951	29.127	105.777	***
510.7	15.351	22.995	74.095	135.415
340.5	10.3859	18.396	55.188	120.085
170.2	6.862526	13.286	43.946	75.628
10.2	1.022	1.7885	10.22	27.083
5.1	0.7931	1.533	5.11	14.308

Table B-3 Shear Stress versus Shear Rate for HEC Polymer.

θ (1/s)	Shear stress (Pa)				
	4 g/l	10 g/l	20 g/l	30 g/l	40 g/l
1021.4	13.797	14.308	16.863	24.528	33.726
510.7	9.198	10.47	13	17.885	27.485
340.5	6.142	8.4	10	15	22.514
170.2	4.251	5.2	6	9	13.797
10.2	1.022	1.5	2.127	2.5	5.11
5.1	0.7665	0.7665	1.022	2	2.555

Table B-4 Shear Stress versus Shear Rate for XC polymer.

θ (1/s)	Shear stress (Pa)				
	4 g/l	10 g/l	20 g/l	30 g/l	40 g/l
1021.4	12.775	33.215	99.645	153.3	
510.7	10.731	22.484	75.294	135.415	
340.5	7.625	16.863	55.2019	117.53	120.085
170.2	4.254075	11.242	33.215	88.914	76.65
10.2	1.022	3.066	10.731	23.506	22.995
5.1	0.7665	2.555	7.9521	12.775	16.863

Table B-5 Shear Stress versus Shear Rate for PVA Polymer.

θ (1/s)	Shear stress (Pa)			
	2 g/0.5l	5 g/0.5l	7 g/o.5l	10 g/0.5l
1021.4	4.5961	4.0854	3.5747	2.5534
510.7	2.5534	2.2981	2.0427	1.532
340.5	1.7874	1.6342	1.532	1.0214
170.2	1.1235	1.0214	1.0214	0.5107
10.2	0.2043	0.1532	0.1532	0.1021
5.1	0.1021	0.1021	0.1021	0.0511

Table B-6 Apparent Viscosity Versus Shear Rate for CMC polymer.

θ (1/s)	Viscosity (Pa. s)				
	4 g/l	10 g/l	20 g/l	30 g/l	40 g/l
1021.4	0.018	0.02	0.048		
510.7	0.028	0.034	0.076	0.245	
340.5	0.033	0.04	0.087	0.312	0.387
170.2	0.039	0.032	0.111	0.411	0.558
10.2	0.1	0.15	0.45	2.25	3.25
5.1	0.1	0.155	0.5	2.502	3.302

Table B-7 Apparent Viscosity versus Shear Rate for CMC Polymer.

θ (1/s)	Viscosity (Pa. s)			
	7 g/l	15 g/l	25 g/l	35 g/l
1021.4	0.021	0.029	0.104	***
510.7	0.03	0.045	0.145	0.265
340.5	0.03	0.054	0.162	0.353
170.2	0.04	0.078	0.258	0.444
10.2	0.1	0.175	1	2.65
5.1	0.1	0.3	1.001	2.802

Table B-8 Apparent Viscosity Versus Shear Rate for HEC polymer.

θ (1/s)	Viscosity (Pa. s)				
	4 g/l	10 g/l	20 g/l	30 g/l	40 g/l
1021.4	0.014	0.014	0.017	0.024	0.033
510.7	0.018	0.02	0.025	0.035	0.054
340.5	0.018	0.025	0.029	0.044	0.066
170.2	0.025	0.031	0.035	0.053	0.081
10.2	0.1	0.147	0.208	0.245	0.5
5.1	0.15	0.15	0.2	0.392	0.5

Table B-9 Apparent Viscosity Versus Shear Rate for XC polymer.

θ (1/s)	Viscosity (Pa. s)				
	4 g/l	10 g/l	20 g/l	30 g/l	40 g/l
1021.4	0.013	0.033	0.098	0.15	***
510.7	0.021	0.044	0.147	0.265	***
340.5	0.022	0.05	0.162	0.345	0.353
170.2	0.025	0.066	0.195	0.522	0.45
10.2	0.1	0.3	1.05	2.3	2.25
5.1	0.15	0.5	1.557	2.502	3.302

Table B-10 Effect of Temperature in Apparent Viscosity for CMC 10 g/L.

Temp.°C	Viscosity (Pa.s)					
	1021.4(1/s)	510.7(1/s)	340.5(1/s)	170.2(1/s)	10.2(1/s)	5.1(1/s)
20	0.020002	0.033914	0.039749	0.032187	0.15042	0.170769
35	0.018501	0.025002	0.027002	0.028502	0.09165	0.100061
45	0.017501	0.022002	0.022502	0.024002	0.06025	0.070042
55	0.015001	0.018001	0.019502	0.021002	0.03350	0.040024

Table B-11Effect of Temperature in Apparent Viscosity for CMC 15 g/L

Temp.°C	Viscosity (Pa.s)					
	1021.4(1/s)	510.7(1/s)	340.5(1/s)	170.2(1/s)	10.2(1/s)	5.1(1/s)
20	0.028502	0.045004	0.054004	0.078006	0.17501	0.300182
35	0.026502	0.032003	0.034503	0.039003	0.12501	0.200121
45	0.024002	0.026002	0.028502	0.033003	0.10000	0.150091
55	0.020002	0.022002	0.024002	0.027002	0.07501	0.100061

Table B-12 Effect of Temperature in Apparent Viscosity for CMC 25 g/L.

Temp.°C	Viscosity (Pa.s)					
	1021.4(1/s)	510.7(1/s)	340.5(1/s)	170.2(1/s)	10.2(1/s)	5.1(1/s)
20	0.103508	0.145011	0.162013	0.25802	1.00008	1.000607
35	0.102008	0.13201	0.147012	0.186015	0.35003	0.400243
45	0.084007	0.108008	0.12451	0.156012	0.25002	0.300182
55	0.082506	0.095007	0.112509	0.156012	0.17501	0.250152

Table B-13 Effect of Temperature in Apparent Viscosity for CMC 40 g/L.

Temp.°C	Viscosity (Pa.s)					
	1021.4(1/s)	510.7(1/s)	340.5(1/s)	170.2(1/s)	10.2(1/s)	5.1(1/s)
20			0.38703	0.558044	3.25025	3.302003
35			0.360028	0.468037	1.90015	2.501518
45		0.288023	0.351027	0.462036	1.00008	1.200728
55		0.211017	0.246019	0.309024	0.60005	0.450273

Table B-14 Effect of Temperature in Apparent Viscosity for HEC 10 g/L

Temp.°C	Viscosity (Pa.s)					
	1021.4(1/s)	510.7(1/s)	340.5(1/s)	170.2(1/s)	10.2(1/s)	5.1(1/s)
20	0.014001	0.017001	0.018327	0.024959	0.14678	0.150091
35	0.011001	0.014001	0.015001	0.022565	0.09737	0.120173
45	0.009001	0.012001	0.012781	0.016864	0.06151	0.083661
55	0.007501	0.010001	0.010682	0.013594	0.04791	0.052942

Table B-15 Effect of Temperature in Apparent Viscosity for HEC 20 g/L

Temp.°C	Viscosity (Pa.s)					
	1021.4(1/s)	510.7(1/s)	340.5(1/s)	170.2(1/s)	10.2(1/s)	5.1(1/s)
20	0.016501	0.022062	0.021612	0.025223	0.20814	0.200121
35	0.012501	0.016001	0.018001	0.020375	0.17501	0.180109
45	0.009001	0.013001	0.012751	0.015001	0.11781	0.130079
55	0.00625	0.009001	0.010501	0.009001	0.05000	0.070042

Table B-16 Effect of Temperature in Apparent Viscosity for HEC 30 g/L.

Temp.°C	Viscosity (Pa.s)					
	1021.4(1/s)	510.7(1/s)	340.5(1/s)	170.2(1/s)	10.2(1/s)	5.1(1/s)
20	0.018001	0.027002	0.025816	0.033367	0.19571	0.200121
35	0.016501	0.023002	0.024002	0.027002	0.15001	0.180209
45	0.013351	0.020002	0.021002	0.022508	0.10001	0.150211
55	0.011001	0.018001	0.018001	0.018001	0.06501	0.100061

Table B-17 Effect of Temperature in Apparent Viscosity for HEC 40 g/L

Temp.°C	Viscosity (Pa.s)					
	1021.4(1/s)	510.7(1/s)	340.5(1/s)	170.2(1/s)	10.2(1/s)	5.1(1/s)
20	0.033003	0.057004	0.052504	0.081006	0.50004	0.500304
35	0.031002	0.046004	0.049504	0.075006	0.35003	0.400243
45	0.029002	0.040003	0.045004	0.051004	0.30002	0.345739
55	0.023002	0.035003	0.036003	0.039003	0.17501	0.150091

Table B-18 Effect of Temperature in Apparent Viscosity for XC 4g/L

Temp. °C	Viscosity (Pa.s)					
	1021.4(1/s)	510.7(1/s)	340.5(1/s)	170.2(1/s)	10.2(1/s)	5.1(1/s)
20	0.012501	0.021002	0.022384	0.024977	0.15001	0.200121
35	0.009001	0.013001	0.015001	0.015001	0.10001	0.150091
45	0.008001	0.011001	0.010501	0.012001	0.07501	0.120073
55	0.007001	0.009001	0.008251	0.009001	0.05001	0.05003

Table B-19 Effect of Temperature in Apparent Viscosity for XC 10g/L

Temp. °C	Viscosity (Pa.s)					
	1021.4(1/s)	510.7(1/s)	340.5(1/s)	170.2(1/s)	10.2(1/s)	5.1(1/s)
20	0.032503	0.044003	0.049504	0.066005	0.30002	0.500304
35	0.028502	0.042003	0.045004	0.060005	0.25002	0.350212
45	0.026502	0.040003	0.042003	0.055504	0.20001	0.250152
55	0.024502	0.037003	0.037503	0.048004	0.12501	0.150091

Table B-20 Effect of Temperature in Apparent Viscosity for XC 20g/L

Temp. °C	Viscosity (Pa.s)					
	1021.4(1/s)	510.7(1/s)	340.5(1/s)	170.2(1/s)	10.2(1/s)	5.1(1/s)
20	0.097508	0.147358	0.162053	0.195015	1.05008	1.557134
35	0.092007	0.138011	0.160867	0.186015	0.55004	0.900546
45	0.083507	0.13401	0.156012	0.180734	0.45003	0.600364
55	0.081111	0.120009	0.145511	0.172396	0.35002	0.400243

Table B-21 Effect of Temperature in Apparent Viscosity for XC 40g/L

Temp. °C	Viscosity (Pa.s)					
	1021.4(1/s)	510.7(1/s)	340.5(1/s)	170.2(1/s)	10.2(1/s)	5.1(1/s)
20			0.352528	0.450035	2.25018	3.302003
35			0.347324	0.444035	2.13522	3.043907
45			0.342913	0.437614	2.01022	2.85173
55			0.33694	0.421533	1.82914	2.579565

Table B-22 Shear Rate versus Shear Stress for Bentonite Suspension.

θ (1/s)	Shear stress (Pa)		
	50 g/l	80 g/l	120 g/l
1021.4	102.2	400	580
510.7	38.325	130	278
340.5	22.995	45	93.676
170.2	10.22	20	51.096
10.2	0.7665	2	3
5.1	0.393	1	1.5

Table B-23 Shear Rate versus Shear Stress for Graphite Suspension.

θ (1/s)	Shear stress (Pa)			
	30 g/l	40 g/l	70 g/l	90 g/l
1021.4	85.848	97.09	127.75	153.3
510.7	40.369	49.056	65.74	66.43
340.5	29.127	30	43.946	39
170.2	7.665	6.5	10.476	12.775
10.2	1.022	1.022	3.066	2.555
5.1	0.2555	0.2555	0.1022	0.0511

Table B-24 Shear Rate versus Shear Stress for Corn Starch Suspension.

θ (1/s)	Shear stress (Pa)					
	300 g/l	400 g/l	500 g/l	600 g/l	700 g/l	800 g/l
1021.4	98	133	140	153	153	***
510.7	45.67	65.65	65	80	50	***
340.5	25	45.99	43	60	12.9	130
170.2	8	16.07	17.49	13	3.2	61.2
10.2	0.511	1	1	0.777	0.695	2.739
5.1	0.5	0.58	0.5	0.67	0.255	1.277

Table B- 25 Apparent Viscosity versus Shear Rate for Bentonite Suspension.

θ (1/s)	Viscosity (Pa.s)		
	50 g/l	80 g/l	120 g/l
1021.4	0.5529	0.3914	0.5676
510.7	0.5441	0.2544	0.5441
340.5	0.275	0.1321	0.275
170.2	0.3	0.1174	0.3
10.2	0.3914	0.1957	0.2936
5.1	0.077	0.19	0.2936

Table B- 26 Apparent Viscosity versus Shear Rate for Graphite Suspension.

θ (1/S)	Viscosity (Pa.s)			
	30 g/l	40 g/l	70 g/l	90 g/l
1021.4	0.084	0.095	0.125	0.15
510.7	0.079	0.096	0.1287	0.13
340.5	0.0855	0.0881	0.129	0.1145
170.2	0.045	0.0382	0.0615	0.075
10.2	0.1	0.1	0.3	0.25
5.1	0.05	0.05	0.02	0.01

Table B- 27 Apparent Viscosity versus Shear Rate for Corn Starch Suspension.

θ (1/S)	Viscosity (Pa.s)					
	300 g/l	400 g/l	500 g/l	600 g/l	700 g/l	800 g/l
1021.4	0.0959	0.1301	0.137	0.1497	0.1497	***
510.7	0.0894	0.1285	0.1272	0.1566	0.1427	***
340.5	0.0734	0.135	0.1262	0.1761	0.1321	0.3816
170.2	0.047	0.0944	0.1027	0.0763	0.06	0.312
10.2		0.0979	0.102	0.076	0.068	0.268
5.1	0.0979	0.1135	0.0979	0.1311	0.05	0.25

Table B-28 Shear Stress Versus Shear Rate for (Bentonite/PVA).

θ (1/s)	Shear stress (Pa)			
	(40+2) g/l	(40+5) g/l	(40+7) g/l	(40+10) g/l
1021.4	35.77	22.995	17.885	30
510.7	25.55	15.33	10.22	20
340.5	17.885	6.643	8.176	13
170.2	10.22	5.11	5.11	9
10.2	6.643	3.577	3.577	2.54
5.1	4.088	1.533	1.022	1.533

Table B-29 Apparent Viscosity versus Shear Rate for (Bentonite/PVA).

Shear rate (1/S)	Viscosity (Pa. s)			
1021.92	0.02936	0.0175	0.0225	0.035
510.96	0.03914	0.02	0.03	0.05
340.64	0.03816	0.024	0.0195	0.0525
170.32	0.05284	0.03	0.03	0.06
10.2192	0.24855	0.35003	0.35003	0.65005
5.1069	0.30018	0.20012	0.30018	0.80049

Table B-30 Bingham Yield Point and Plastic Viscosity Versus Shear Rate for (Bentonite/PVA).

Conc. g/l	Bingham yield point	Plastic Viscosity
4	2.7611	0.0123
10	2.372	0.0085
14	2.0149	0.0209
20	6.0086	0.3311

Table B-31 Model Selection for Bentonite/PVA at Concentration (80+4) g/L Using Add-in in Microsoft Excel.

Shear rate	Sum of Square Error				
	Newtonian	Bingham	Power Law	With Yield	Robertson
1021.4	30.6414	36.9908	28.832	21.5828	29.3372
510.69	15.3207	19.3577	18.2611	15.8012	20.9229
340.46	10.2138	13.48	13.9798	13.1668	17.1693
170.23	5.1069	7.60226	8.85423	9.64029	12.2449
10.214	0.30641	2.07722	1.38699	2.72236	3.10551
5.1069	0.15321	1.90089	0.87847	1.99449	2.21484

Table B-32 Model Selection for Bentonite/PVA at Concentration (80+10) g/L Using Add-in in Microsoft Excel.

Shear rate	Sum of Square Error				
	Newtonian	Bingham	Power Law	With Yield	Robertson
1021.4	20.428	20.167	17.304	16.58	17.611855
510.69	10.214	10.639	11.871	11.899	12.477729
340.46	6.8092	7.4634	9.5224	9.8258	10.207798
170.23	3.4046	4.2874	6.5324	7.1236	7.2597917
10.214	0.2043	1.302	1.415	2.198	2.0735656
5.1069	0.1021	1.2067	0.9707	1.7299	1.6597702

Table B- 33 Model Selection for Bentonite/PVA at Concentration (80+14) g/L Using Add-in in Microsoft Excel.

Shear rate	Sum of Square Error				
	Newtonian	Bingham	Power Law	With Yield	Robertson
1021.4	25.5345	21.4385	14.0143	14.1537	14.67557646
510.69	12.7673	11.5542	10.3843	10.3067	10.47143416
340.46	8.5115	8.25949	8.71398	8.57668	8.596918824
170.23	4.25575	4.96475	6.45686	6.2896	6.139967844
10.214	0.25535	1.86768	1.91237	1.955	1.62509095
5.1069	0.12767	1.76884	1.41702	1.52005	1.208293144

Table B-34 Model Selection for Bentonite/PVA at Concentration (80+20) g/L Using Add-in in Microsoft Excel.

Shear rate	Sum of Square Error				
	Newtonian	Bingham	Power Law	With Yield	Robertson
1021.4	49.026	40.248	27.129	32.727	32.017243
510.69	24.513	22.374	21.285	24.987	24.302351
340.46	16.342	16.416	18.469	21.359	20.695957
170.23	8.171	10.458	14.49	16.371	15.757204
10.214	0.4903	4.8575	5.4129	5.8265	5.7824792
5.1069	0.2451	4.6787	4.2468	4.5997	4.8392518

الخلاصة

هذا البحث يهتم بدراسة الخواص الريولوجية للمحاليل البوليمرات، والعوالق. البوليمرات المستخدمة في البحث هي : XC – أكسانثان كم بوليمر ، CMC - كاربوكسي مثيل سيليلوز ، HEC - هايدروكسي مثيل سيليلوز ، PVA - بولي فنيل الكحول. العوالق المستخدمة : البنتونايت، الكرافايت و نشأ الذرة.

الخواص الريولوجية لهذه المواد أستنتجت من أستعمالي لجهاز (Fann VG.35A) و حدود الجهاز مابين ٣- ٦٠٠ دورة في كل دقيقة حيث أنه يقيس اجهاد القص (shear stress) المصاحب لكل معدل قص مسلط (shear rate).

ست وسبعون تجربة أجريت ضمن حدود الجهاز للتراكيز المحصورة مابين ٤-٤٠ غرام \ لتر لكل البوليمرات المستخدمة (CMC, HEC and XC) ومن ٢-١٠ غرام \ لتر لمادة بولي فنيل الكحول، والعوالق التي أستخدمتها كانت ضمن حدود مختلفة لكل مادة، فلبنتونايت من 50 الى 120 غرام \ لتر، الكرافايت من 30 الى 90 غرام \ لتر، ونشأ الذرة كان من 300 الى 800 غرام \ لتر وكانت حدود الحرارة للتجارب التي أجريتها ما بين ٠-٥٥ درجة مئوية.

ومن خلال النتائج العملية وجدة أنه كلما زاد تركيز البوليمير في المحاليل فإن دليل سلوك الجريان (n) يقل وأنه ضمن حدود مابين (0.7-0.4) عند 20 درجة مئوية، وزيادة تركيز العوالق يؤدي الى أن دليل سلوك الجريان (n) يزداد ويصبح ضمن حدود مابين (1-1.3) عند 35 درجة مئوية. تم أيجاد معادلات رياضية التي تبين تأثير التركيز على دليل سلوك الجريان (n) معادلة لكل بوليمر وعالق مستخدم.

أن لزوجة البوليمرات الثلاثة المستخدمة في عملي أثبتت أنها تقل كلما أزدادت درجة الحرارة ومعدل القص المسلط عليها ، وكذلك وجد أن لزوجة العوالق تزداد كلما زادة معدل القص المسلط.

وتم اعتماد النموذج الرياضي (Power Law Model) لأيجاد الخواص الريولوجية لكل من المحاليل البوليمرات والعوالق.

أن التغير بدرجات الحرارة أثرت على قيمتي (n) و (k) ، ان الزيادة في درجة الحرارة تسبب زيادة في قيمة (n) وتقلل قيمة (k).

تم استخدام برنامج مايكروسوفت ايكسيل لايجاد افضل نموذج رياضي يمثل النتائج العملية .
وقد وجد بان النموذج رياضي (Bingham plastic model) هو الافضل لتمثيل الخواص
الريولوجية لأضافة مادة PVA polymer بتراكيز مختلفة الى مادة البنيونايت.
أن اضافة مادة بولي فنيل الكحول للبتونايت يؤثر على الخواص الريولوجية حيث انه يعمل
على تعديل قيم الزوجة الظاهرة للبتونايت. أن التجارب العملية أثبتت أن الزوجة الظاهرة لمادة
البتونايت (بدون بوليمر) تزداد مع زيادة معدل القص.
ان Bingham yield stress (τ_B)، يقل عند اضافة مادة بولي فنيل الكحول الى ان يصل
لتركيز مابين 14- 15 غرام \ لتر حيث يبدأ بالزيادة.

شكر و تقدير

اولاً وقبل كل شيء الحمد والشكر لله على تمام الصحة وقوة الأيمان التي ساعدتني على تخطي الصعاب التي واجهتني طيلة فترة البحث. واتقدم بالشكر الجزيل الى الاستاذ الدكتور قاسم جبار سليمان رئيس قسم الهندسة الكيمياءوية. اود ان اعبر عن خالص شكري وامتناني وعرفاني بالجميل للدكتور كمال شاكر عبد المسيح الذي تفضل بأكمال متابعة بحثي وما قدمه لي من اهتمام كبير ولما أبدا لي من توجيهات قيمة ساعدتني على إنجاز هذا العمل. ولا أنسى أن أشكر من ربياني على طريق المعرفة والخير وأنا أتشرفه

بصما أبي وأمي الحنونة

وكذلك من لزميني بالدعاء اخي محمود . مروى وزينب اخواتي.

وكذلك لا أنسى أعمز من الوجود رفيق دربي الذي وقفه الى جانبي

في هذه الفترة زوجي حيدر.

منار طاهر ناصر

دراسة الخواص الريولوجية لمحاليل البولمرات والعوالق

رسالة

مقدمة الى كلية الهندسة في جامعة النهريين
وهي جزء من متطلبات نيل درجة ماجستير علوم
في الهندسة الكيمياوية

من قبل

منار ظاهر ناصر

(بكوريوس علوم في الهندسة الكيمياوية ٢٠٠٦)

١٤٣٠

٢٠٠٩

جمادي الآخر

آيار